Supporting Information

Development of Allosteric Small Molecule APOBEC3B Inhibitors from *In Silico* Screening

Katherine F. M. Jones[1⊥], Özlem Demir[2⊥], Mackenzie K. Wyllie[3], Michael J. Grillo[1], Clare Morris[2], Sophia P. Hirakis[2], Rahul Dadabhau Kardile[3], Michael A. Walters[3,4], Reuben S. Harris[5,6], Rommie E. Amaro[2*], and Daniel A. Harki[1,3*]

[1] Department of Chemistry, University of Minnesota, Minneapolis, MN, USA

[2] Department of Chemistry and Biochemistry, University of California – San Diego, La Jolla, CA, USA

[3] Department of Medicinal Chemistry, University of Minnesota, Minneapolis, MN, USA

[4] Institute for Therapeutics Discovery and Development, University of Minnesota, Minneapolis, MN, USA

[5] Department of Biochemistry & Structural Biology, University of Texas Health Science Center San Antonio, San Antonio, TX, USA

[6] Howard Hughes Medical Institute, University of Texas Health Science Center San Antonio, San Antonio, TX, USA

[⊥] These authors contributed equally to this work

1 Methods

1.1 Synthesis

Unless otherwise noted, reactants and glassware were not dried before use, and reactions were stirred with a Teflon-coated stir bar. Reaction solvents acetonitrile (CH_3CN), dichloromethane (CH_2Cl_2), and tetrahydrofuran (THF) were dried by passage over a column of activated alumina using a solvent purification system (MBraun). Dimethylformamide (DMF) was dried by passage over a column of molecular sieves using a solvent purification system (MBraun). Reactions were monitored using thin layer chromatography with EMD Chemicals Silica Gel 60 F_{254} glass plates (250 µm thickness) and visualized with UV irradiation at either 254 nm or 365 nm. Flash chromatography was performed with a Teledyne-Isco CombiFlash NextGen instrument, equipped with both a UV-Vis detector and an ELSD, using Redisep Rf High Performance silica gel columns (Teledyne-Isco). ^{1}H NMR (500 MHz) and ^{13}C NMR (125 MHz) were collected on a Bruker Advance NMR spectrometer at room temperature. NMR chemical shifts (δ) are recorded relative to TMS (0.05% v/v, δ = 0.0) or residual solvent signal (δ = 7.26 ppm for $CDCl_3$, δ = 2.50 ppm for DMSO-d_6, or δ = 3.31 ppm for MeOD) for ^{1}H NMR and the solvent signal for ^{13}C NMR (δ = 77.0 for $CDCl_3$, δ = 40.0 for DMSO-d_6, or δ = 49.0 ppm for MeOD). ^{1}H peak broadening and additional ^{13}C resonances are observed for compounds **23**, **24**, and **25**, which are attributed to conformational restriction of the substituted piperidine. This observation is consistent with a prior report.[1] HRMS data were collected on an Orbitrap Elite (Thermo) mass analyzer at 240,000 resolution with electrospray ionization in positive mode. Reverse-phase purification was performed on a preparative-scale Agilent 1200 series instrument. The preparative column was an Agilent Zorbax SB-C18 (21.2 x 250 mm, 7 µm pore). Mobile phase A = H_2O + 0.1% TFA, mobile phase B = MeCN + 0.1% TFA, flow rate = 30 mL/min. Elution: 90:10 A:B for 0-2 min, gradient to 30:70 A:B from 2-22 min, gradient to 5:95 A:B from 22 min to 28 min, isocratic at 5:95 A:B from 28-30 min.

*1.1.1 Synthesis of 1-benzyl-3-ethylpiperidin-3-ol (**19**)*

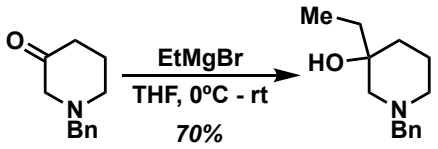

18 **19**

To a suspension of N-benzyl-3-piperidone HCl salt (**18**, 4.51 g, 20.0 mmol) in dry THF (40 mL) in a flame-dried flask was added EtMgBr (1.0 M in THF, 50 mL, 50 mmol) slowly at 0°C under N_2

and then warmed to room temperature overnight. Saturated NH_4Cl solution (75 mL) was carefully added, and the reaction mixture was concentrated in vacuo to remove the THF and ether. The crude material was diluted with water (50 mL) and extracted with CH_2Cl_2 (50 mL) three times, then the combined organic layers were dried over Na_2SO_4, concentrated *in vacuo* then purified by flash chromatography (0-50% EtOAc in hexanes gradient) resulting in a pale-yellow oil, **19** (2.41 g, 11.0 mmol) in 70% yield.

^{1}H NMR (500 MHz, $CDCl_3$): δ 7.36 – 7.21 (m, 6H), 3.62 – 3.44 (m, 2H), 3.24 (s, 1H), 2.79 (d, *J* = 11.0 Hz, 1H), 2.59 (dt, *J* = 10.9, 2.2 Hz, 1H), 2.03 – 1.85 (m, 2H), 1.77 (qt, *J* = 12.7, 4.3 Hz, 1H), 1.67 – 1.58 (m, 1H), 1.54 (ddq, *J* = 13.5, 5.6, 2.8 Hz, 1H), 1.45 (qd, *J* = 7.5, 4.8 Hz, 2H), 1.20 (td, *J* = 13.0, 4.9 Hz, 1H), 0.90 (t, *J* = 7.6 Hz, 3H).

HRMS: $C_{14}H_{22}NO$ Calc'd $[M+H]^+$: 220.1701, Found: 220.1686.

*1.1.2 Synthesis of 1-(4-bromobenzoyl)-3-ethylpiperidin-3-ol (**20**)*

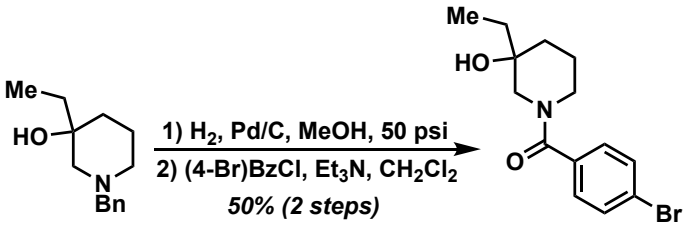

19 **20**

To a solution of **19** (2.41 g, 11.0 mmol) in MeOH (55 mL, 0.2 M) was added Pd/C (10% w/w) then the mixture was placed under vacuum and purged several times with N_2 and then H_2. The mixture was then shaken under 50 psi H_2 overnight on a Parr hydrogenator. The mixture was filtered through Celite and concentrated *in vacuo*, yielding a pale-yellow oil. The crude product (782 mg, 6.05 mmol) was used in the next step without further purification.

The crude intermediate was dissolved in anhydrous CH_2Cl_2 (12.1 mL, 0.5 M), then Et_3N (1.27 mL, 9.08 mmol) and 4-bromobenzoyl chloride (1.46 g, 6.66 mmol) was added. The solution was stirred overnight under N_2 then concentrated *in vacuo*. The resulting crude material was taken up in EtOAc (25 mL), washed with saturated NH_4Cl solution (20 mL), water (20 mL), and brine (20 mL). The organic layer was dried over Na_2SO_4, concentrated *in vacuo*, and purified by flash chromatography (0-10% MeOH in CH_2Cl_2) yielding the product, **20**, as a white solid (545 mg, 1.75 mmol) in 50% yield over two steps.

^{1}H NMR (500 MHz, MeOD): δ 7.61 (dd, *J* = 13.3, 7.9 Hz, 2H), 7.37 (dd, *J* = 25.6, 8.0 Hz, 2H), 4.08 (dd, *J* = 162.9, 13.0 Hz, 1H), 3.41 (dd, *J* = 37.7, 13.5 Hz, 1H), 3.29 – 3.02 (m, 2H), 1.84 (dd, *J* = 47.3, 12.2 Hz, 1H), 1.76 – 1.68 (m, 1H), 1.68 – 1.45 (m, 3H), 1.45 – 1.24 (m, 1H), 0.89 (dt, *J* = 93.7, 7.6 Hz, 3H).

^{13}C NMR (126 MHz, MeOD): δ 170.9, 170.5, 135.2, 134.9, 131.5, 131.2, 129.2, 128.3, 123.4, 69.7, 69.5, 56.8, 51.0, 42.5, 34.2, 34.1, 31.6, 31.6, 21.6, 20.4, 6.0, 5.7.

HRMS: $C_{14}H_{18}BrNO_2$ Calc'd $[M+H]^+$: 312.0599, Found: 312.0585.

*1.1.3 Synthesis of 4'-(3-ethyl-3-hydroxypiperidine-1-carbonyl)-4-fluoro-[1,1'-biphenyl]-3-carboxamide (**10***)*

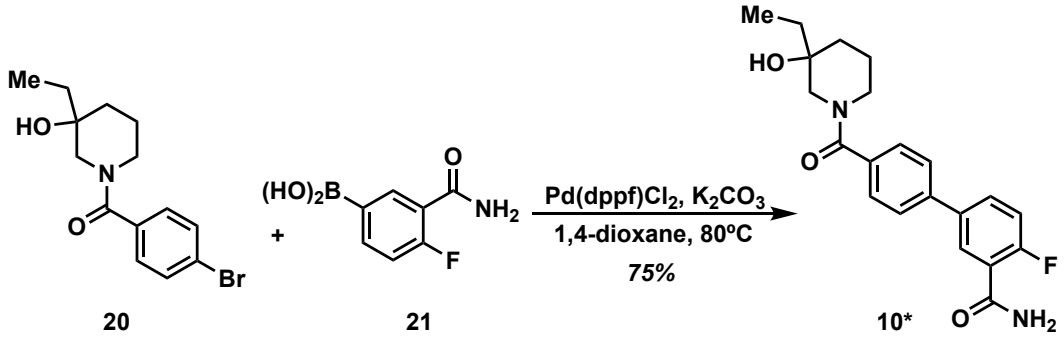

A solution of **20** (187 mg, 0.450 mmol), (3-carbamoyl-4-fluorophenyl)boronic acid (**21**, 90.6 mg, 0.495 mmol), and K_2CO_3 (5 M in H_2O, 270 µL) in 1,4-dioxane (20 mL, 0.02 M) was degassed by placing the flask under vacuum and purging several times with N_2, then $Pd(dppf)Cl_2$ (36.7 mg, 0.045 mmol) was added and the mixture heated to 60°C overnight. The dioxane was evaporated *in vacuo*, and the resulting crude material was diluted with EtOAc (20 mL) and water (20 mL), then filtered through celite. The organic layer was washed with water (15 mL) and brine (20 mL), dried over Na_2SO_4, concentrated in *vacuo* and then purified by flash chromatography (0-100% EtOAc in hexanes) yielding a light brown foamy solid. The product was further purified by reverse-phase preparative HPLC (described in General) yielding the final product, **10***, (125 mg, 0.337 mmol) as a foamy white solid with high purity in 75% yield.

^{1}H NMR (500 MHz, DMSO): δ 7.86 – 7.60 (m, 7H), 7.60 – 7.44 (m, 2H), 4.43 – 4.33 (m, 1H), 4.14 – 3.94 (m, 1H), 3.19 – 3.04 (m, 2H), 1.76 (s, 1H), 1.40 (dd, *J* = 125.6, 53.4 Hz, 5H), 0.81 (d, J = 90.4 Hz, 3H).

^{13}C NMR (126 MHz, DMSO): δ 165.4, 161.3, 159.3, 144.1, 144.0, 131.4, 131.4, 128.7, 127.9, 127.1, 123.0, 123.0, 114.7, 114.6, 69.1, 49.1, 34.8, 7.4.

^{19}F NMR (471 MHz, $CDCl_3$): δ -115.30.

HRMS: $C_{21}H_{23}FN_2O_3$ Calc'd $[M+H]^+$: 371.1771, Found: 371.1756.

*1.1.4 Synthesis of 1-{3'-amino-4'-fluoro-[1,1'-biphenyl]-4-carbonyl}-3-ethylpiperidin-3-ol (**23**)*

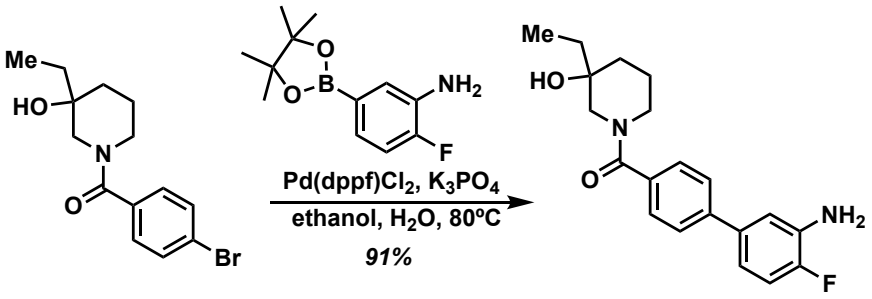

20 **23**

A solution of 1-(4-bromobenzoyl)-3-ethylpiperidin-3-ol (**20**, 150 mg, 0.480 mmol), 2-fluoro-5-(4,4,5,5-tetramethyl-1,3,2-dioxaborolan-2-yl)aniline (114 mg, 0.480 mmol), and K_3PO_4 (1.0 M in H_2O, 1.44 mL) in ethanol (2.5 mL) was degassed by vacuuming and purging several times with N_2. Next, Pd(dppf)Cl_2 (19.6 mg, 0.024 mmol) was added, and the reaction was heated to reflux for 4 hours. After this time, the reaction mixture was cooled to room temperature, diluted with water (10 mL) then extracted with CH_2Cl_2 (15 mL, 3x). The combined organics were washed with saturated brine (10 mL), dried over Na_2SO_4, concentrated *in vacuo*, and purified on a silica gel column (0-20% MeOH in CH_2Cl_2) yielding 1-{3'-amino-4'-fluoro-[1,1'-biphenyl]-4-carbonyl}-3-ethylpiperidin-3-ol (**23**) as an off-white foamy solid in 91% yield (150 mg, 0.438 mmol).

^{1}H NMR (500 MHz, $CDCl_3$): δ 7.53 - 7.46 (m, 4H), 7.04 – 7.97 (m, 2H), 6.89 – 6.86 (m, 1H), 4.33 (bs, 1H), 3.70 – 3.51 (bd, 3H), 3.10 – 3.00 (m, 2H), 1.91 – 1.83 (m, 1H), 1.76 (bs, 1H), 1.51 (bs, 4H), 0.92 (bs, 3H).

^{13}C NMR (126 MHz, $CDCl_3$): δ 171.5, 151.5 (d, $J_{(C-F)}$ = 240 Hz), 141.7, 136.7 (d, $J_{(C-F)}$ = 2 Hz), 134.58, 134.5, 134.4 (d, $J_{(C-F)}$ = 13 Hz), 127.5, 126.7, 117.3 (d, $J_{(C-F)}$ = 7Hz), 115.6 (d, $J_{(C-F)}$ = 3 Hz) , 115.4 (d, $J_{(C-F)}$ = 19 Hz), 70.3, 56.9, 51.8, 48.4, 42.6, 34.5, 32.9, 31.7, 22.1, 20.8, 6.9 (note: extra peaks are due to conformational restrictions).

^{19}F NMR (471 MHz, $CDCl_3$): δ -136.5

HRMS: $C_{21}H_{23}FN_2O_3$ Calc'd $[M+H]^+$: 343.1822, Found: 343.1806.

*1.1.5 Synthesis of N-{4'-[(3-ethyl-3-hydroxy-1-piperidyl)carbonyl]-4-fluoro-3-biphenylyl}chloroacetamide (**24**)*

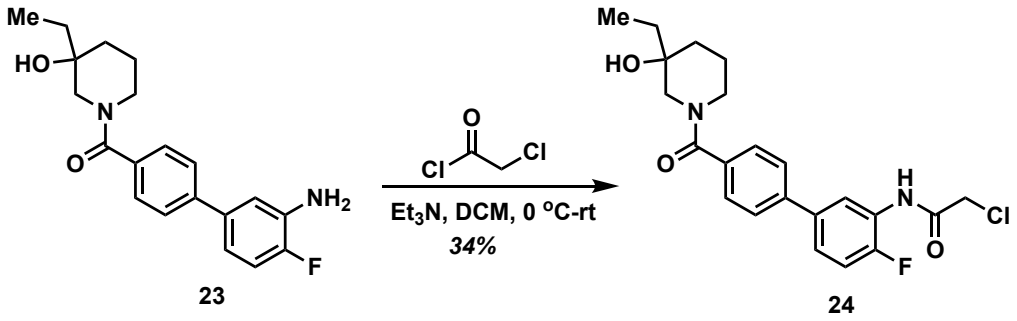

To a solution of 1-{3'-amino-4'-fluoro-[1,1'-biphenyl]-4-carbonyl}-3-ethylpiperidin-3-ol (**23**, 150 mg, 0.438 mmol) in CH_2Cl_2 (3 mL) was added Et_3N (79 µL, 0.569 mmol). The mixture was cooled to 0°C and to the reaction mixture was added chloroacetyl chloride (42 µL, 0.526 mmol) in CH_2Cl_2 (1 mL). The reaction mixture was stirred and allowed to warm to room temperature for 2 h. The reaction was monitored by TLC and upon consumption of starting material, the reaction mixture was concentrated *in vacuo*. The residue was redissolved in EtOAc (20 mL) and washed with water (15 mL) and brine (10 mL). The organic layer was dried over Na_2SO_4, concentrated in *vacuo* and then purified by flash chromatography (0-100% EtOAc in hexanes). The product was further purified by reverse-phase HPLC, as detailed in the General section, yielding N-{4'-[(3-ethyl-3-hydroxy-1-piperidyl)carbonyl]-4-fluoro-3-biphenylyl}chloroacetamide (**24**) as a white solid in 34% yield (62 mg, 0.148 mmol).

^{1}H NMR (500 MHz, MeOD): δ 10.2 (s, 1H), 8.22 (d, *J* = 5.5 Hz, 1H), 7.66 (d, *J* = 7.3 Hz, 2H), 7.53 – 7.47 (m, 3H), 7.41 – 7.38 (m, 1H), 4.39 (s, 2H), 4.34 (bs, 1H), 3.97 (bs, 0.5H), 3.54 (bs, 0.5H), 3.32 (bs, 1H), 3.14 - 3.05 (m, 1H), 1.75 – 1.21 (m, 6H), 0.89 (s, 1H), 0.70 (s, 2H).

^{13}C NMR (126 MHz, DMSO-d_6): δ 169.3, 168.9, 165.3, 153.4 (d, $J_{(C-F)}$ = 248 Hz), 139.6, 135.9 (d, $J_{(C-F)}$ = 3 Hz), 135.6, 128.2, 127.3, 126.5, 126.2, 125.9 (d, $J_{(C-F)}$ = 12 Hz), 124.1 (d, $J_{(C-F)}$ = 7 Hz), 122.3, 116.2 (d, $J_{(C-F)}$ = 20 Hz), 68.6, 56.4, 50.9, 47.4, 43.1, 41.9, 34.9, 32.2, 31.0, 21.8, 20.6, 7.1, 6.9 (note: extra peaks are due to conformational restrictions).

^{19}F NMR (471 MHz, CDCl3): δ -132.3

HRMS: $C_{22}H_{24}ClFN_2O_3$ Calc'd $[M+H]^+$: 419.1537, Found: 419.1523.

*1.1.6 Synthesis of -[4'-(3-ethyl-3-hydroxypiperidine-1-carbonyl)-4-fluoro-[1,1'-biphenyl]-3-yl]prop-2-enamide (**25**)*

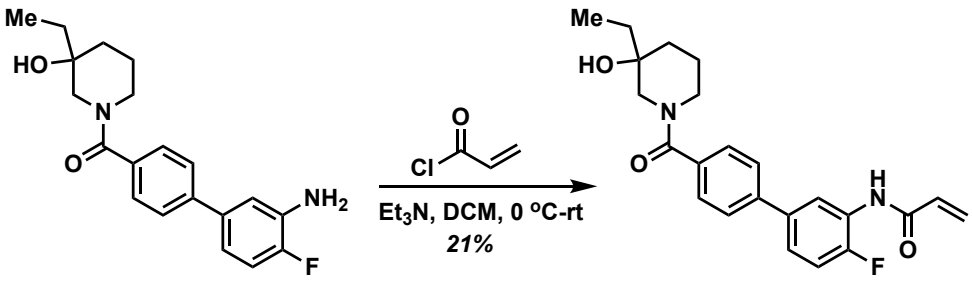

To a solution of 1-{3'-amino-4'-fluoro-[1,1'-biphenyl]-4-carbonyl}-3-ethylpiperidin-3-ol (**23**, 200 mg, 0.584 mmol) in CH_2Cl_2 (3 mL) was added Et_3N (106 µL, 0.759 mmol). The mixture was cooled to 0°C and to the reaction mixture was added acryloyl chloride (57 µL, 0.701 mmol). in CH_2Cl_2 (1 mL). The reaction mixture was stirred and allowed to warm to room temperature for 2 h. The reaction was monitored by TLC and upon consumption of starting material, the reaction mixture was concentrated *in vacuo*. The residue was redissolved in EtOAc (20 mL) and washed with water (15 mL) and brine (10 mL). The organic layer was dried over Na_2SO_4, concentrated in *vacuo* and then purified by flash chromatography (0-100% EtOAc in hexanes). The product was further purified by reverse-phase C18 column chromatography (0-100% MeCN in water) yielding N-[4'-(3-ethyl-3-hydroxypiperidine-1-carbonyl)-4-fluoro-[1,1'-biphenyl]-3-yl]prop-2-enamide (**25**) as a white solid in 21% yield (48 mg, 0.121 mmol).

^{1}H NMR (500 MHz, $CDCl_3$): δ 8.69 (d, *J* = 5.9 Hz,1H), 7.62 (s, 1H), 7.59 (d, *J* = 8.0 Hz, 2H), 7.49 (d, *J* = 7.9 Hz, 2H), 7.29 – 7.26 (m, 1H), 7.18 – 7.14 (m, 1H), 6.48 (d, *J* = 16.8 Hz, 1H), 6.35 – 6.30 (m, 1H), 5.83 (d, *J* = 10.2 Hz, 1H), 4.33 (bs, 1H), 3.70 – 3.52 (m, 1H), 3.11 – 3.01 (m, 2H), 2.10 – 1.53 (m, 8H), 0.99 – 0.85 (m, 3H).

^{13}C NMR (126 MHz, $CDCl_3$): δ 171.6, 171.1, 163.6, 152.4 (d, *J* = 245 Hz), 141.2, 135.7 (d, $J_{(C-F)}$ = 248 Hz), 130.7, 128.3, 127.5, 126.9, 126.3 (d, $J_{(C-F)}$ = 10 Hz), , 123.0 (d, $J_{(C-F)}$ = 7Hz), 120.9, 115.1 (d, $J_{(C-F)}$ = 20 Hz), , 70.4, 60.3, 57.1, 53.3, 51.8, 48.4, 42.6, 34.5, 32.8, 31.8, 29.6, 22.2, 20.9, 14.1, 6.9 (note: extra peaks are due to conformational restrictions).

^{19}F NMR (471 MHz, CDCl3): δ -133.1

HRMS: $C_{23}H_{25}FN_2O_3$ Calc'd $[M+H]^+$: 397.1928, Found: 397.1910.

1.2 Computational modeling and screening

1.2.1 Molecular dynamics simulations identifying allosteric site and virtual screening

Using POVME3.0 program for active-site-shape-based clustering, eight A3Bctd conformations were selected as cluster representatives of eight clusters from our prior molecular dynamics simulations of apo and nucleic acid-bound A3Bctd.[2,3] Each A3Bctd conformation was then evaluated for binding hot spots with FTMap.[4] FTprod was then used to process and compare all FTMap data.[5] Cluster0 and Cluster6 representative frames were selected for virtual screening against the active site and the putative allosteric site as they had the most-populated FTMap probes at those sites, respectively. Schrodinger's Glide was then used in standard precision mode to virtually screen ChemBridge Diversity Set of 110,000 compounds for the two sites.[6,7] A metal constraint was used for the zinc at the active site during active site virtual screen. Docking scores and ligand efficiencies were used to rank and select compounds for experimental testing.

1.2.2 Ligand parameterization

Parameters for **10** were generated with the Antechamber module of Amber18[8] using the Generalized Amber Force Field[9,10] with RESP HF 6-31G* charges calculated by Gaussian program.[11] The initial pose of compound **10** in A3B cluster 6 virtual screening was used as an input for induced fit docking to define the binding site and pose of the ligand. Using the induced-fit docking module of Schrodinger (version 2022u1), twenty-one different poses of A3B in complex with **10** were generated. Nine of the highest scoring poses (that had better than -319 kcal/mol) of **10** were selected and simulated for 100 ns for 3 replicates each using the Amber MD engine. After 100ns, the three most stable poses (poses 3, 6, and 8) were simulated for an additional 400 ns, for a total of 500 ns (**Figure S82**). Of these three poses, pose 6 displayed the highest stability at the allosteric site throughout all replicates and was simulated for a total of 1 μs x three replicates.

*1.2.3 Molecular dynamics simulations with **10** and analysis*

Simulations of A3Bctd and A3A with nucleotides were parameterized using the AMBER FF19SB forcefield for protein atoms, and OL15 forcefield for DNA atoms. The A3Bctd starting structure was based on the 5TD5 PDB structure, with amino acid substitutions returned to wild type amino acid sequence as described in previous work.[12,13] A3A starting structure was based on the PDB structure 5SWW, and missing loops and mutated residues were returned to wild type amino acid sequence.[13] The catalytic zinc was modeled using the Cationic Dummy Atom Model, and the zinc was modeled as being bound to an $^{-}$OH ion to represent the activated water molecule as is present

in A3Bctd pre-catalysis. All systems were solvated in a TIP3P water box with a buffer of 10 Å, and ions were added to neutralize charge and obtain a concentration of 0.150 M sodium chloride solution. PROPKA was used to predict the protonation states of the sidechains.[14,15] Cysteine residues, as they were of particular interest for sidechain dynamics, were not locked into disulfide bonds. Ambertools' tLeap was used to build the final topology and coordinate files necessary for simulations.[8]

A3Bctd and A3A in complex with the **10** (and without ssDNA) were simulated for a total of 3 μs of simulation time per system. Each system underwent sequential energy minimization, followed by gradual heating and equilibration according to the following protocol. The initial energy minimization was performed on all atom excluding hydrogen with a restraint weight of 100.0 kcal/mol/Å^2 for 500 cycles. A second minimization of 500 cycles restrained all atoms except the protein including the ligand using a reduced restraint weight of 50.0 kcal/mol/Å^2. A third minimization run allowed the sidechains to minimize, restraining only backbone atoms (CA, C, N, O) with a restraint weight of 100.0 kcal/mol/Å^2. The fourth and final minimization run allowed an unrestrained minimization of all atoms in the system. It was conducted with 1,000,000 cycles using constant volume periodic boundary conditions using a 10Å cutoff for non-bonded interactions. In the heating step 250, positional restraints were applied to protein atoms, excluding hydrogen with a restraint weight of 2.0 kcal/mol/Å^2. The simulation started at 0.0 K and gradually heated to 310.0 K using a Langevin equilibration scheme (Nosé-Hoover thermostat). In the subsequent equilibration steps performed in three stages, each 250 ps, we utilized isotropic pressure control (ntb=2, ntp=1, pres0=1.0) to maintain a target pressure. In subsequent equilibration stages, the Nosé-Hoover thermostat-controlled temperature fluctuations, keeping the system at a constant temperature of 310.0 K using a relaxation parameter of 5.0. Nonbonded interactions were maintained with a cutoff of 10 Å, and positional restraints were released for increased system flexibility. A restraint was applied to the protein atoms and ligand atoms, excluding hydrogen with a restraint weight of 3.0 kcal/mol/Å^2. The final equilibration ran simulation ran for 125,000 timesteps with a timestep of 2 fs.

Each system (A3Bctd-**10**, A3Bctd-**10**-DNA, A3A-**10**, A3A-**10**-DNA) was simulated for 1 μs x 3 replicates of unrestrained MD simulations in an NPT ensemble at 310K with a timestep of 2 fs using the Amber22 Molecular Mechanics Engine.[8] Hydrogen bonding information and atomic distances were calculated using CPPTRAJ.[16] Contact analysis was performed using the MDTraj package Pycontact[17] with a maximum atom-atom distance cutoff of 5.0 Å, an angle cutoff for hydrogen bonds of 120 degrees, and a distance cutoff for hydrogen bonds of 2.5 Å as

recommended by PyContact. The same protocol was repeated for A3Bctd and A3A in complex with the ligand in addition to ssDNA for a total of 12 μs of simulation time. Simulations were performed on a mix of computing resources that include our own GPU clusters as well as the NCSA Delta supercomputer resource.

1.3 Protein expression and purification

The A3Bctd protein utilized in these studies was expressed in *Sf9* insect cells and purified by affinity chromatography by GenScript Biotech Corporation. The protein construct contains the sequence of A3B amino acid (aa) 193-382, followed by a non-cleavable MycHis$_6$ tag, based on Uniprot accession: Q9UH17-1. Upon delivery of the protein, >95% purity was established with a 4-12% polyacrylamide gel stained with Coomassie blue, and the protein kinetic activity was confirmed. A3A was expressed in HEK293T mammalian cells, according to a previous published protocol.[13] A3A was based on Uniprot accession: P31941-1 encompassing the full sequence (amino acids 1-199).

1.4 Deaminase assay initial screening

Assays were performed as previously described,[18] with a few modifications. Compounds were suspended in DMSO at 20 mM stock concentrations. Compounds were diluted to 1.5 mM in A3 assay buffer (50 mM Tris, pH 7.4, 100 mM NaCl, 1 mM EDTA, 10% glycerol, 0.5% Triton X-100), and 10 μL was added to each respective well of a Nunc 384-well black flat-bottom plate. Recombinant A3Bctd was diluted to 10 ng/μL in A3 assay buffer, and A3A was diluted to 1 ng/μL, and 10 μL of diluted protein was added to plate wells. Compound and protein were incubated at 37°C. After 30 minutes, 10 μL of oligo substrate (5′-FAM-AAATAT**C**CCAAAGAGAGA-TAMRA-3′, purchased from IDT), diluted to 0.2 μM in 1x TE buffer, was added to all wells, then incubated for 30 minutes at 37°C. Next, 3 μL of 4 M NaOH was added to hydrolyze the ssDNA substrate, which was incubated for 30 minutes at 37°C, then neutralized by dilution with 2 M Tris, pH 7.9 (40 μL). The plates were cooled to 4°C before reading fluorescence on a Synergy H1 microplate reader (BioTek), with an excitation wavelength of 490 nm and an emission wavelength of 520 nm. The ChemBridge ID and associated compound numbering are described in **Table S1**. Activity was normalized to the DMSO control, and background was subtracted through monitoring the fluorescence of wells containing only the oligo nucleotide. Data were processed in Microsoft Excel and analyzed using Prism v9.1.2 (GraphPad). IC_{50} values were determined by a non-linear fit

using the [Inhibitor] vs. response – Variable slope (four parameter) model. Data points and error bars are the mean and standard deviation of N = 3 technical replicates.

1.5 Repurchased compound screening

Compounds determined to be hits in the initial screening process were repurchased from Hit2Lead. Compounds were purified by preparative HPLC, then reanalyzed by analytical HPLC for purity. Of the 21 compounds repurchased, 17 compounds were able to be purified to >95% by analytical HPLC analysis at 215 and 254 nm. Purified compounds were screened as described in section 1.4, with minor experimental changes. Recombinant A3Bctd was diluted to 20 ng/µL instead of 10 ng/µL, the oligo was 5′-labeled with AlexaFluor488 instead of FAM, and the oligo was diluted to 0.3 µM instead of 0.2 µM. The full reaction (compound, protein, and oligo) was incubated for 45 minutes, instead of 30 minutes.

1.6 UDG control inhibition assay

The UDG control assay was performed similar to the deaminase assay as described in **1.4**. Compounds were diluted to 3 mM in A3 assay buffer, and 10 µL of each compound was added to the plate. To prepare the UDG (5 U/mL, New England BioLabs), 1 µL of stock UDG was diluted to 2 mL in A3 assay buffer, and 10 µL of diluted UDG was added to the appropriate wells. Compounds and UDG were incubated for 30 minutes at 37°C. Meanwhile, the oligo substrate (5′-FAM-AAATAT**U**CCAAAGAGAGA-TAMRA-3′, purchased from IDT) was diluted to 0.2 µM in 1X TE buffer, then 10 µL was added to each well and the reaction was incubated for 45 minutes. The reaction was quenched with the addition of 3 µL of 4 M NaOH, incubated for 30 minutes at 37°C, then cooled to 4°C before reading on a Synergy H1 microplate reader (BioTek). Data were analyzed using Prism v9.1.2 (GraphPad), with a non-linear fit using the [Inhibitor] vs. response – Variable slope (four parameter) model. Data points and error bars are the mean and standard deviation of N = 3 technical replicates.

1.7 Fluorescence polarization assay

Competitive fluorescence polarization assay was adapted from previous direct binding fluorescence polarization assays developed by our group.[19,20] A3Bctd was diluted to 2.7 µM and tracer (5′-AlexaFluor546-ATTATGTCGTTGGATTTATTT-3′) was diluted to 15 nM in a 50:50 mix of protein buffer (25 mM Tris HCl pH 6.0, 75 mM NaCl, 0.5 mM EDTA) and DNA buffer (10 mM Tris HCl pH 6.0, 0.5 mM EDTA). In a black low volume Corning 384-well plate, 20 µL of this

premixed solution was added to appropriate wells. Compounds were dispensed with an HP D300 digital dispenser with the DMSO normalized to 3%. Plates were shaken on an orbital rotating block at 1500 rpm for 1 minute to mix, then centrifuged at 1000 rpm for 1 minutes. The reaction was incubated for 20 minutes at room temperature, then read on a Tecan Spark, with a monochromator-based excitation wavelength of 530 $\pm$ 5 nm and a filter-based emission wavelength of 620(10) nm. Anisotropy values were background corrected based on the average of $N \geq 8$ technical replicates of wells containing tracer only. Data were analyzed using Prism v9.1.2 (GraphPad), with a non-linear fit using the specific binding with Hill slope model. Data points and error bars are the mean and standard deviation of N = 3 technical replicates.

1.8 CPMG NMR

This assay was performed similar to our previously reported protocol.[21] Protein stocks were exchanged into 50 mM NaH_2PO_4/Na_2HPO_4, pH 7.5, 150 mM NaCl, 10% D_2O, then concentrated via molecular weight cutoff filter (3 kDa, 0.5 mL, MilliporeSigma). Protein concentration was assessed by BCA, then diluted to 20.2 µM in buffer. Compound stocks were diluted to 10 mM from 100 mM in DMSO-d_6. To 49.5 µL of 20.2 µM A3Bctd protein was added 0.5 µL of 10 mM compound, for a final protein concentration of 20 µM and a final compound concentration of 100 µM. For compound alone spectra, 0.5 µL of the 10 mM DMSO-d_6 compound stock was added to 49.5 µL of buffer. Samples were prepared in 1.5 mL Eppendorf tubes, vortexed, and briefly centrifuged using a tabletop mini centrifuge (7000 rpm, 30 sec), prior to being added to 1.7-mm NMR tubes.

Spectra were acquired on a Bruker 700-MHz Avance III with a CryoProbe, with an 800 ms T_2 relaxation delay filter in the CPMG pulse sequence. Data were processed in MestreNova v14.1.0 (Mestrelab Research) software. After processing, the DMSO signal in overlaid spectra were normalized to each other. The selected peak was measured by the intensity of the signal in both spectra, and the intensity of the peak in the protein + compound sample was divided by the intensity of the peak in the compound alone sample, then multiplied by 100 to give the relative signal attenuation as a percentage.

1.9 Intact protein mass spectrometry

Protein samples were desalted into assay buffer (10mM Tris, pH 8.0), and concentration was determined via nanodrop. Protein concentration was adjusted to 26.3 µM using assay buffer, and 47.5 µL of this solution was transferred to a 0.6 mL Eppendorf tubes. Stock solutions of

compounds **25** (chloroacetamide) and **26** (acrylamide) were diluted in DMSO at the following concentrations (10 mM, 5 mM, 2.5 mM, 0.5 mM). 2.5 µL of the DMSO stocks were added to the 47.5 µL solution of protein (final volume = 50 µL, final protein concentration = 25 µM). The final concentrations of the compounds were 500 µM (10 mM stock), 250 µM (5 mM stock), 125 µM (2.5 mM stock), and 25 µM (0.5 mM stock). These solutions were then left to incubate for one or three hours at 37 °C. After incubation, these solutions were then desalted using 0.5 mL 7 kD Zeba desalting spin columns (ThermoScientific). Protein samples were analyzed with an UltiMate™ 3000 liquid chromatography system (ThermoFisher) in-line with an Orbitrap Elite (ThermoFisher) hybrid mass spectrometer. The LC eluent system was water +0.5% formic acid (Eluent A) and acetonitrile +0.5% formic acid (Eluent B). The LC column was a Zorbax 300 SB-C3 Rapid Resolution HD column, 2.1x100 mm, 1.8 µm particle size (Agilent). The LC gradient (400 µL/min flow rate, 10 µL injection) total time was 4 minutes, with the following steps: 0 min, 20% B; 0.75 min, 100% B; 1.5 min, 20% B; 3 min, 100% B; 3.5 min, 100% B; 4.0 min, 20% B. The first ramp up and down was used to desalt the sample, and the column flow was sent to waste for the first 1.5 min; the second ramp up resulted in elution of the protein. The Orbitrap settings were as follows: FTMS analyzer in positive mode, 30,000 resolution, m/z scan range of 600-2000. Resulting spectra were deconvoluted with the Protein Deconvolution software (ThermoFisher) with the following settings: m/z range = 800-2000, S/N threshold = 3, relative abundance threshold = 5. Percent adduction was calculated by dividing the intensity of the adduct species by the sum of the intensities, multiplied by 100. % Adducted = [(intensity of mass adduct species)/(intensity of unadducted species + intensity of mass adduct species)] x 100. N = 2 biological replicates.

1.10 Bottom-up protein digestion with 25

Incubation and desalt of A3A and A3Bctd was conducted as described in **1.9**, where A3A was incubated with 250 µM and A3Bctd with 500 µM **24** and then desalted with 0.5 mL 7kD Zeba desalting spin columns. The solutions were then dried via SpeedVac overnight. Roughly 5 µg of each protein sample were separately reconstituted in 20 µL of denaturing buffer (8 M Urea, 50 mM DTT, 100 mM NH_4HCO_3) and incubated for one hour at 37 °C to denature the proteins. 20 µL of 50 mM iodoacetamide (IAA) was added to each of the samples and incubated in the dark at room temperature for 30 minutes, to alkylate exposed cysteines. 160 µL of dilution buffer (50 mM NH_4HCO_3, 1 mM $CaCl_2$) and 20 µL of acetonitrile was added to each sample to reduce the concentration of Urea. Glu-C endoproteinase (ThermoScientific) was reconstituted in MilliQ water at a concentration of 0.01 µg/µL, and 10 µL were added to each sample for a final amount of 0.1 µg (1:50, enzyme:protein). This solution was then left to incubate overnight at 37 °C. The next

day 10 µL of 0.01 µg/µL, for a final amount of 0.1 µg (1:50, enzyme:protein) of Trypsin Gold (Promega) was added to samples and left to incubate for four hours at 37 °C. 20 µL of glacial acetic was then added to quench the reaction, and then the samples were concentrated to 80 µL using a SpeedVac. The solutions were then adjusted to 0.5% TFA, prior to desalting by manufacture protocol using 100 µL Pierce C18 Tips (ThermoScientific). Samples were then evaporated to dryness overnight using SpeedVac. Samples were reconstituted in 2% acetonitrile, 98% water containing 0.1% formic acid, at 0.2 µg/µL. 3µL of sample were loaded onto a home-packed analytical C18 reverse phase column with a 10 µm emission tip (75 µm × 200 mm [New Objective, Woburn, MA], with Luna C18 5 µm particles [Phenomenex, Torrance, CA]) via UltiMate™ 3000 liquid chromatography system (ThermoScientific). Peptides were eluted with buffer A (0.1% formic acid in water) and buffer B (0.1% formic acid in acetonitrile) with the following gradient profile: 0-5.5 min for loading, 2% B, flowrate 1 µL/min; 6-12 min, 2%-10% B, 0.3 µL/min; 12-52 min, 10%-25% B, 0.3 µL/min; 52-57 min, 25%-40% B, 0.3 µL/min; 57-58 min, 40%-85% B, 0.3 µL/min; 58-62 min 85% B, 0.3 µL/min; 62-63 min, 85%-2% B, 0.3 µL/min; 63-65 min, 2% B, 1.0 µL/min. Mass spectrometry was obtained on an Orbitrap Fusion Tribrid Mass Spectrometer (ThermoFisher) in positive nanospray ionization mode. The mass spectrometer conditions were: spray voltage 2.2 kV, ion transfer tube temperature 300 °C. MS survey scans were performed with a cycle time of 3 s. After each survey scan, the 10 to 20 most abundant precursor ions with $z > 1$ were selected for fragmentation using higher energy collisional dissociation (HCD). MS^1 resolution was at 120,000 with a scan range of 375-1500. MS^2 resolution was fixed at 15,000. N = 3 biological replicates of the digestion and mass spectrometry analysis were performed. The resulting data was analyzed using Proteome Discoverer 3.0 (ThermoScientific) for chromatogram processing and fragment spectra isolation. Peptides were analyzed by referencing the A3Bctd and A3A protein sequences from a FASTA file created in-house, with cysteine carbamidomethylation and the compound **24** molecular weight set as dynamic modifications.

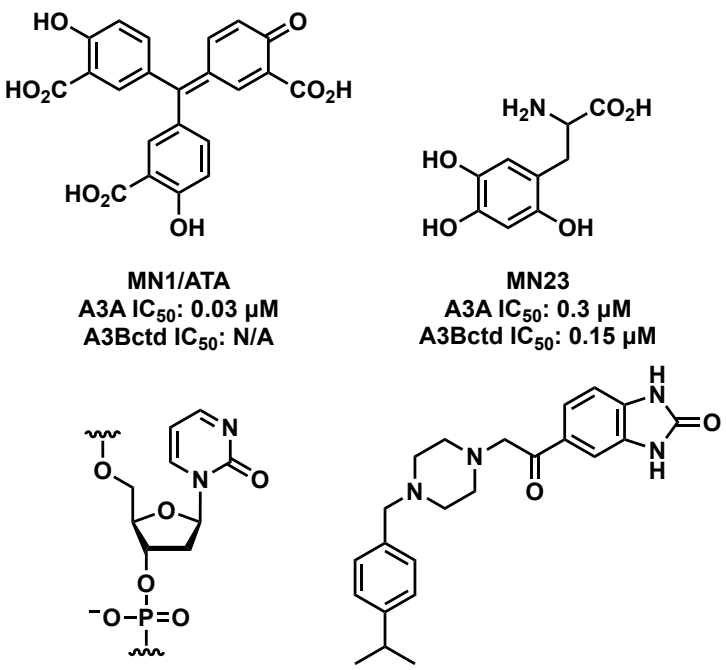

Figure S1. Figures of known A3A/A3B inhibitors, along with their published potencies. MN1 and MN23 were used as positive controls for screening.

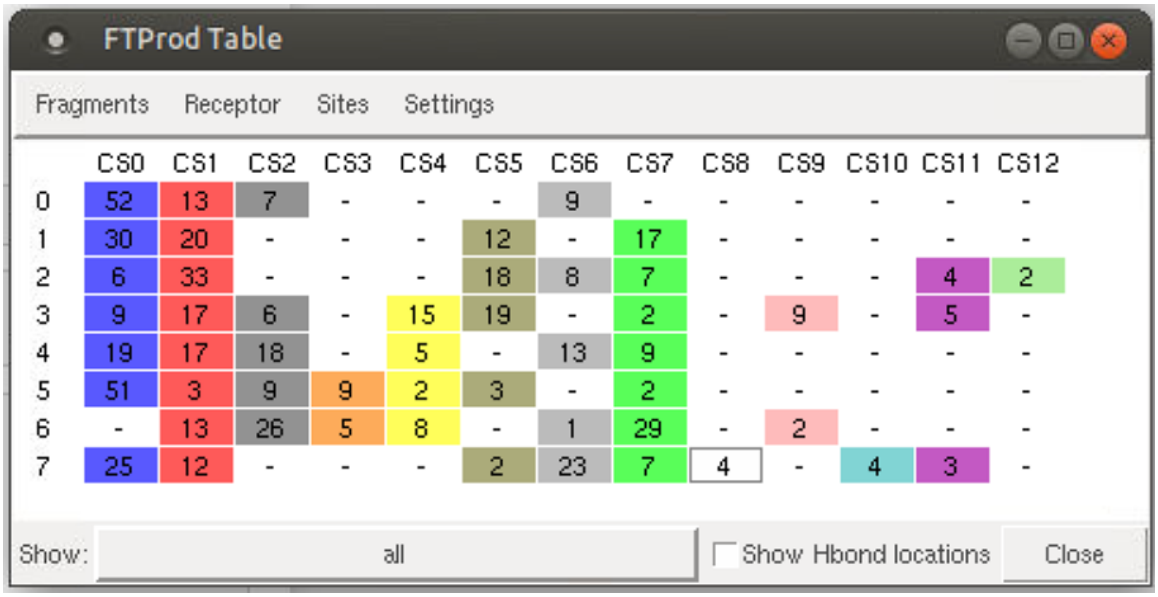

	CS0	CS1	CS2	CS3	CS4	CS5	CS6	CS7	CS8	CS9	CS10	CS11	CS12
0	52	13	7	-	-	-	9	-	-	-	-	-	-
1	30	20	-	-	-	12	-	17	-	-	-	-	-
2	6	33	-	-	-	18	8	7	-	-	-	4	2
3	9	17	6	-	15	19	-	2	-	9	-	5	-
4	19	17	18	-	5	-	13	9	-	-	-	-	-
5	51	3	9	9	2	3	-	2	-	-	-	-	-
6	-	13	26	5	8	-	1	29	-	2	-	-	-
7	25	12	-	-	-	2	23	7	4	-	4	3	-

Figure S2. FTProd results showing the distribution of binding hot spots for eight cluster representative A3Bctd structures (from 0 to 7). Cluster0 and Cluster6 have the largest and second largest FTMap probe populations for the active site (CS0) and the putative allosteric site (CS7), respectively. Number of FTMap probes for each site is tabulated in the below table. CS stands for consensus site.

Table S1. Compounds selected as hits from primary screening and their individual biological replicate activity values (% residual deaminase activity). [⊥]In the second replicate of the primary screen, the column containing this compound had a missed liquid addition – therefore all the values for the compounds in that row were excluded from analysis. Out of an abundance of caution, the compound was selected for further confirmation testing.

Compound	ChemBridge ID	Replicate 1	Replicate 2
4	33616296	16.4	24.2
5	69830916	7.4	15.0
7	54214567	23.8	N/A[⊥]
8	21647897	17.7	12.2
10	22128731	-8.1	1.1
11	9123731	23.7	22.8
14	81965134	19.8	7.1
17	79828650	18.1	27.5
27	64062448	19.8	21.9
28	7741584	12.4	7.3
29	33650212	14.6	24.7
30	27048541	-4.6	0.3
31	93915334	-3.6	-3.2
32	15818196	-4.3	2.4
33	82460954	-5.9	-1.2
34	44060191	-4.7	-3.1
35	49253890	18.5	10.3
36	5541604	3.5	14.1
37	7954304	5.4	5.8
38	7740811	-0.4	1.6
39	7961510	3.0	2.8
40	9152831	16.4	29.5
41	9287220	6.6	7.4

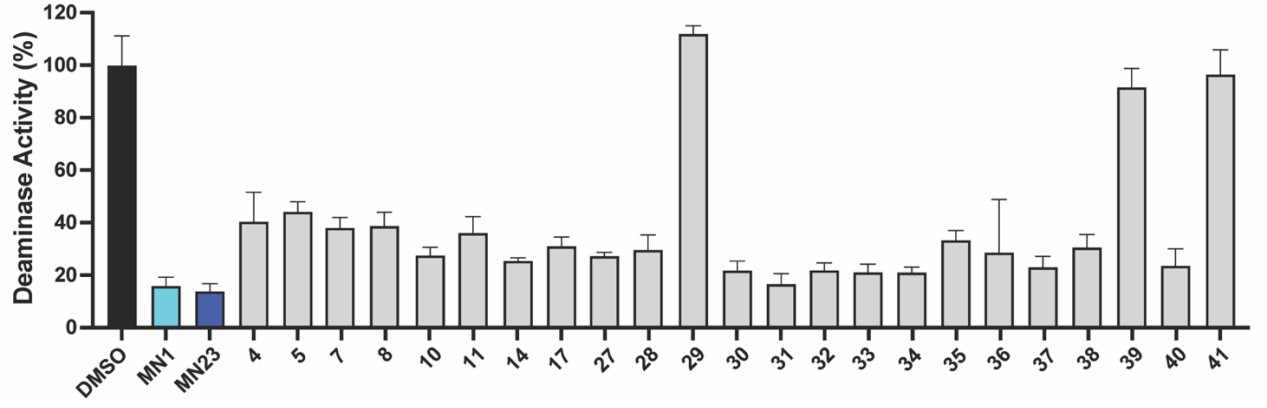

Figure S3. Single point re-testing of compounds selected as hits from the initial screening. Compounds tested at 500 μM concentration in the fluorescence-based activity assay against A3Bctd. Bars are the mean of N ≥ 3 technical replicates, errors bars are the standard deviation.

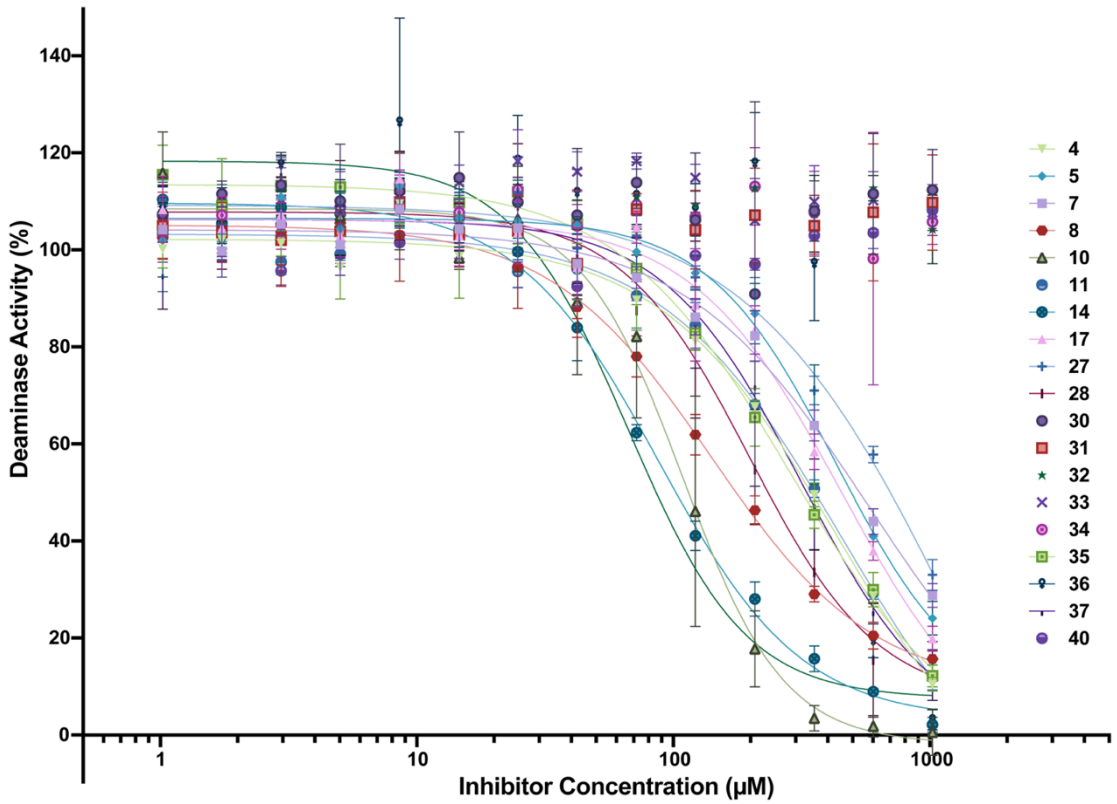

Figure S4. Dose response testing of compounds that confirmed in the single point response (**Figure S3**).

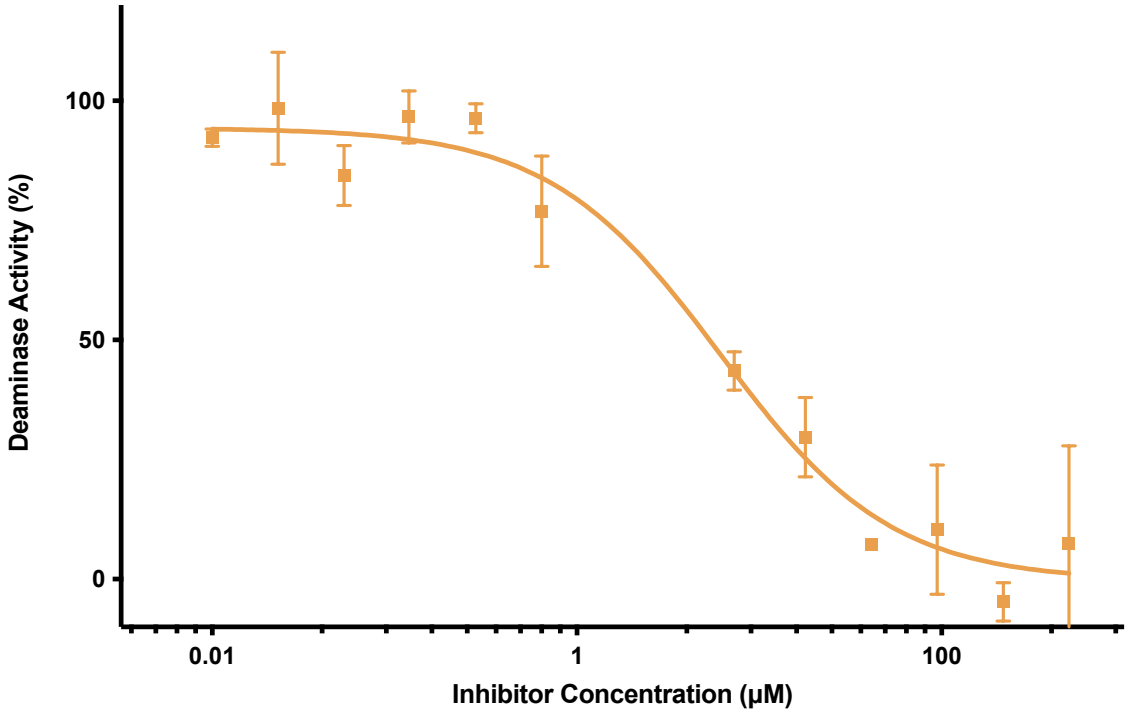

Figure S5. Dose response of unpurified **38**.

Table S2. Purities of repurchased compounds analyzed by analytical HPLC after preparative HPLC purification. ****27** hydrolyzed quickly in water. After every purification, as soon as the sample was dissolved in water to analyze by HPLC, the sample was already degraded to <95% purity, see HPLC trace below. [§]**28** precipitates in water when diluted to be analyzed by HPLC.

Compound #	215 nm purity (%)	254 nm purity (%)	Compound #	215 nm purity (%)	254 nm purity (%)
1	95.2	97.2	11	99.7	99.2
2	99.5	99.9	12	98.6	96.8
3	99.6	99.8	13	98.1	98.3
4	97.8	99.1	14	99.6	99.9
5	95.7	95.1	15	97.4	98.4
6	99.6	99.9	16	97.9	98.5
7	95.7	96.0	17	95.8	95.5
8	98.7	98.7	27	N/A**	N/A**
9	95.8	98.6	28	N/A[§]	N/A[§]
10	95.1	98.2			

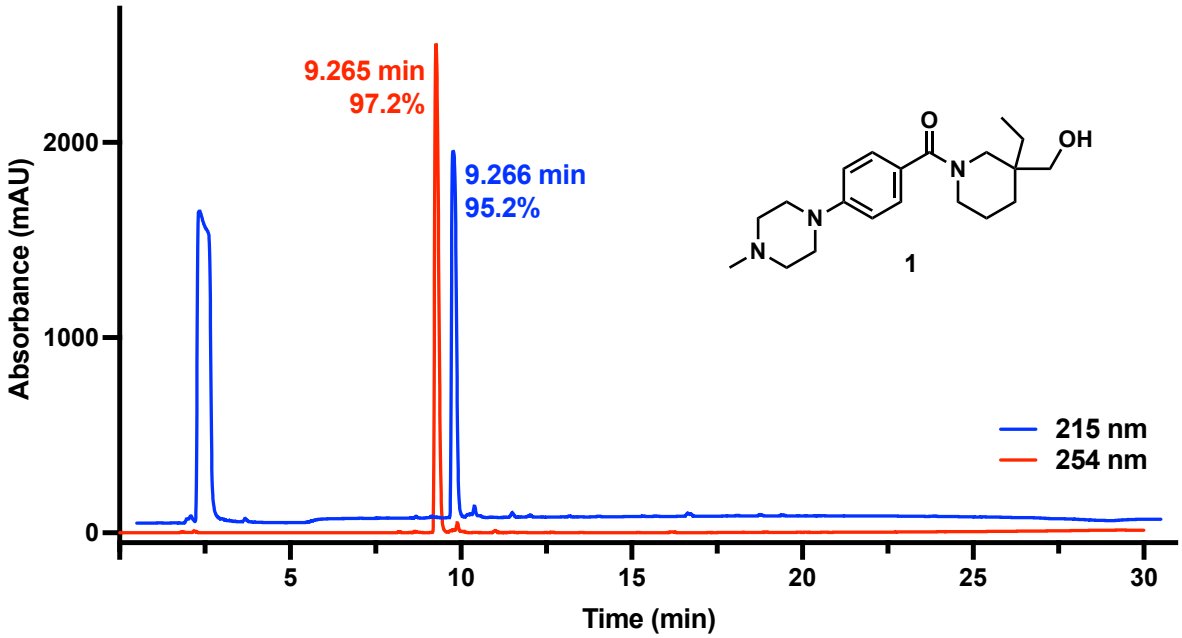

Figure S6. HPLC trace of **1**. Peak at RT = 2.5 min is DMSO-d_6.

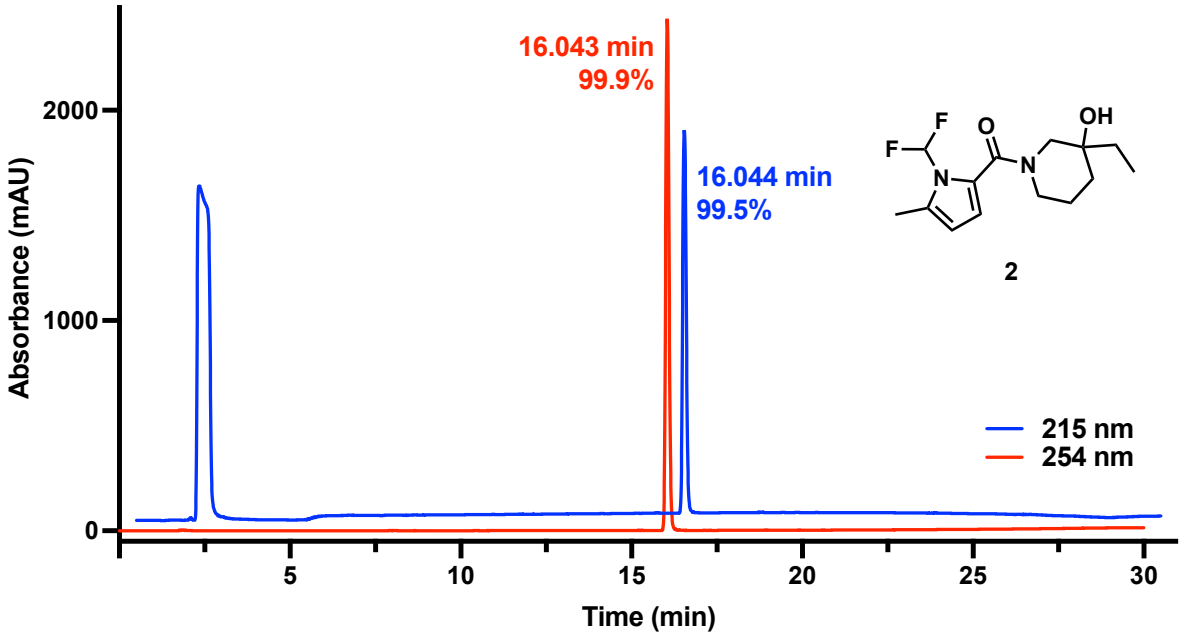

Figure S7. HPLC trace of **2**. Peak at RT = 2.5 min is DMSO-d_6.

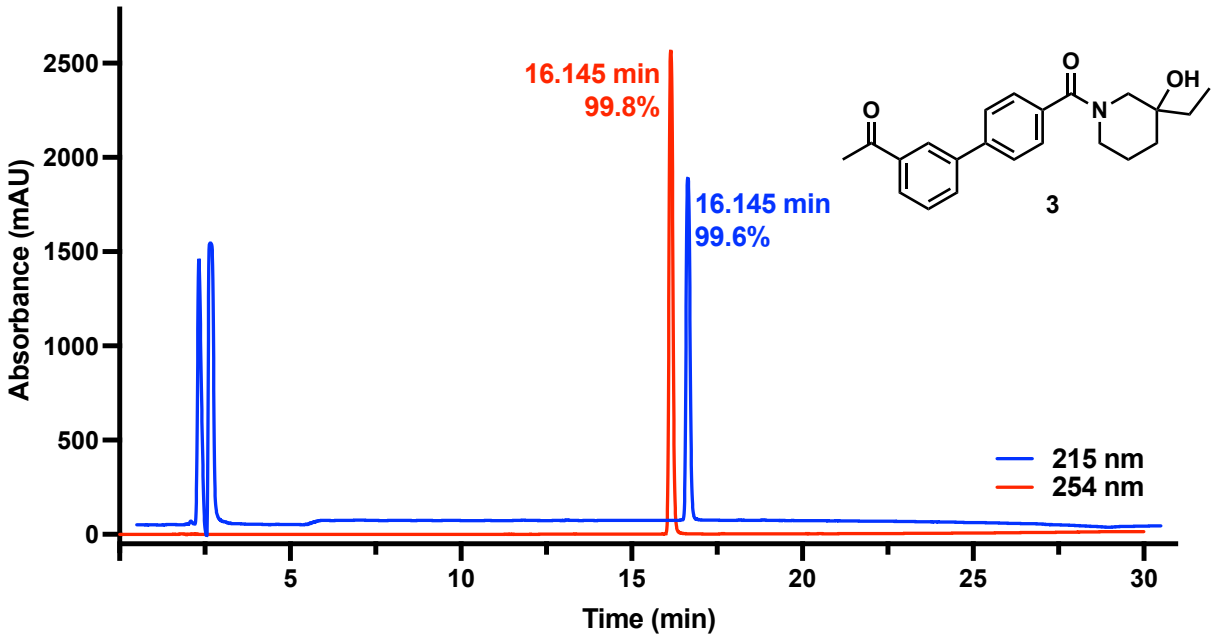

Figure S8. HPLC trace of **3**. Double peak at RT = 2.5 min is DMSO-d_6.

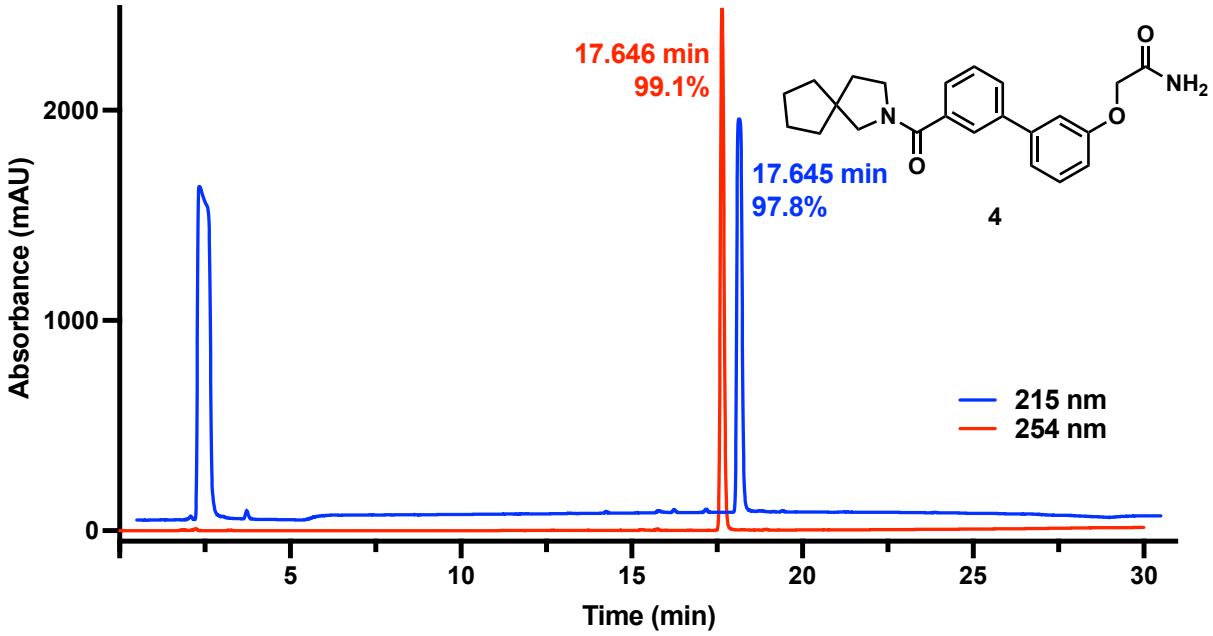

Figure S9. HPLC trace of **4**. Peak at RT = 2.5 min is DMSO-d_6.

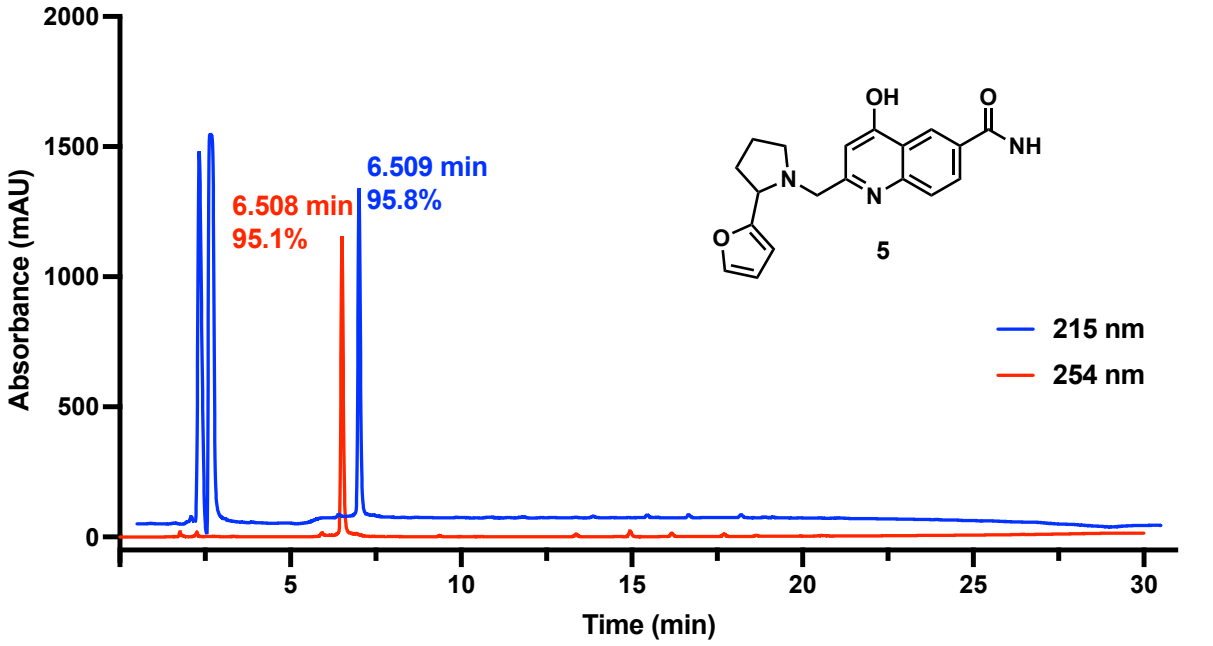

Figure S10. HPLC trace of **5**. Double peak at RT = 2.5 min is DMSO-d_6.

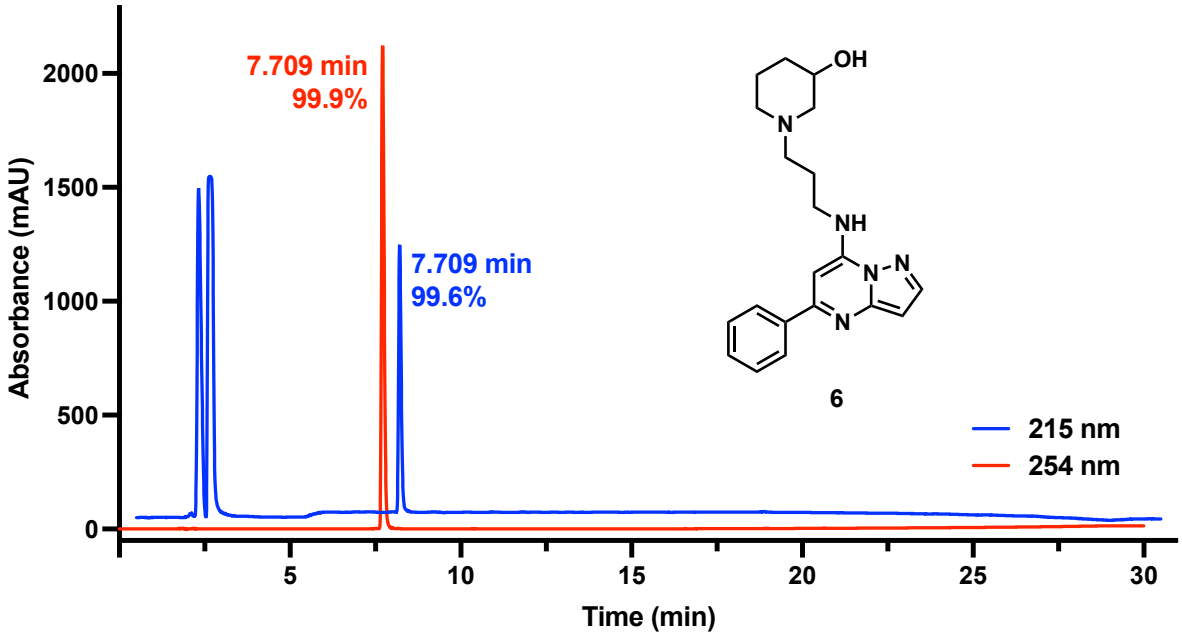

Figure S11. HPLC trace of **6**. Double peak at RT = 2.5 min is DMSO-d_6.

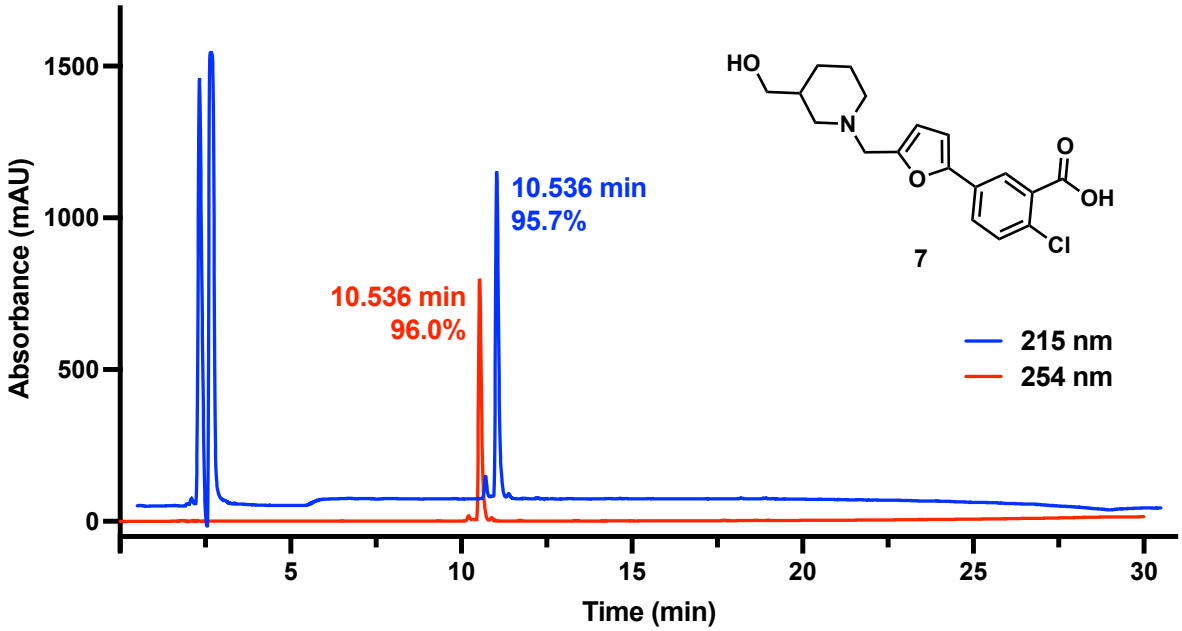

Figure S12. HPLC trace of **7**. Double peak at RT = 2.5 min is DMSO-d_6.

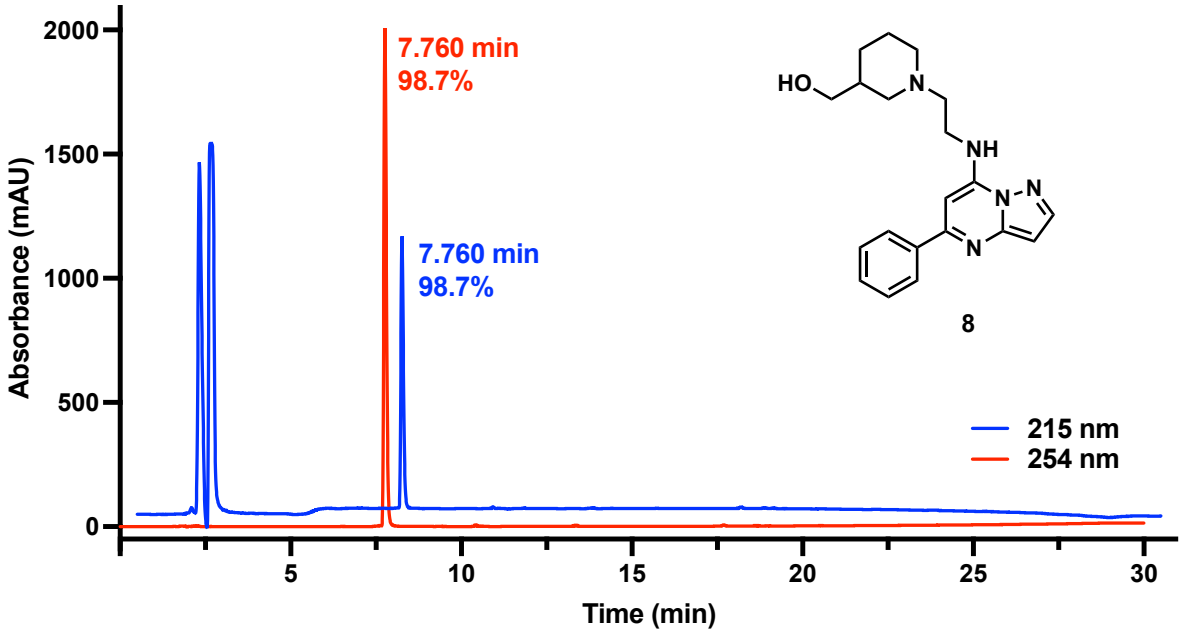

Figure S13. HPLC trace of **8**. Double peak at RT = 2.5 min is DMSO-d_6.

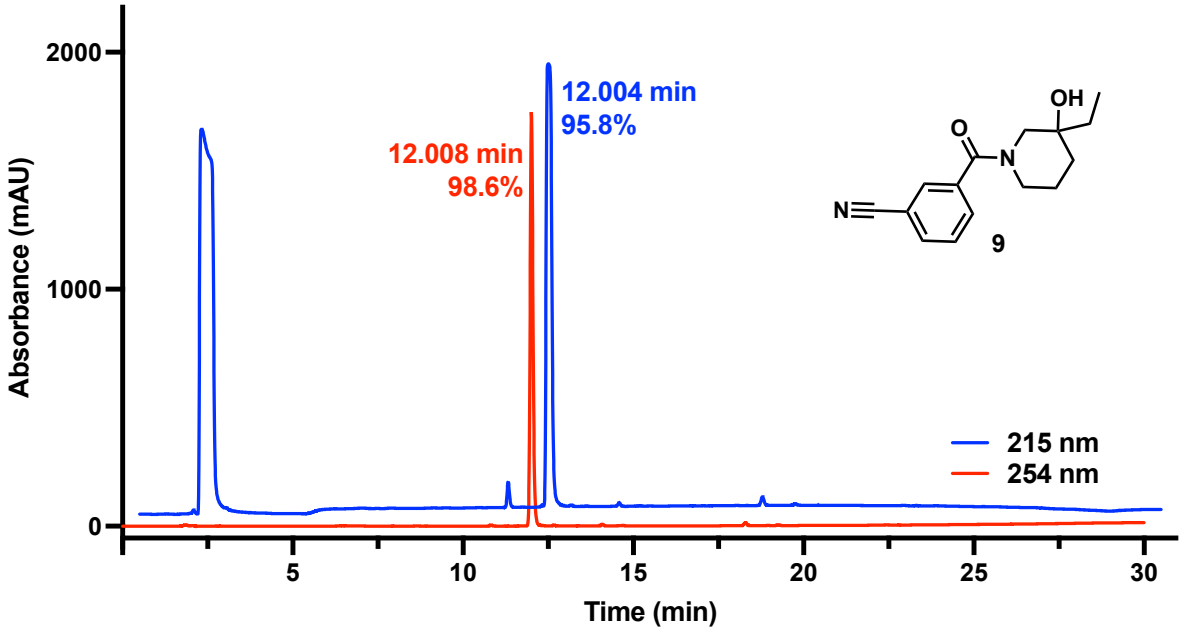

Figure S14. HPLC trace of **9**. Peak at RT = 2.5 min is DMSO-d_6.

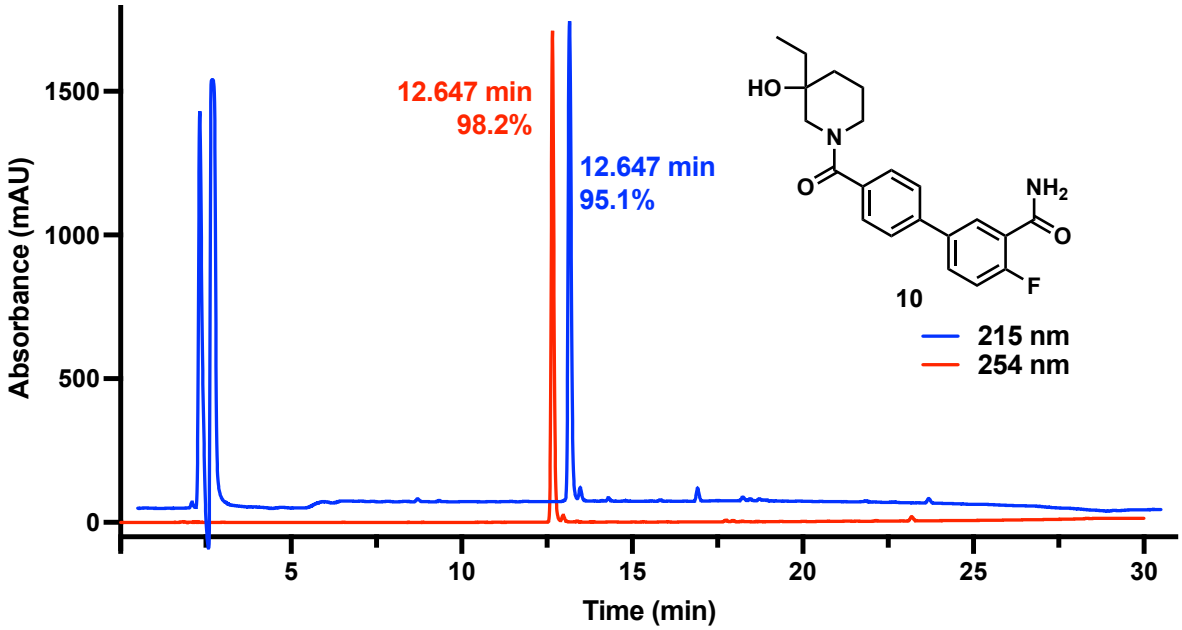

Figure S15. HPLC trace of **10**. Double peak at RT = 2.5 min is DMSO-d_6.

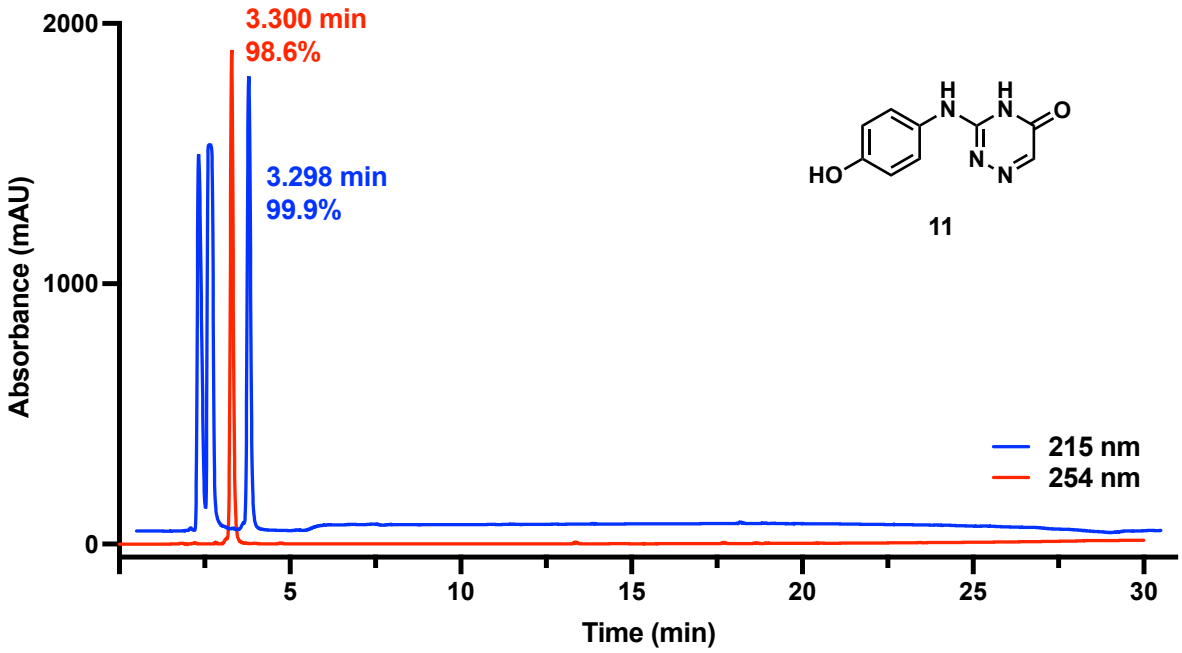

Figure S16. HPLC trace of **11**. Double peak at RT = 2.5 min is DMSO-d_6.

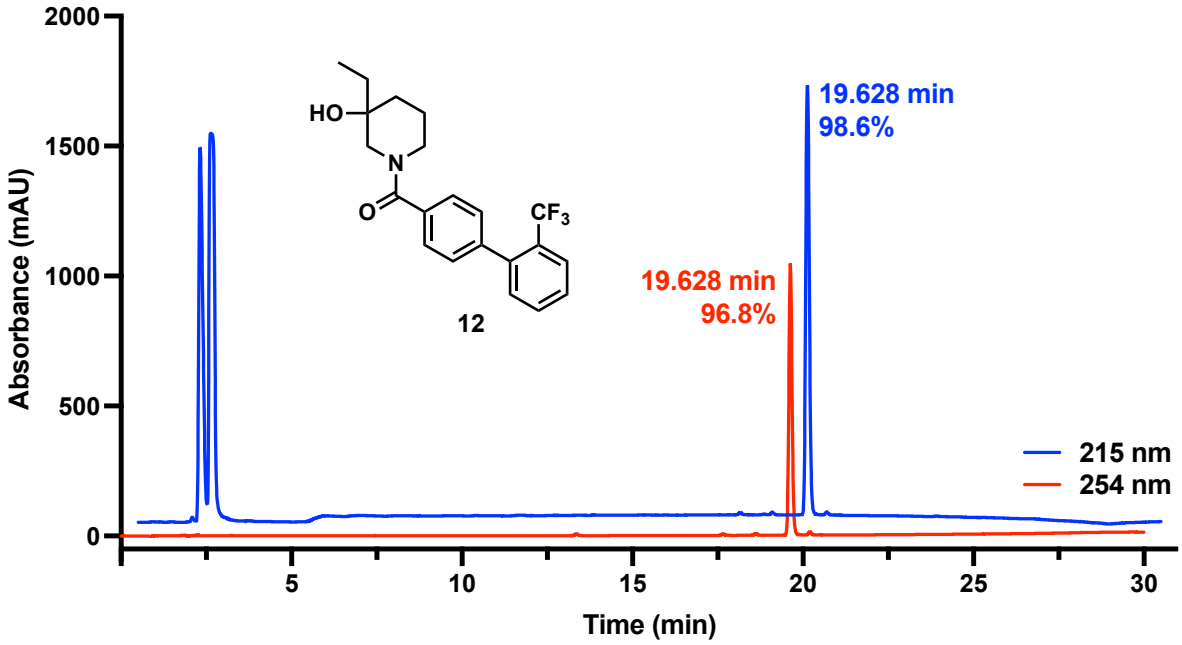

Figure S17. HPLC trace of **12**. Double peak at RT = 2.5 min is DMSO-d_6.

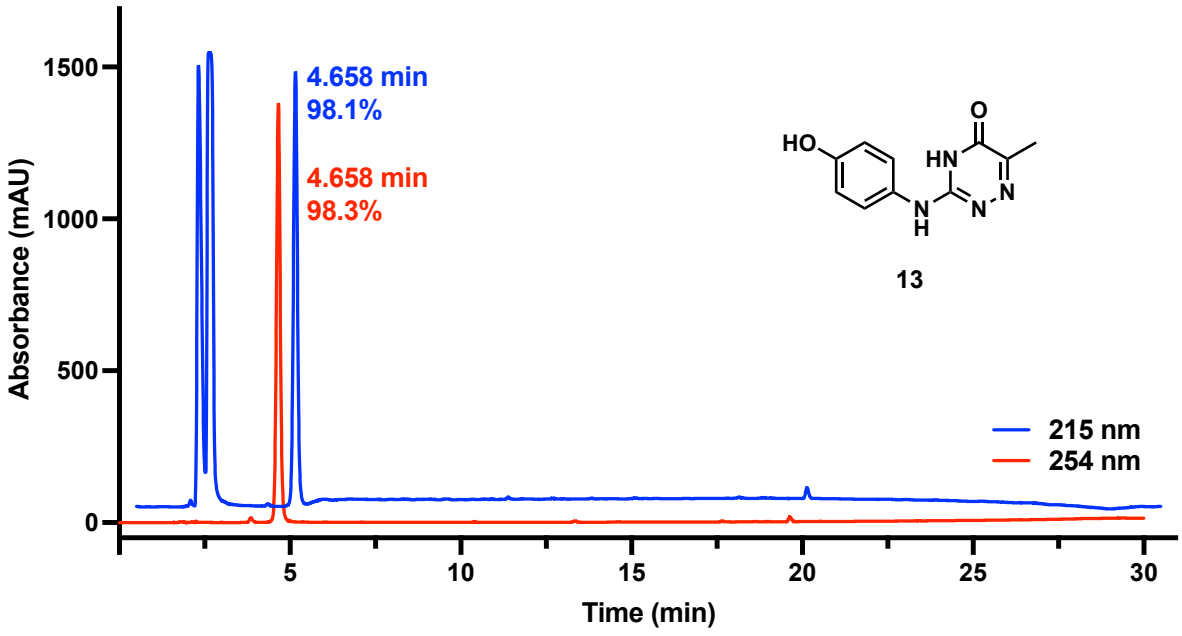

Figure S18. HPLC trace of **13**. Double peak at RT = 2.5 min is DMSO-d_6.

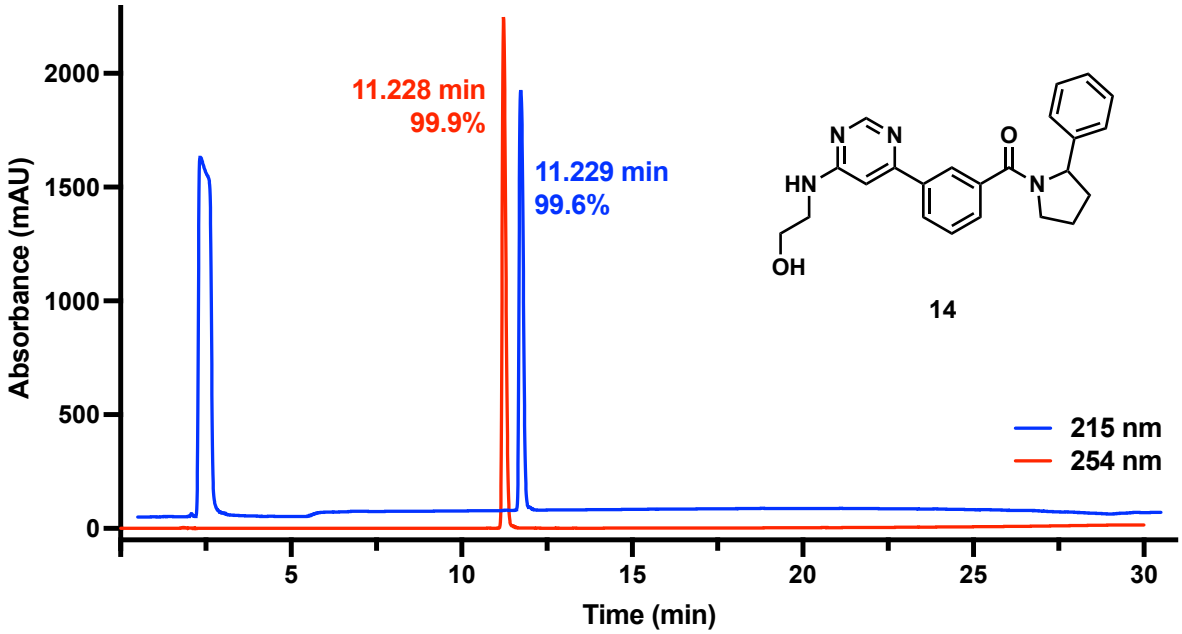

Figure S19. HPLC trace of **14**. Peak at RT = 2.5 min is DMSO-d_6.

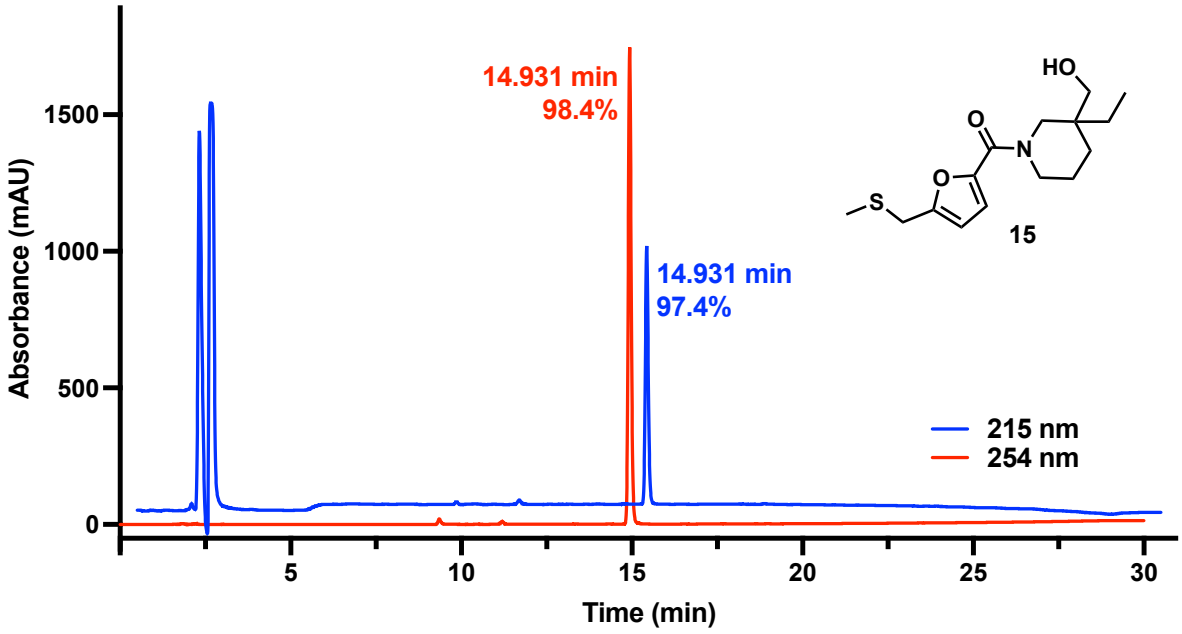

Figure S20. HPLC trace of **15**. Double peak at RT = 2.5 min is DMSO-d_6.

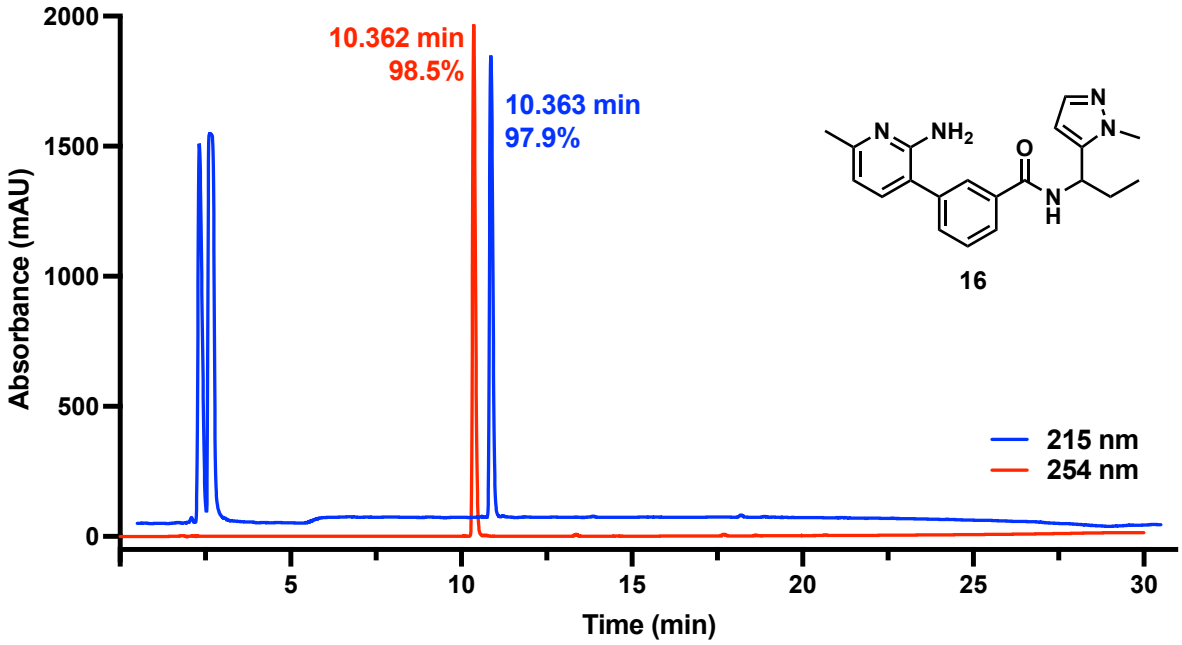

Figure S21. HPLC trace of **16**. Double peak at RT = 2.5 min is DMSO-d_6.

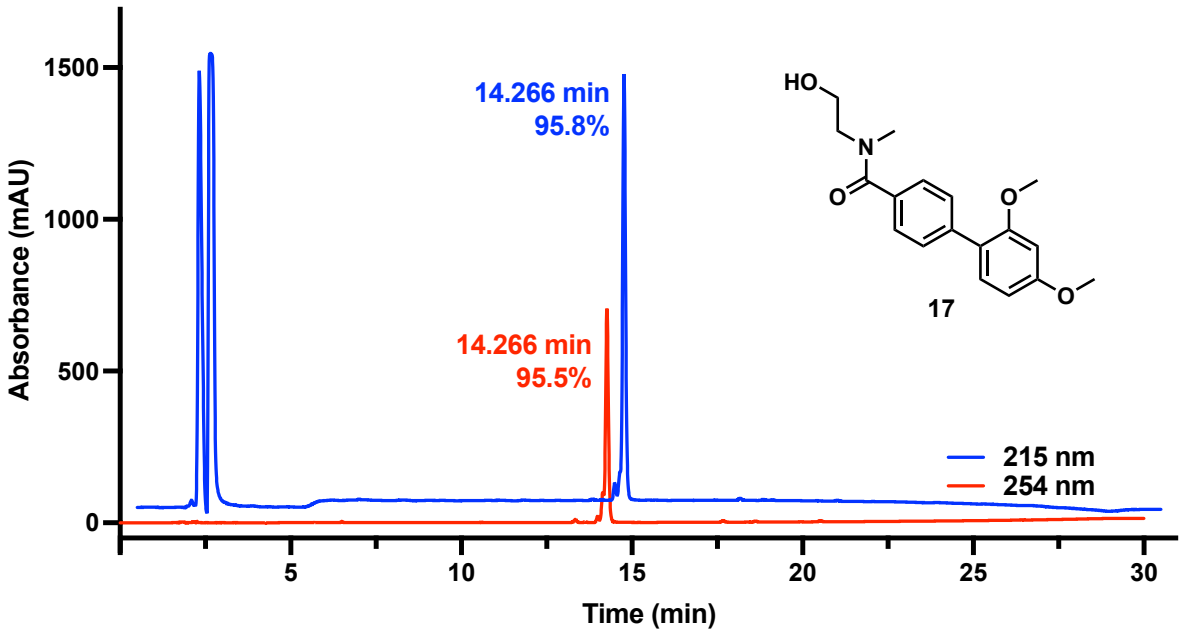

Figure S22. HPLC trace of **17**. Double peak at RT = 2.5 min is DMSO-d_6.

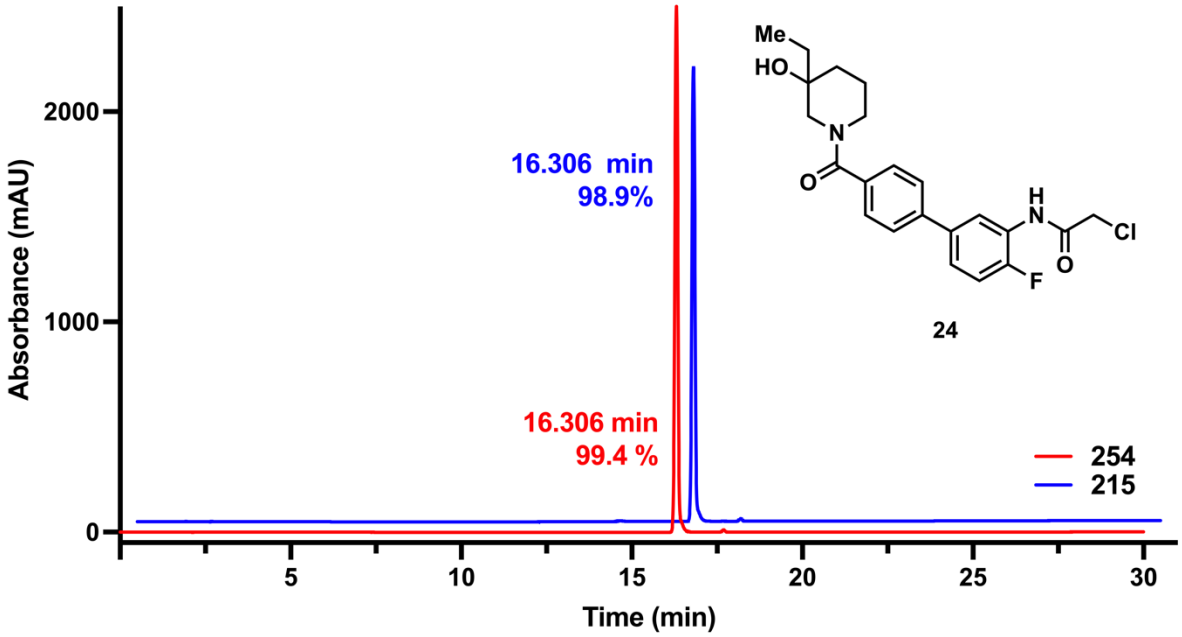

Figure S23. HPLC trace of **24**.

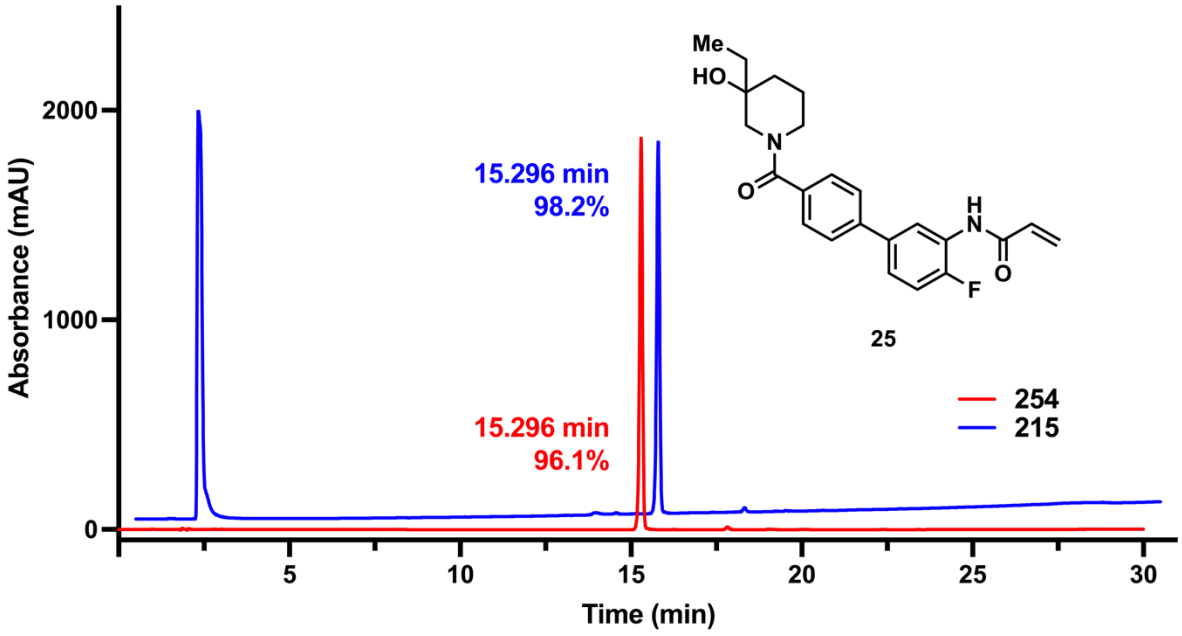

Figure S24. HPLC trace of **25**.

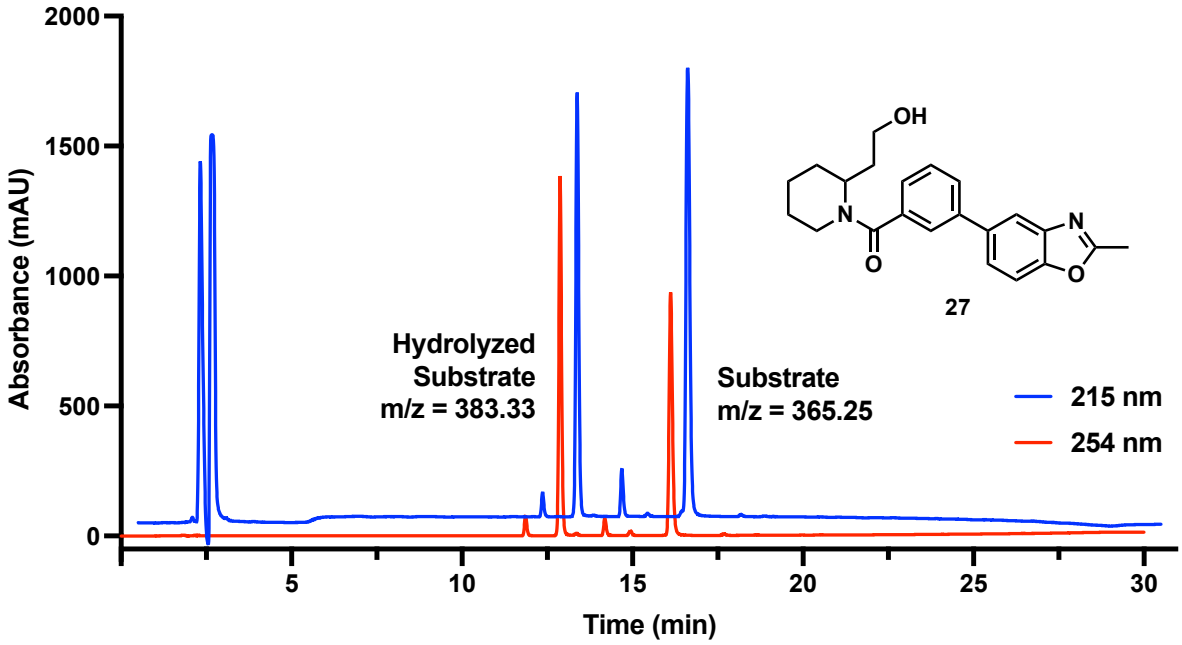

Figure S25. HPLC trace of **27**. Double peak at RT = 2.5 min is DMSO-d_6.

Table S3. LC-MS analysis of purified compound stocks tested in dose response.

Compound	Calc $[M+H]^+$	Found $[M+H]^+$	Compound	Calc $[M+H]^+$	Found $[M+H]^+$
1	346.2	346.4	10	371.2	371.3
2	287.2	287.2	11	205.2	205.2
3	352.2	352.3	12	378.4	378.3
4	379.2	379.3	13	219.2	219.2
5	338.4	338.3	14	389.2	389.3
6	352.5	352.3	15	298.2	298.3
7	350.8	350.2	16	350.4	350.3
8	352.2	352.3	17	316.4	316.3
9	259.2	259.2			

Table S4. Summary of results of control testing for primary hit inhibition of UDG in coupled activity assay. UDG activity is the average ± SEM of two biological replicates. **There was not enough material to test compound **7**, but when the compound was tested in the activity assay against A3A, it did not inhibit, indicating the compound is likely not an inhibitor of UDG.

Compound	UDG Activity (%)	Compound	UDG Activity (%)
5	108 ± 4	12	108 ± 3
6	101 ± 5	13	108 ± 4
7	N/A**	14	110 ± 5
8	99.5 ± 4.8	15	97.8 ± 3.2
9	92.4 ± 3.3	16	103 ± 3
10	97.8 ± 3.8	17	105 ± 3
11	96.0 ± 3.5		

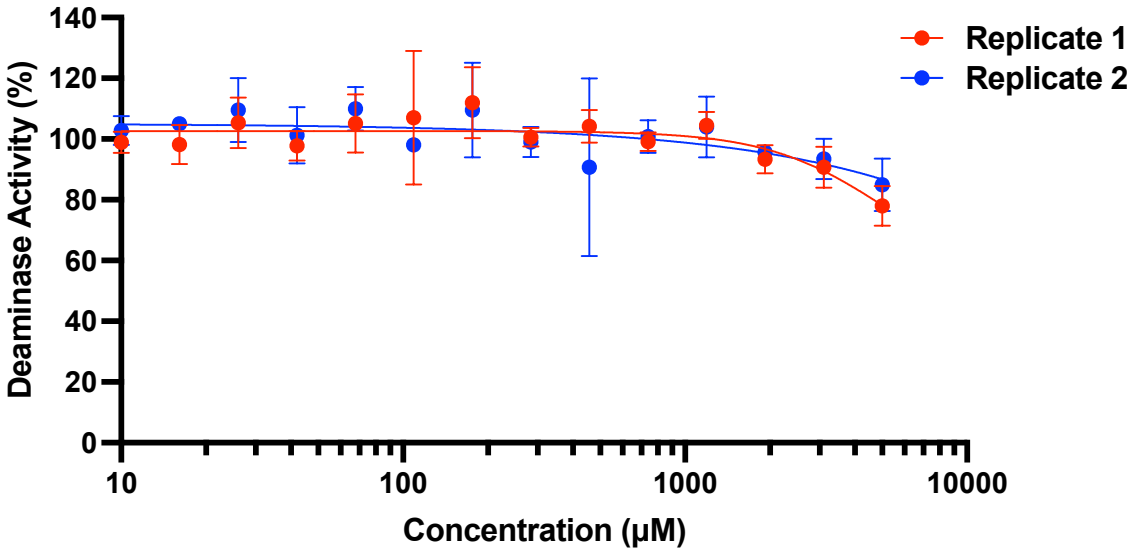

Figure S26. Two biological replicates of the deaminase activity assay with A3Bctd against **1**. Each point is mean ± standard deviation of N = 3 technical replicates. IC_{50} values were unable to be determined.

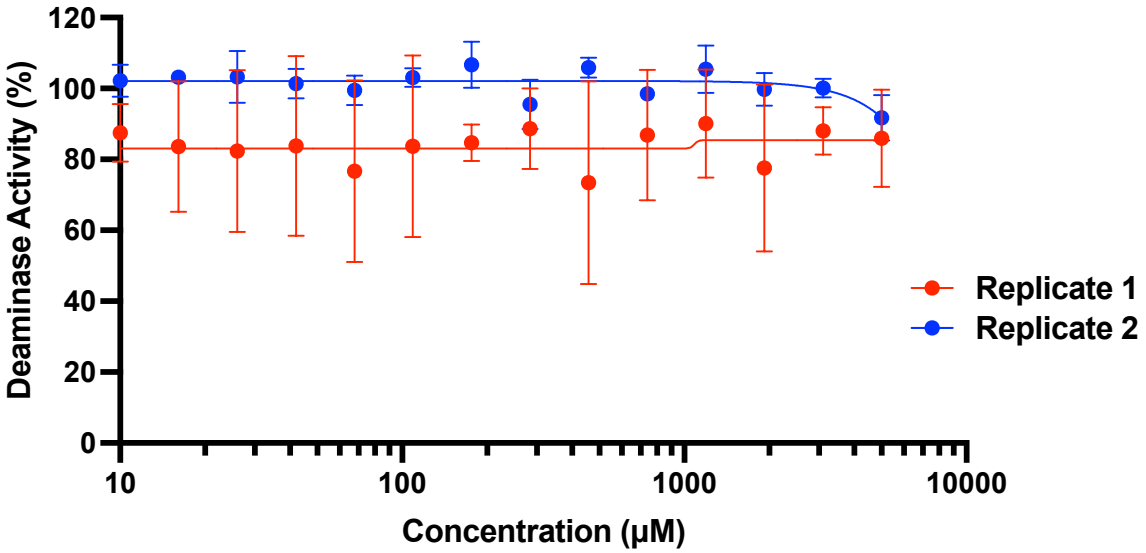

Figure S27. Two biological replicates of the deaminase activity assay with A3Bctd against **2**. Each point is mean ± standard deviation of N = 3 technical replicates. IC_{50} values were unable to be determined.

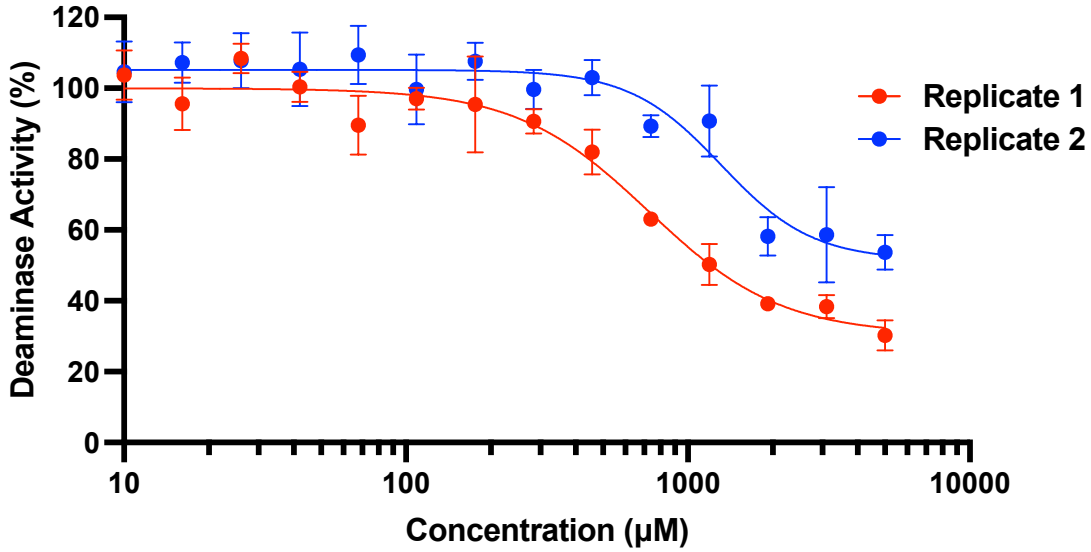

Figure S28. Two biological replicates of the deaminase activity assay with A3Bctd against **3**. Each point is mean ± standard deviation of N = 3 technical replicates. IC_{50} values were unable to be determined.

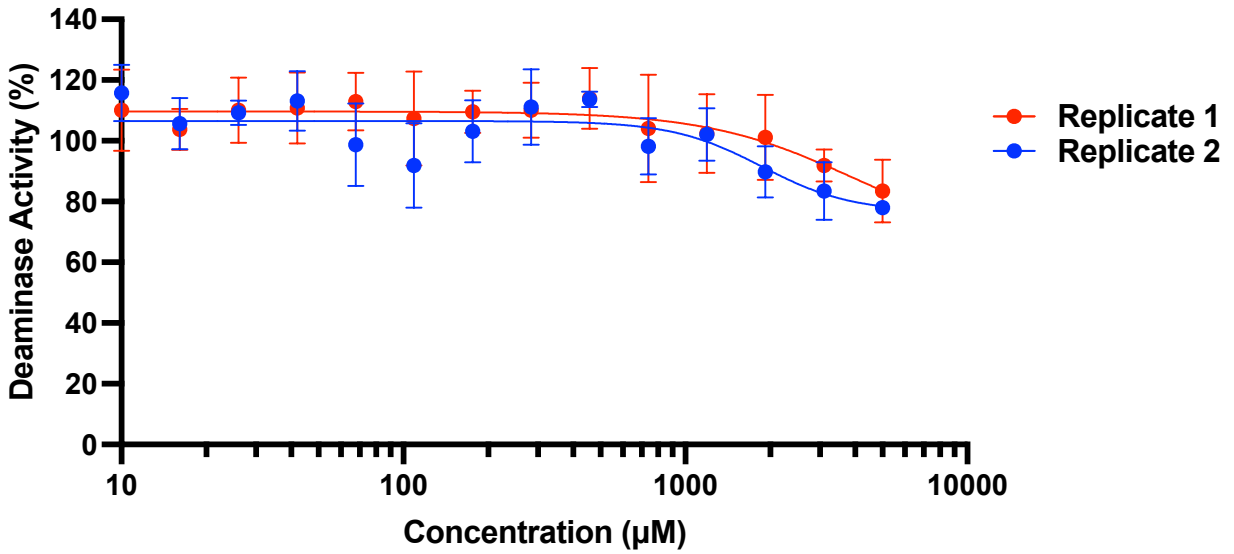

Figure S29. Two biological replicates of the deaminase activity assay with A3Bctd against **4**. Each point is mean ± standard deviation of N = 3 technical replicates. IC_{50} values were unable to be determined.

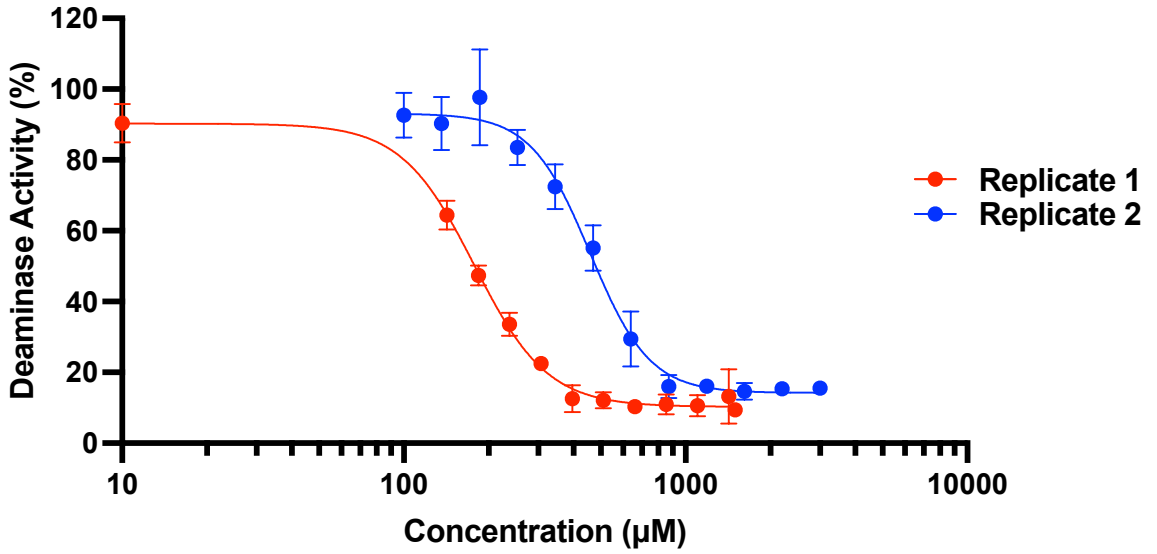

Figure S30. Two biological replicates of the deaminase activity assay with A3Bctd against **5**. Each point is mean ± standard deviation of N = 3 technical replicates. IC_{50} values ± SEM: Replicate 1 = 178 ± 5 μM, Replicate 2 = 458 ± 18 μM.

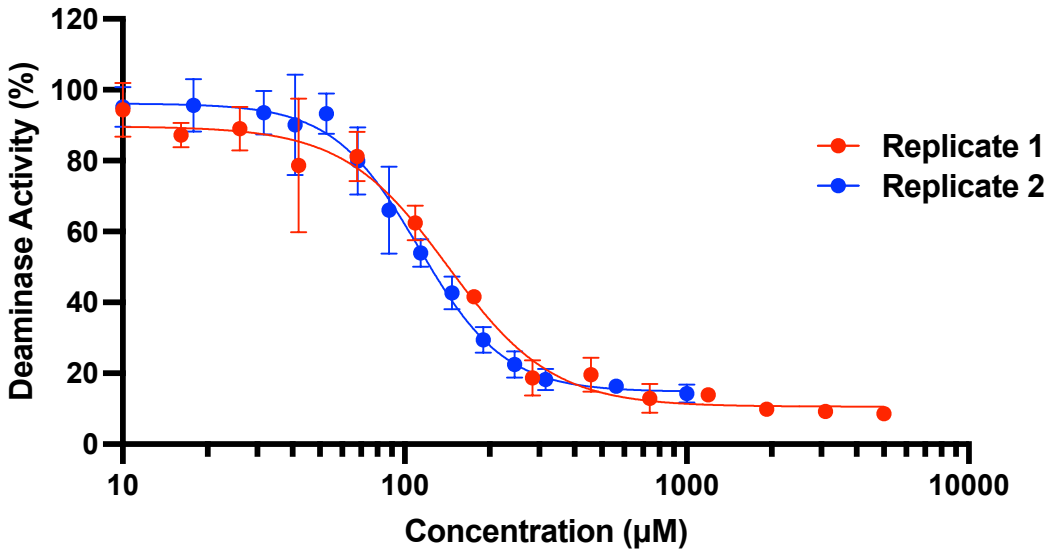

Figure S31. Two biological replicates of the deaminase activity assay with A3Bctd against **6**. Each point is mean ± standard deviation of N = 3 technical replicates. IC_{50} values ± SEM: Replicate 1 = 142 ± 10 μM, Replicate 2 = 112 ± 6 μM.

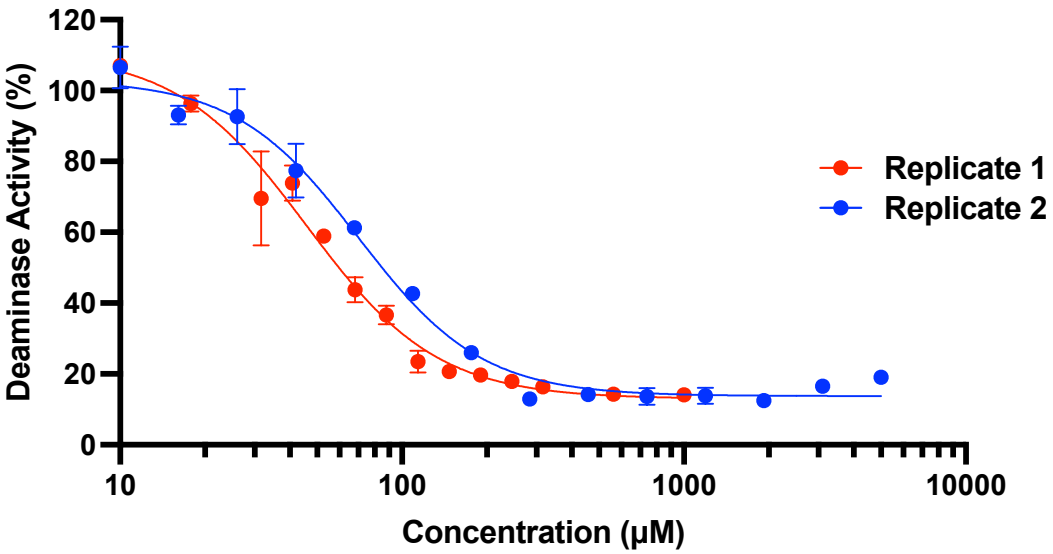

Figure S32. Two biological replicates of the deaminase activity assay with A3Bctd against **7**. Each point is mean ± standard deviation of N = 3 technical replicates. IC_{50} values ± SEM: Replicate 1 = 70.1 ± 3.9 μM, Replicate 2 = 45.8 ± 3.0 μM.

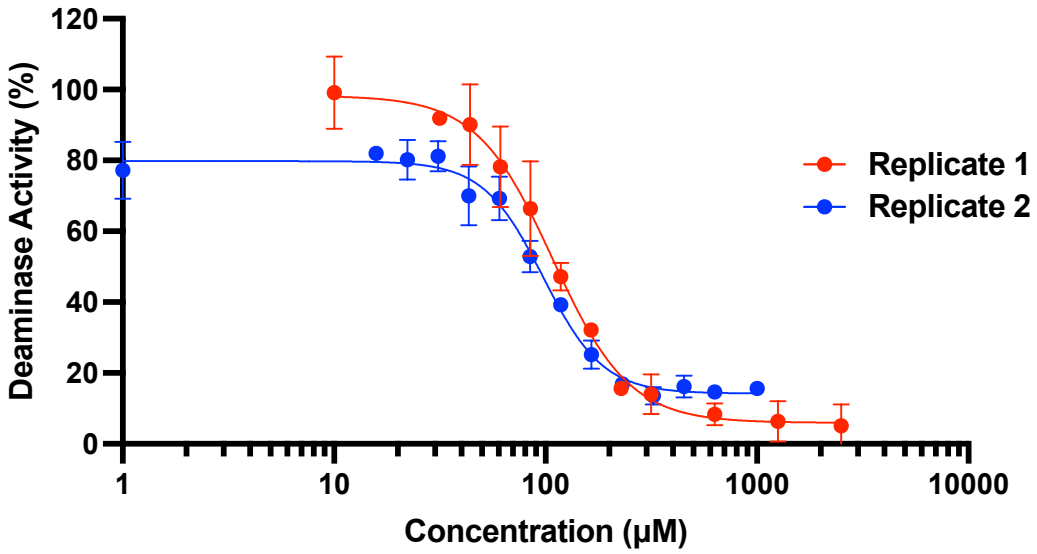

Figure S33. Two biological replicates of the deaminase activity assay with A3Bctd against **8**. Each point is mean ± standard deviation of N = 3 technical replicates. IC_{50} values ± SEM: Replicate 1 = 108 ± 6 μM, Replicate 2 = 97.6 ± 4.1 μM.

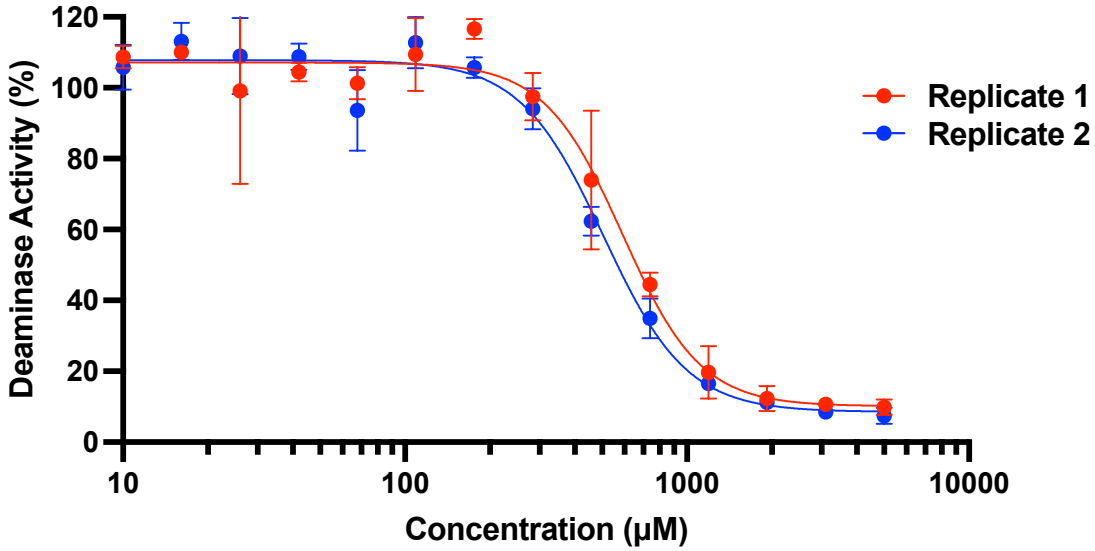

Figure S34. Two biological replicates of the deaminase activity assay with A3Bctd against **9**. Each point is mean ± standard deviation of N = 3 technical replicates. IC_{50} values ± SEM: Replicate 1 = 591 ± 40 μM, Replicate 2 = 506 ± 25 μM.

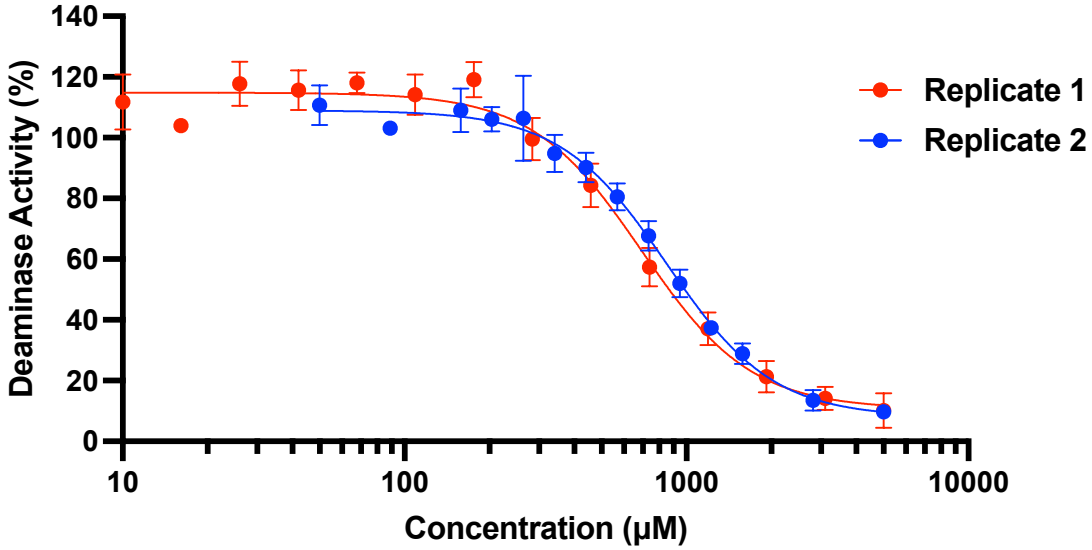

Figure S35. Two biological replicates of the deaminase activity assay with A3Bctd against **10**. Each point is mean ± standard deviation of N = 3 technical replicates. IC_{50} values ± SEM: Replicate 1 = 693 ± 43 μM, Replicate 2 = 851 ± 38 μM.

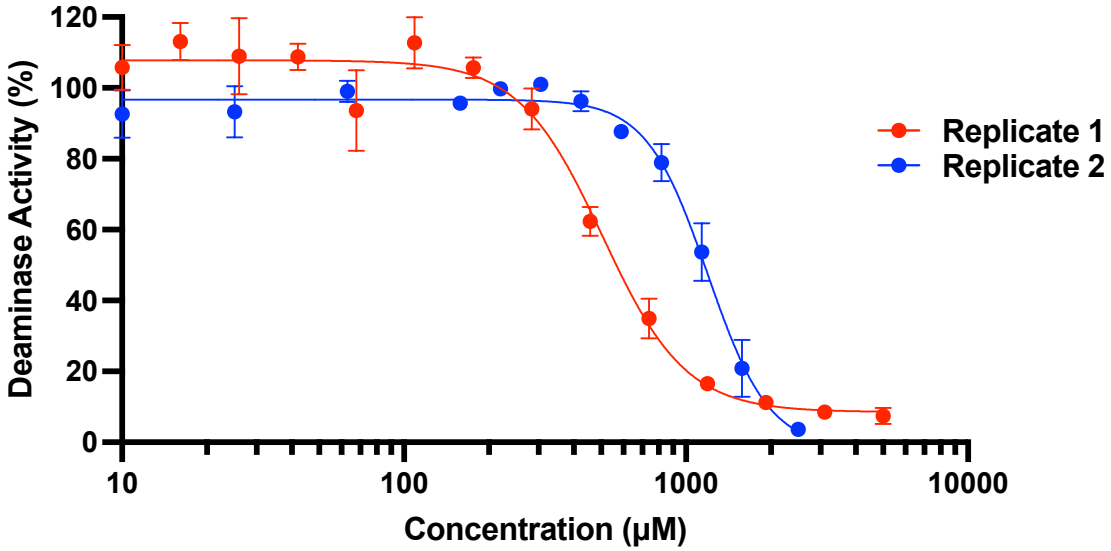

Figure S36. Two biological replicates of the deaminase activity assay with A3Bctd against **11**. Each point is mean ± standard deviation of N = 3 technical replicates. IC_{50} values ± SEM: Replicate 1 = 505 ± 25 μM, Replicate 2 = 1190 ± 45 μM.

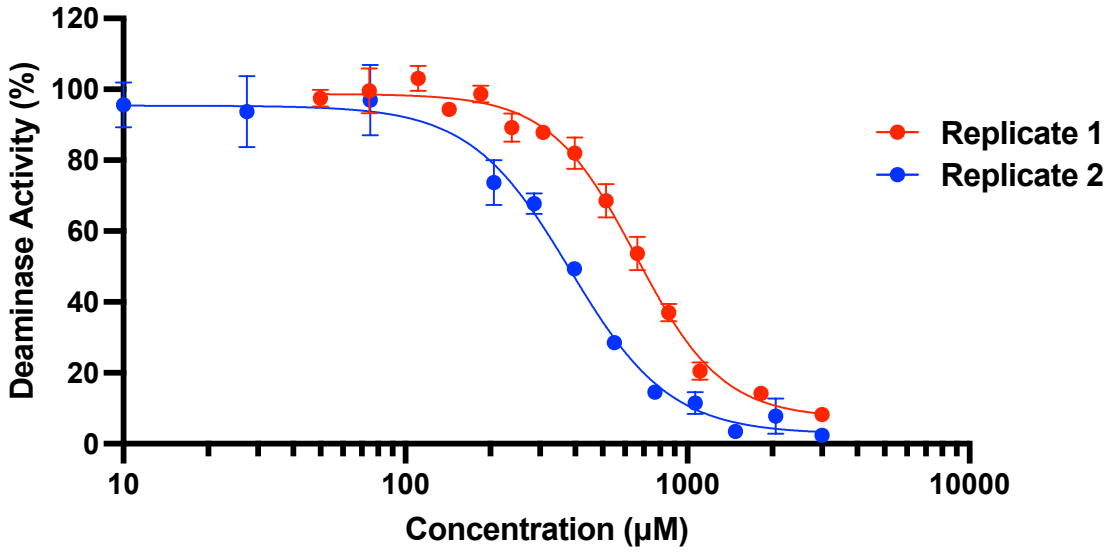

Figure S37. Two biological replicates of the deaminase activity assay with A3Bctd against **12**. Each point is mean ± standard deviation of N = 3 technical replicates. IC_{50} values ± SEM: Replicate 1 = 656 ± 19 μM, Replicate 2 = 383 ± 17 μM.

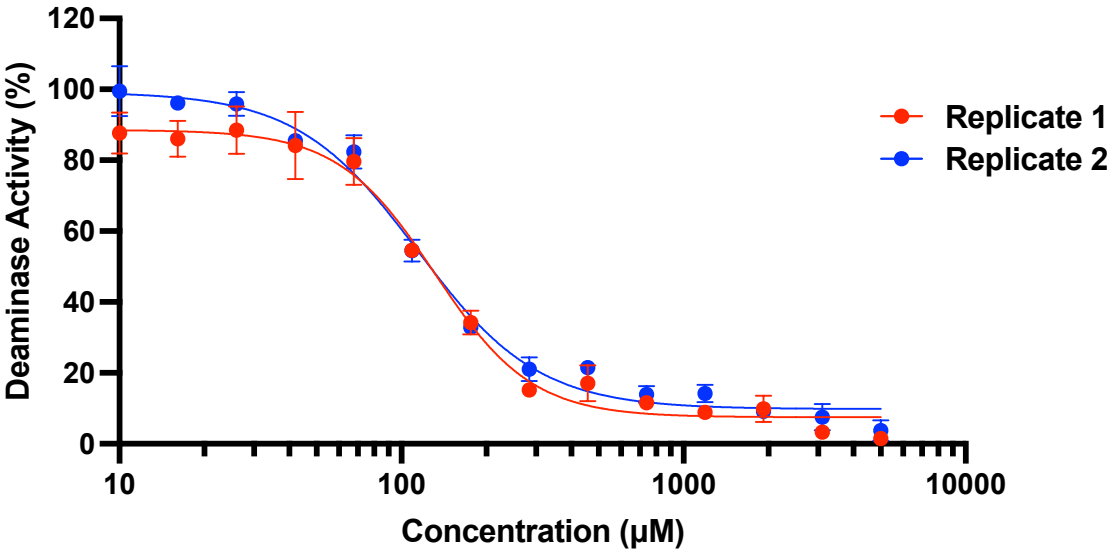

Figure S38. Two biological replicates of the deaminase activity assay with A3Bctd against **13**. Each point is mean ± standard deviation of N = 3 technical replicates. IC_{50} values ± SEM: Replicate 1 = 131 ± 7 μM, Replicate 2 = 114 ± 6 μM.

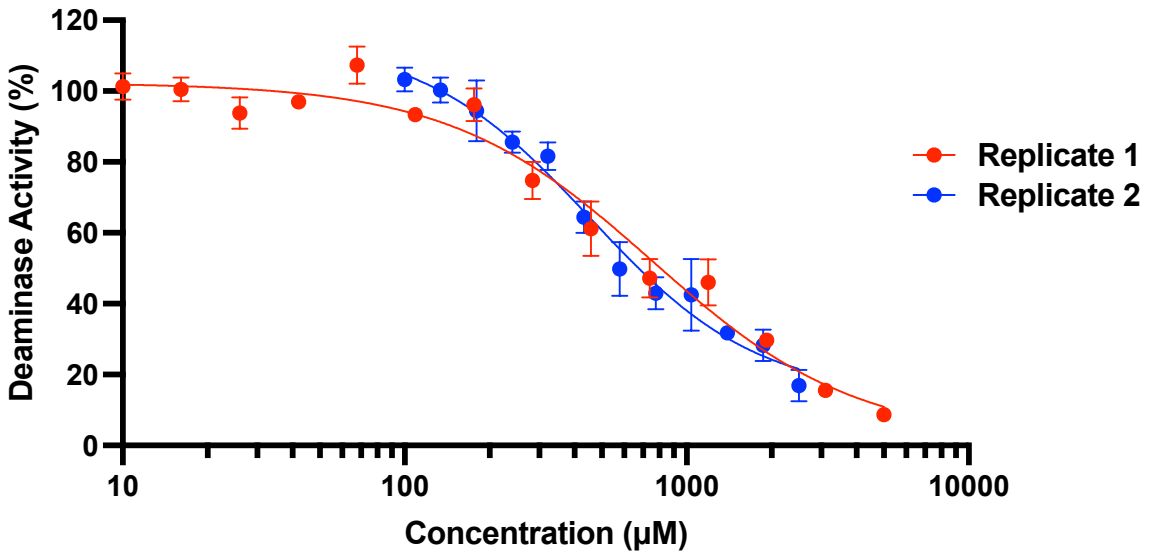

Figure S39. Two biological replicates of the deaminase activity assay with A3Bctd against **14**. Each point is mean ± standard deviation of N = 3 technical replicates. IC_{50} values ± SEM: Replicate 1 = 757 ± 122 μM, Replicate 2 = 455 ± 52 μM.

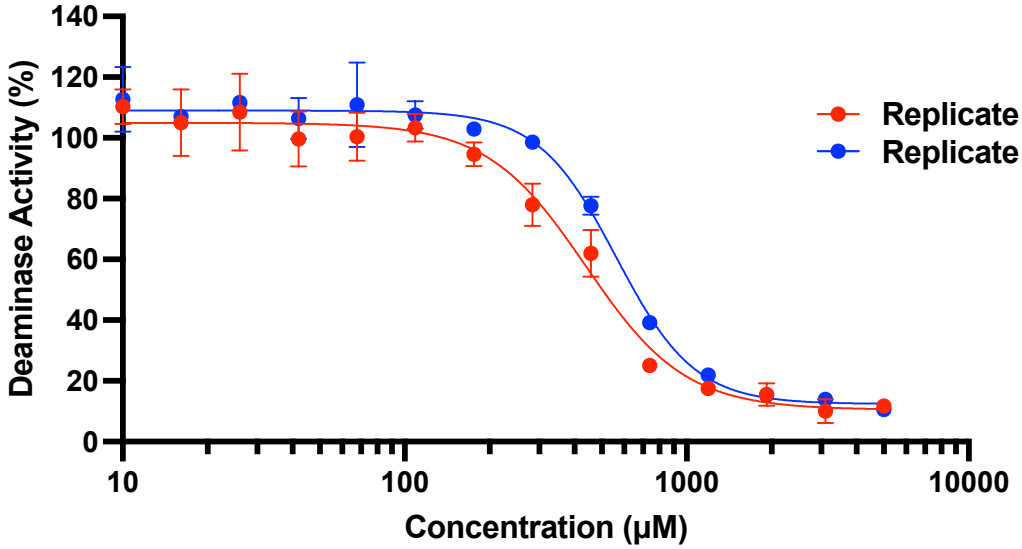

Figure S40. Two biological replicates of the deaminase activity assay with A3Bctd against **15**. Each point is mean ± standard deviation of N = 3 technical replicates. IC_{50} values ± SEM: Replicate 1 = 439 ± 26 μM, Replicate 2 = 563 ± 20 μM.

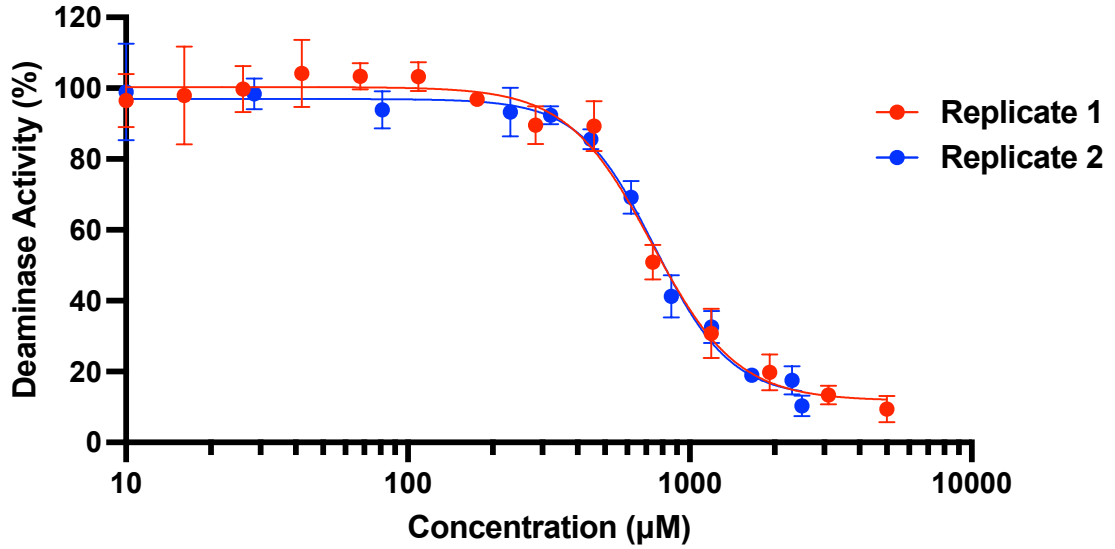

Figure S41. Two biological replicates of the deaminase activity assay with A3Bctd against **16**. Each point is mean ± standard deviation of N = 3 technical replicates. IC_{50} values ± SEM: Replicate 1 = 734 ± 42 μM, Replicate 2 = 754 ± 34 μM.

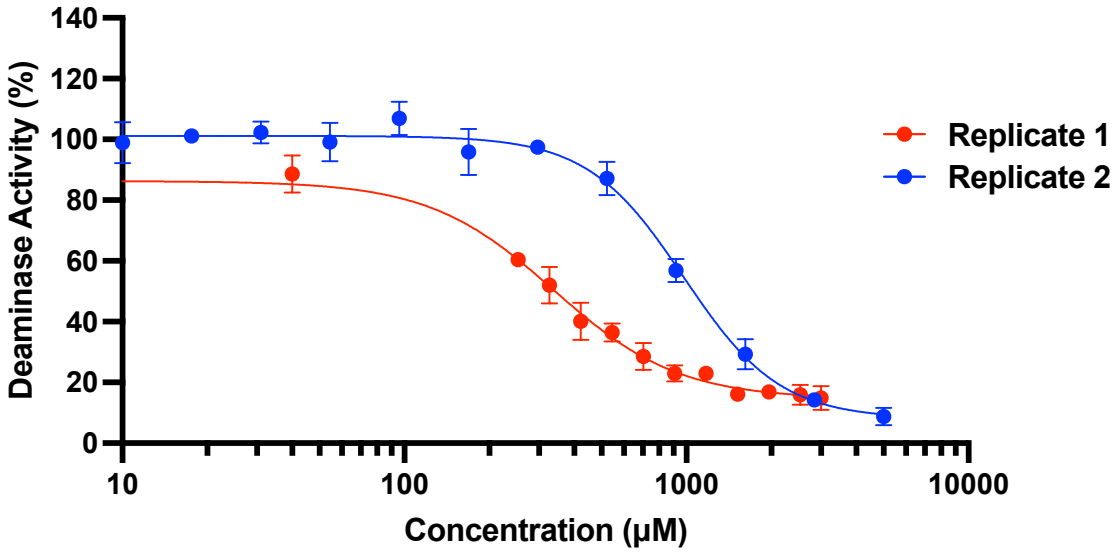

Figure S42. Two biological replicates of the deaminase activity assay with A3Bctd against **17**. Each point is mean ± standard deviation of N = 3 technical replicates. IC_{50} values ± SEM: Replicate 1 = 338 ± 17 μM, Replicate 2 = 979 ± 49 μM.

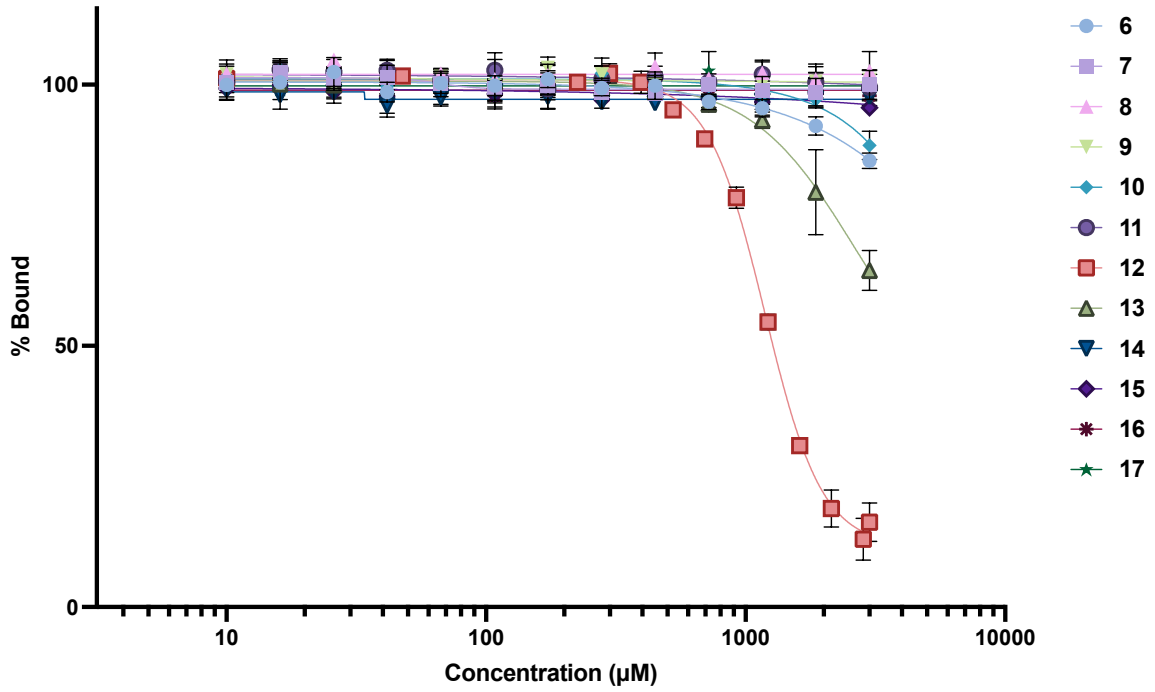

Figure S43. One biological replicate of compounds tested against A3Bctd in the fluorescence polarization assay. Each point is mean ± standard deviation of N = 3 technical replicates. The IC_{50} of **12** is measured to be 1.1 mM.

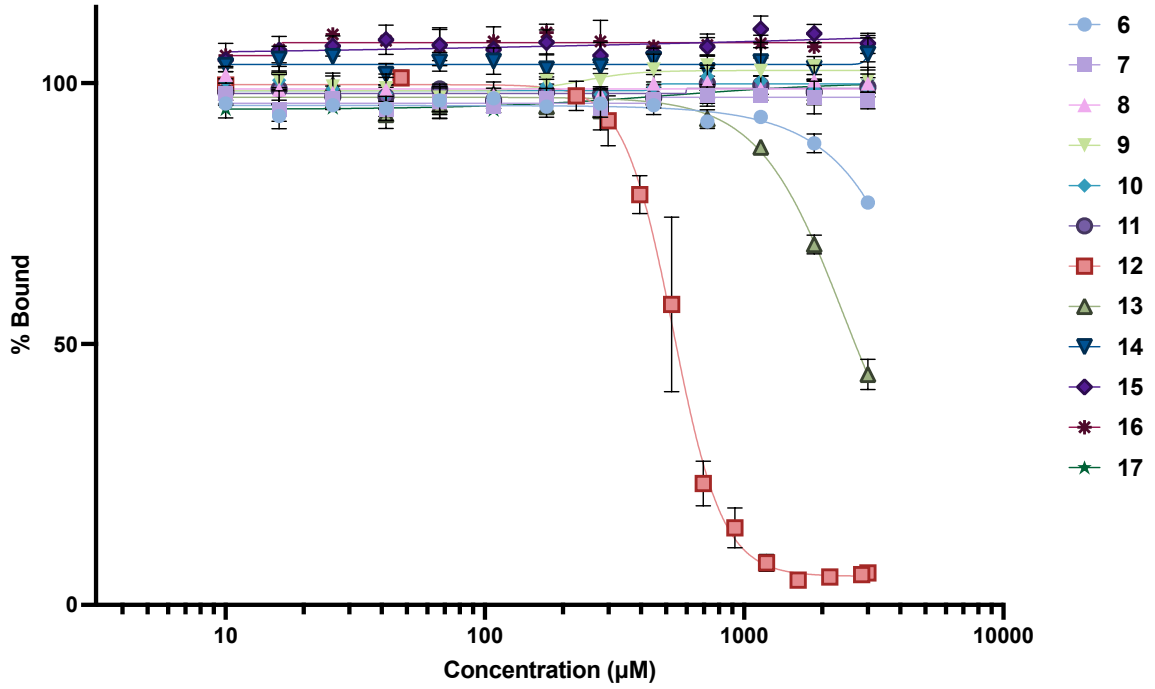

Figure S44. One biological replicate of compounds tested against A3Bctd in the fluorescence polarization assay. Each point is mean ± standard deviation of N = 3 technical replicates. The IC_{50} of **12** is measured to be 533 μM.

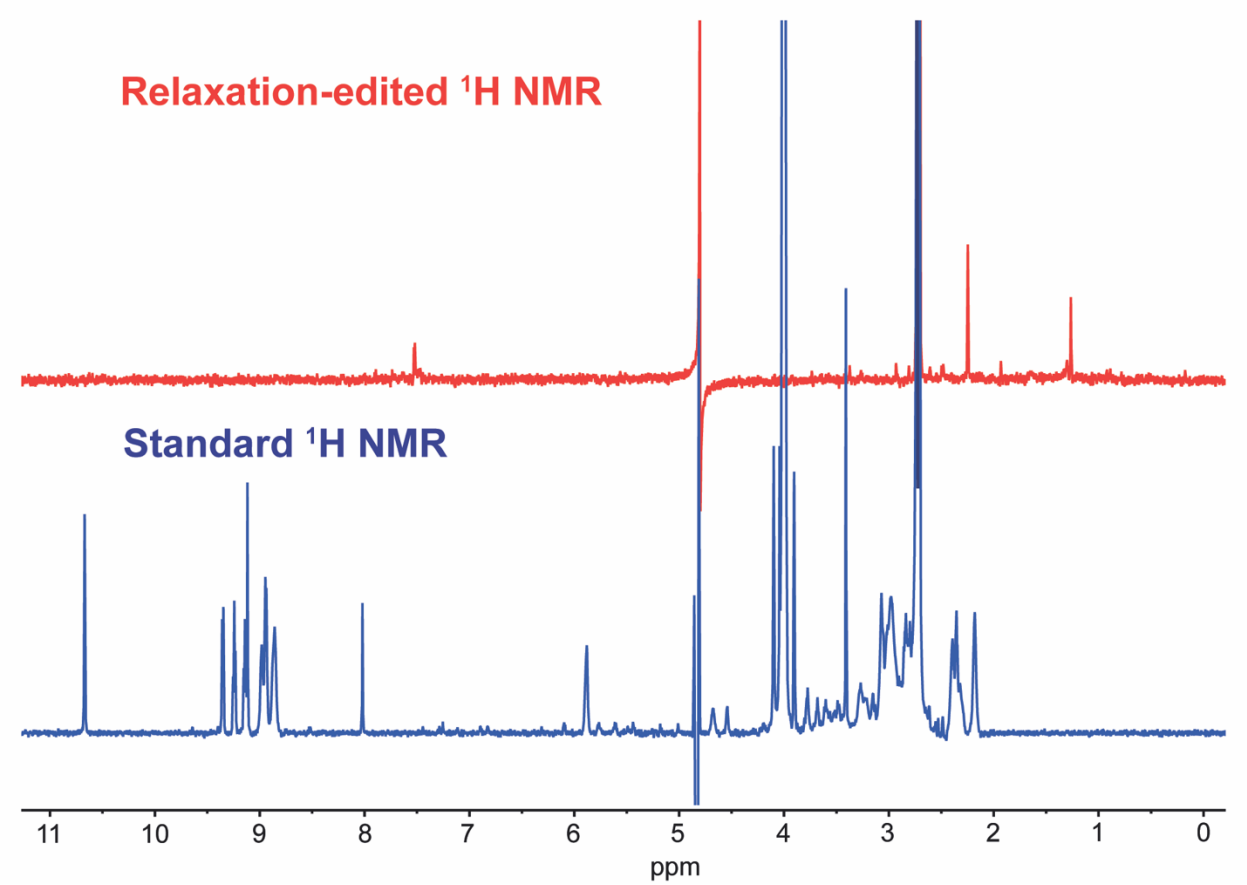

Figure S45. Comparison of relaxation-edited ^{1}H NMR to standard ^{1}H NMR of **12**. The disappearance of peaks upon implementing a T_2-relaxation delay indicates the aggregation of compound in solution.

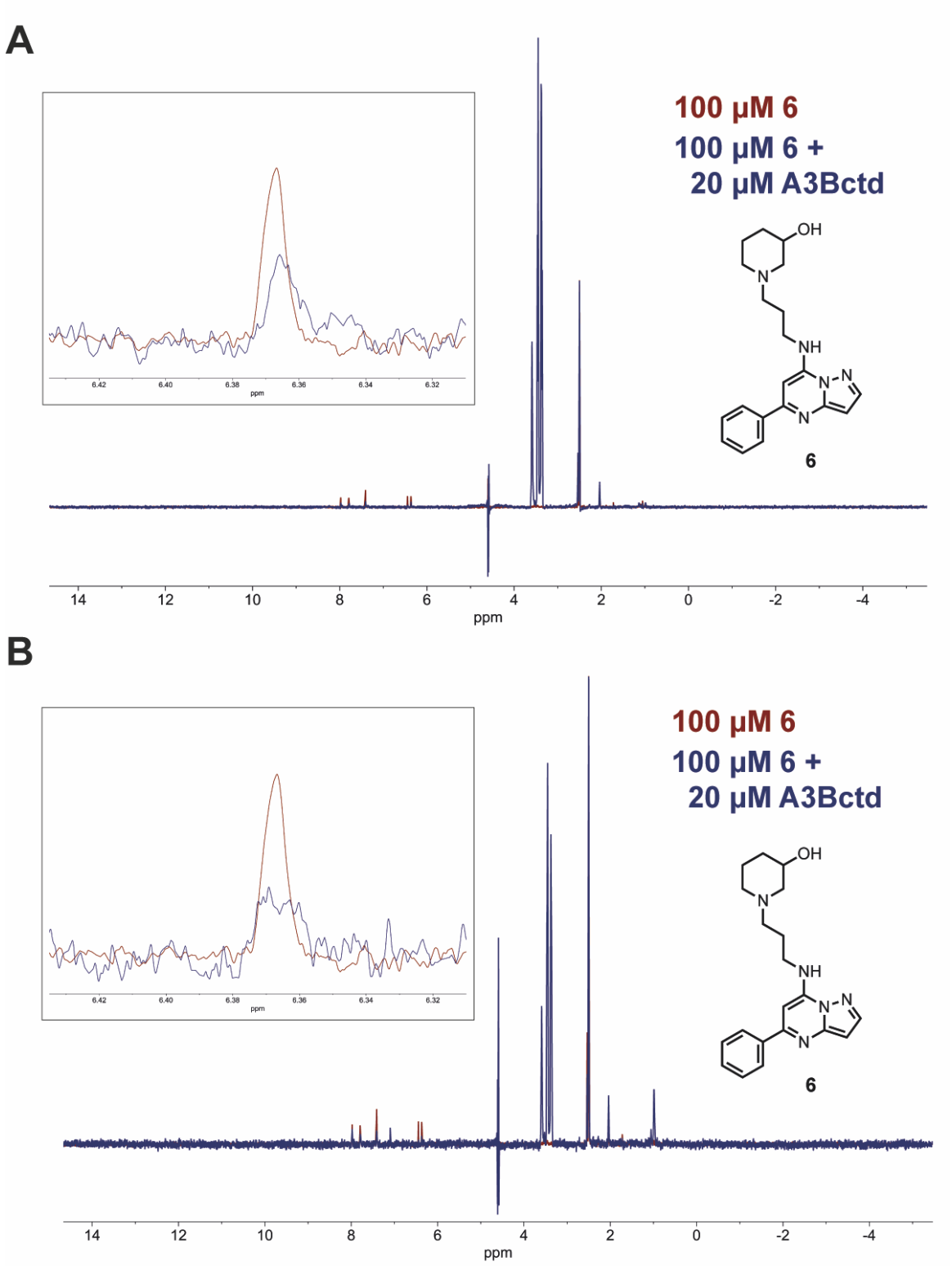

Figure S46. Biological replicate 1 (A) and 2 (B) of ligand-observed ^{1}H CPMG NMR, measuring the binding of **6** to A3Bctd. Red spectrum is compound alone, blue spectrum is compound incubated with protein. Peak used to measure signal attenuation is at 6.37 ppm. Spectra are normalized to DMSO peak at 2.5 ppm.

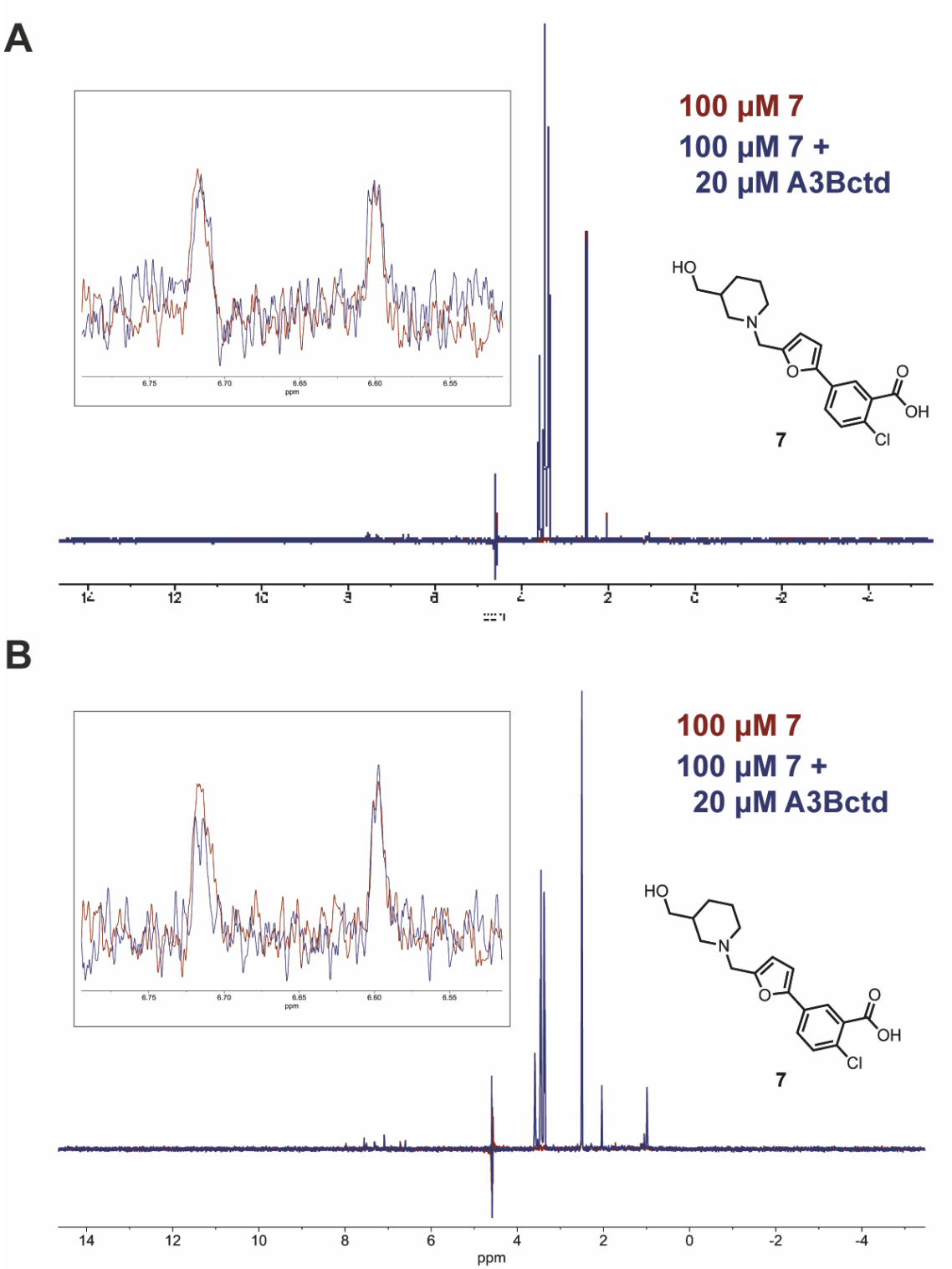

Figure S47. Biological replicate 1 (A) and 2 (B) of ligand-observed ^{1}H CPMG NMR, measuring the binding of **7** to A3Bctd. Blue spectrum is compound alone, red spectrum is compound and protein. Peak used to measure signal attenuation is at 6.72 ppm. Spectra are normalized to DMSO peak at 2.5 ppm.

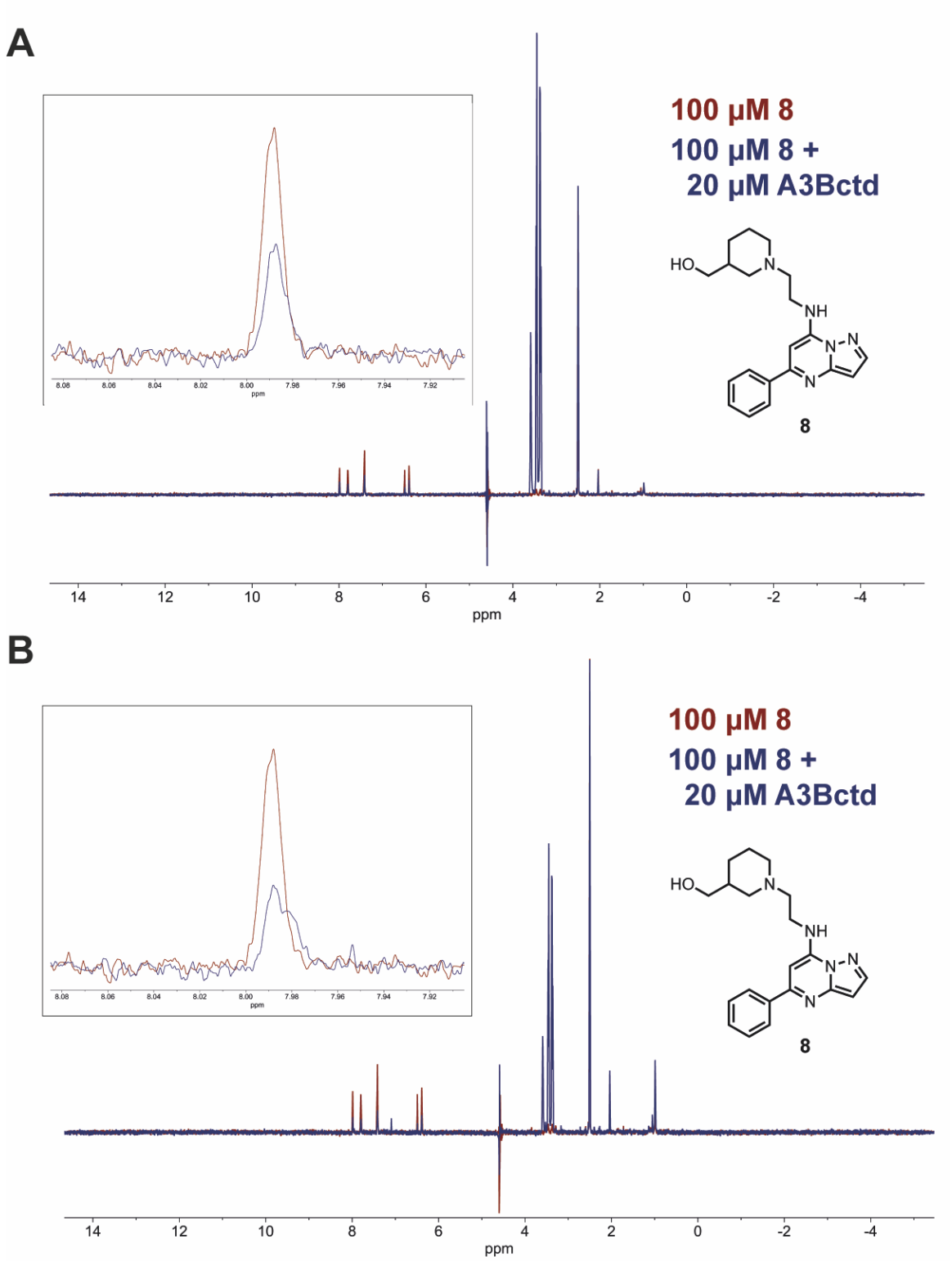

Figure S48. Biological replicate 1 (A) and 2 (B) of ligand-observed ^{1}H CPMG NMR, measuring the binding of **8** to A3Bctd. Red spectrum is compound alone, blue spectrum is compound incubated with protein. Peak used to measure signal attenuation is at 7.99 ppm. Spectra are normalized to DMSO peak at 2.5 ppm.

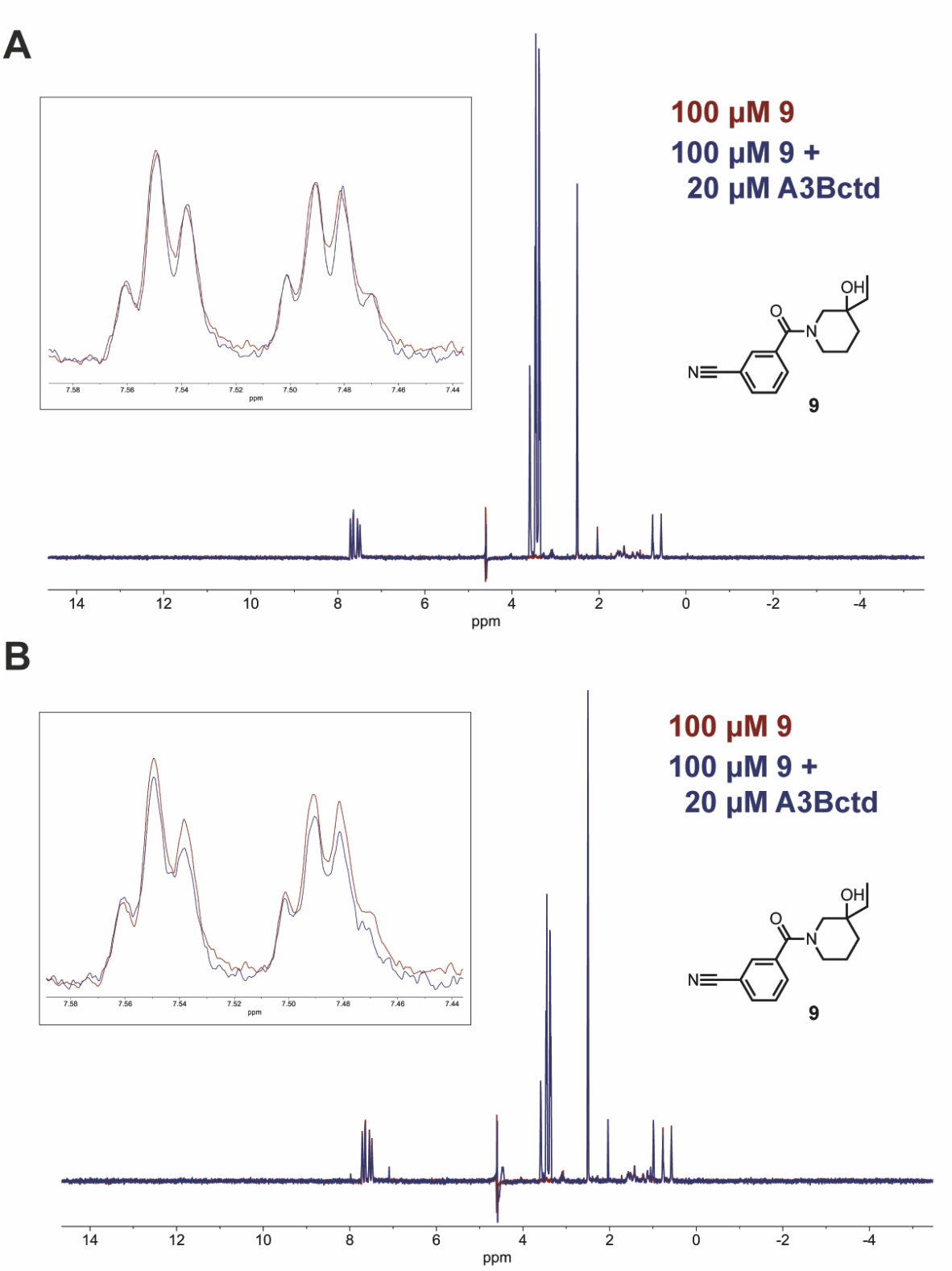

Figure S49. Biological replicate 1 (A) and 2 (B) of ligand-observed ^{1}H CPMG NMR, measuring the binding of **9** to A3Bctd. Red spectrum is compound alone, blue spectrum is compound incubated with protein. Peak used to measure signal attenuation is at 7.55 ppm. Spectra are normalized to DMSO peak at 2.5 ppm.

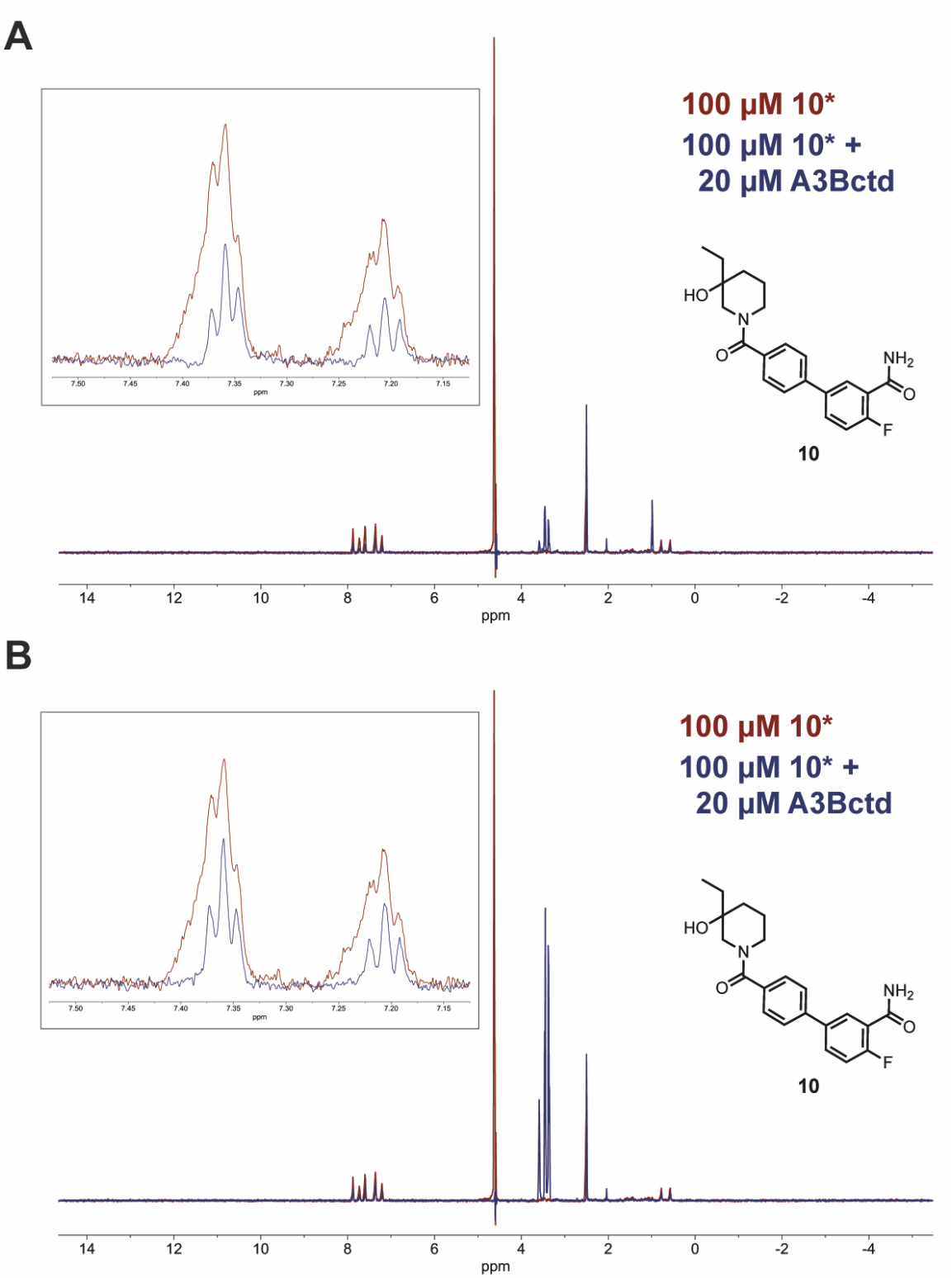

Figure S50. Biological replicate 1 (A) and 2 (B) of ligand-observed ^{1}H CPMG NMR, measuring the binding of **10*** to A3Bctd. Red spectrum is compound alone, blue spectrum is compound incubated with protein. Peak used to measure signal attenuation is at 7.36 ppm. Spectra are normalized to DMSO peak at 2.5 ppm.

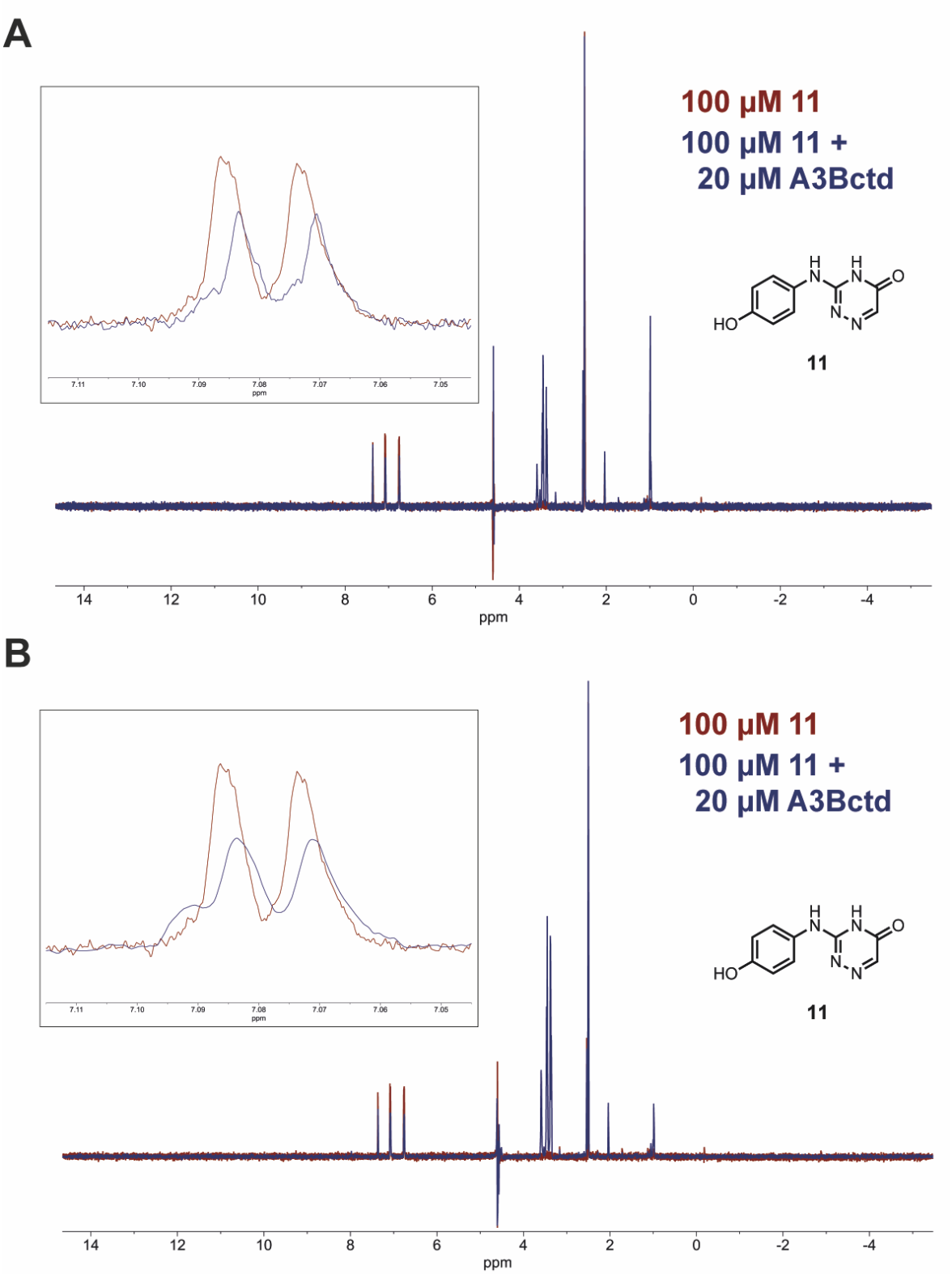

Figure S51. Biological replicate 1 (A) and 2 (B) of ligand-observed ^{1}H CPMG NMR, measuring the binding of **11** to A3Bctd. Red spectrum is compound alone, blue spectrum is compound incubated with protein. Peak used to measure signal attenuation is at 7.09 ppm. Spectra are normalized to DMSO peak at 2.5 ppm.

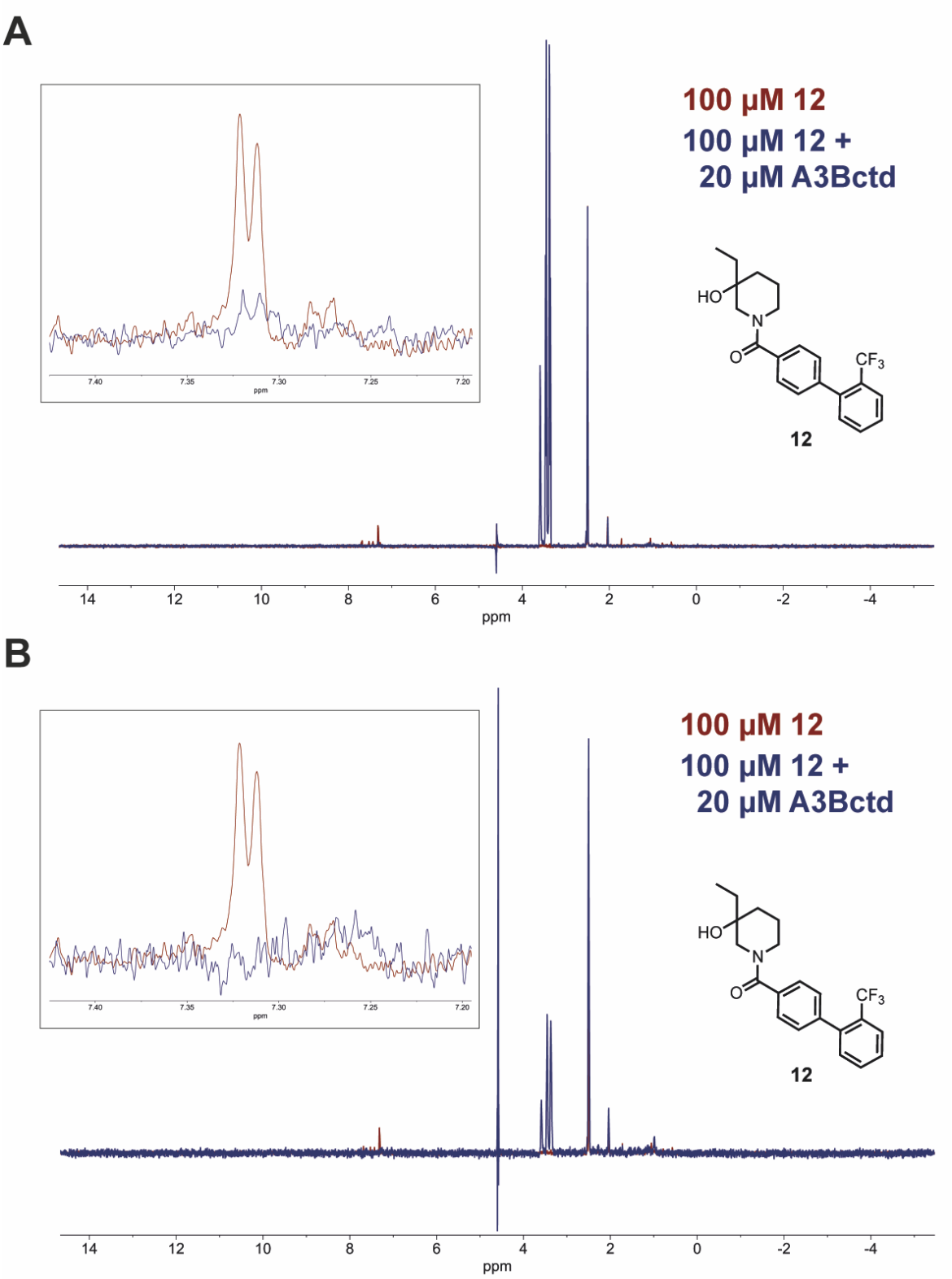

Figure S52. Biological replicate 1 (A) and 2 (B) of ligand-observed ^{1}H CPMG NMR, measuring the binding of **12** to A3Bctd. Red spectrum is compound alone, blue spectrum is compound incubated with protein. Peak used to measure signal attenuation is at 7.32 ppm. Spectra are normalized to DMSO peak at 2.5 ppm.

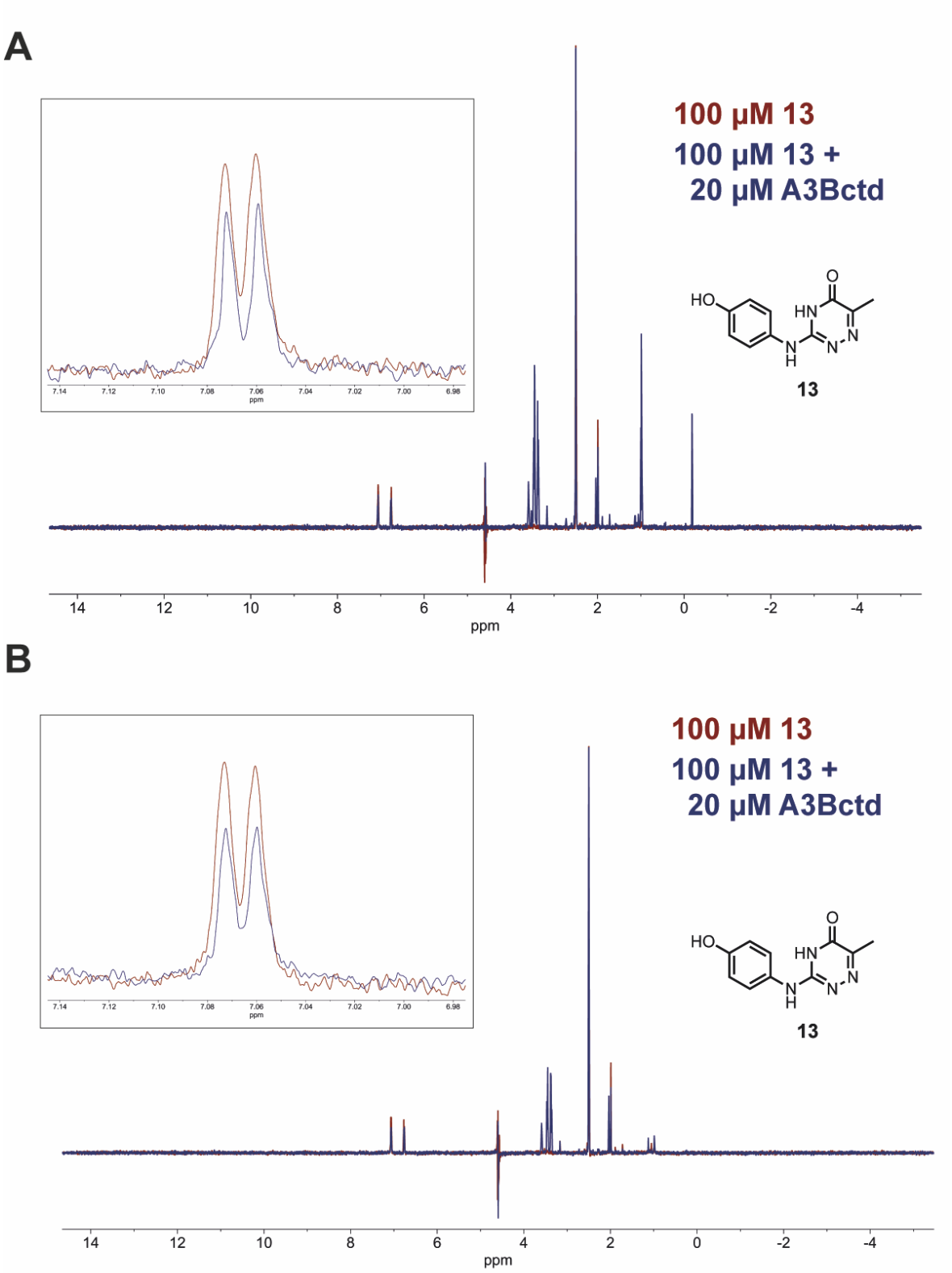

Figure S53. Biological replicate 1 (A) and 2 (B) of ligand-observed ^{1}H CPMG NMR, measuring the binding of **13** to A3Bctd. Red spectrum is compound alone, blue spectrum is compound incubated with protein. Peak used to measure signal attenuation is at 7.06 ppm. Spectra are normalized to DMSO peak at 2.5 ppm.

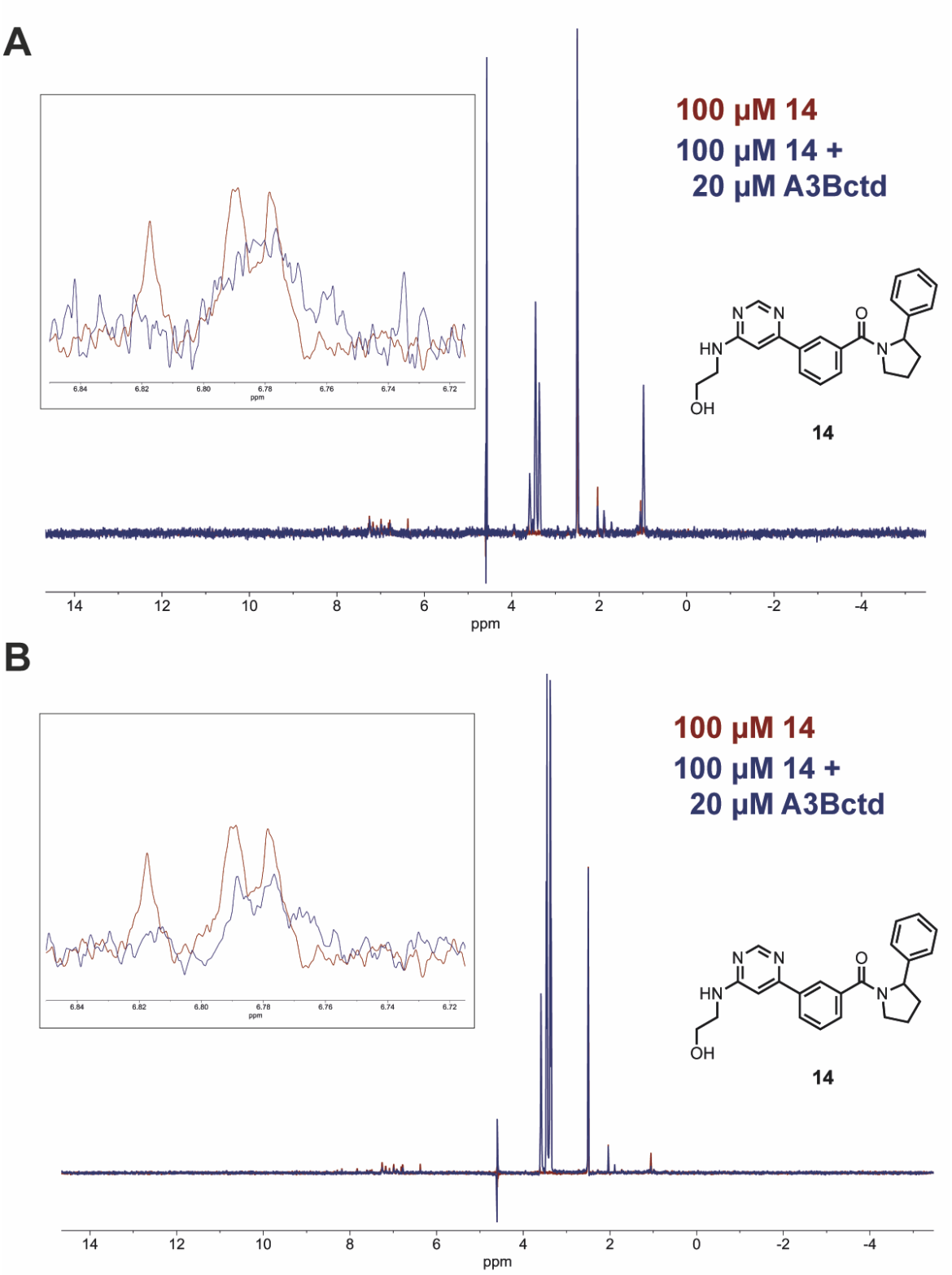

Figure S54. Biological replicate 1 (A) and 2 (B) of ligand-observed ^{1}H CPMG NMR, measuring the binding of **14** to A3Bctd. Red spectrum is compound alone, blue spectrum is compound incubated with protein. Peak used to measure signal attenuation is at 6.79 ppm. Spectra are normalized to DMSO peak at 2.5 ppm.

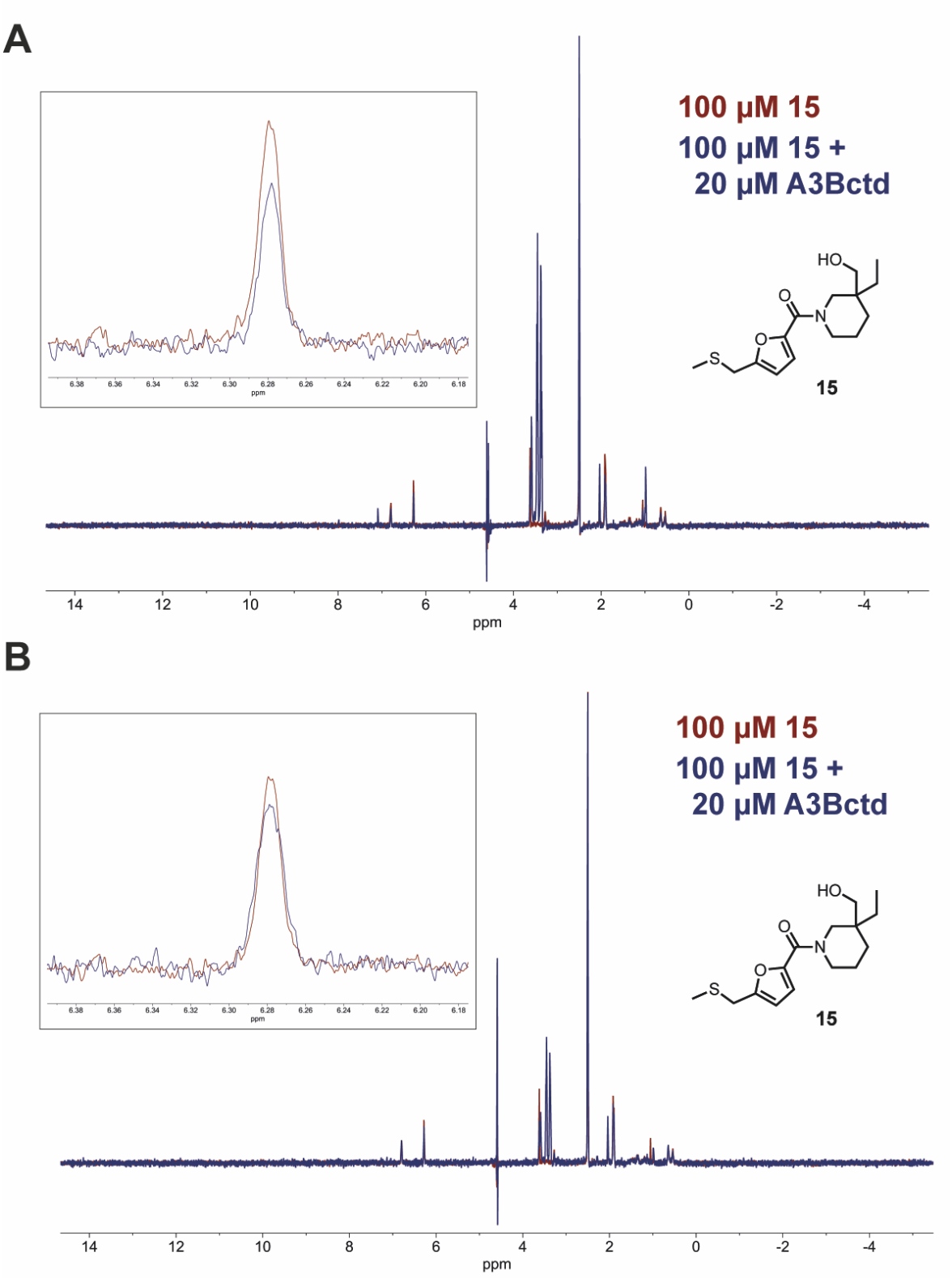

Figure S55. Biological replicate 1 (A) and 2 (B) of ligand-observed ^{1}H CPMG NMR, measuring the binding of **15** to A3Bctd. Red spectrum is compound alone, blue spectrum is compound incubated with protein. Peak used to measure signal attenuation is at 6.28 ppm. Spectra are normalized to DMSO peak at 2.5 ppm.

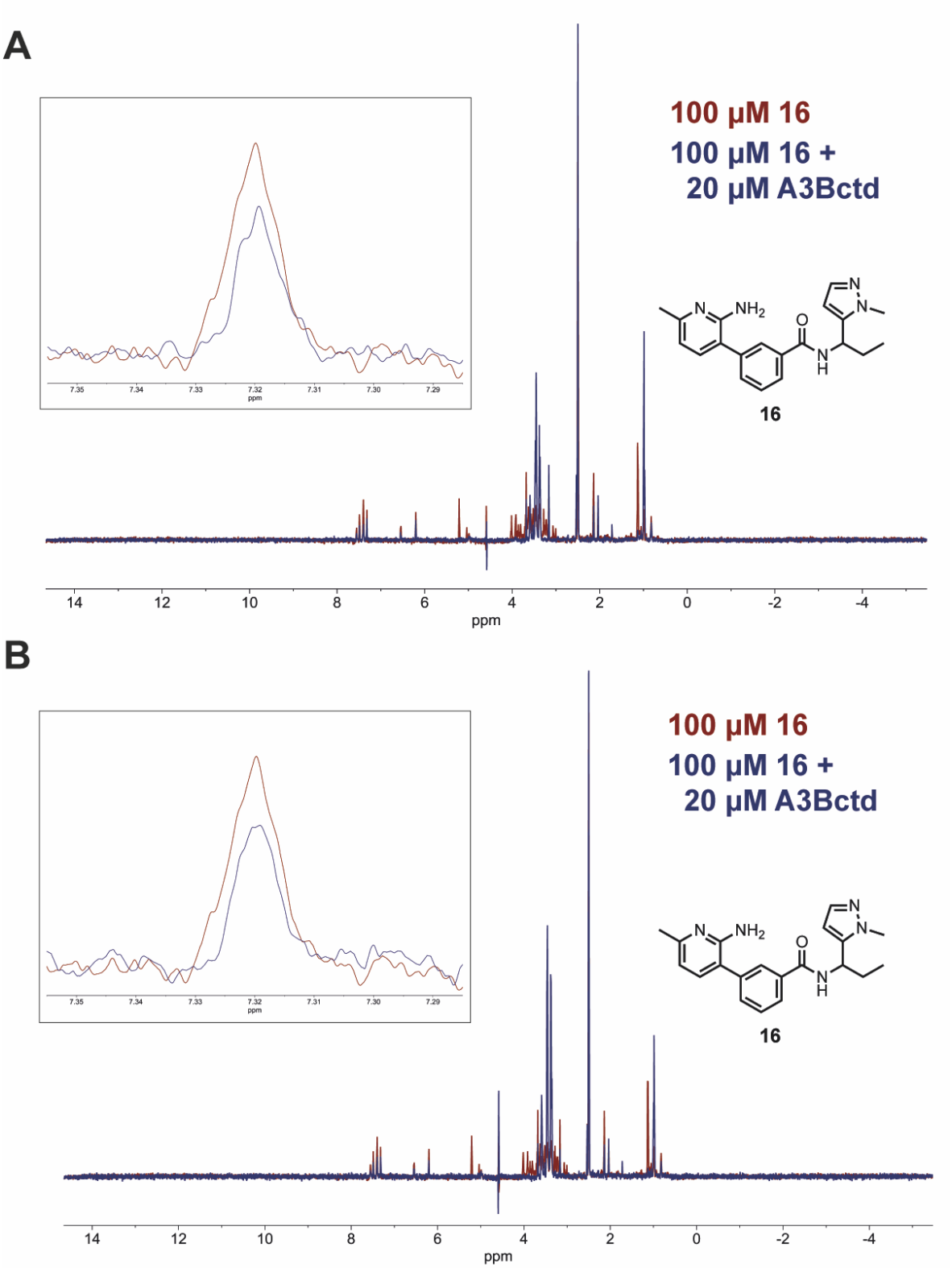

Figure S56. Biological replicate 1 (A) and 2 (B) of ligand-observed ^{1}H CPMG NMR, measuring the binding of **16** to A3Bctd. Red spectrum is compound alone, blue spectrum is compound incubated with protein. Peak used to measure signal attenuation is at 7.32 ppm. Spectra are normalized to DMSO peak at 2.5 ppm.

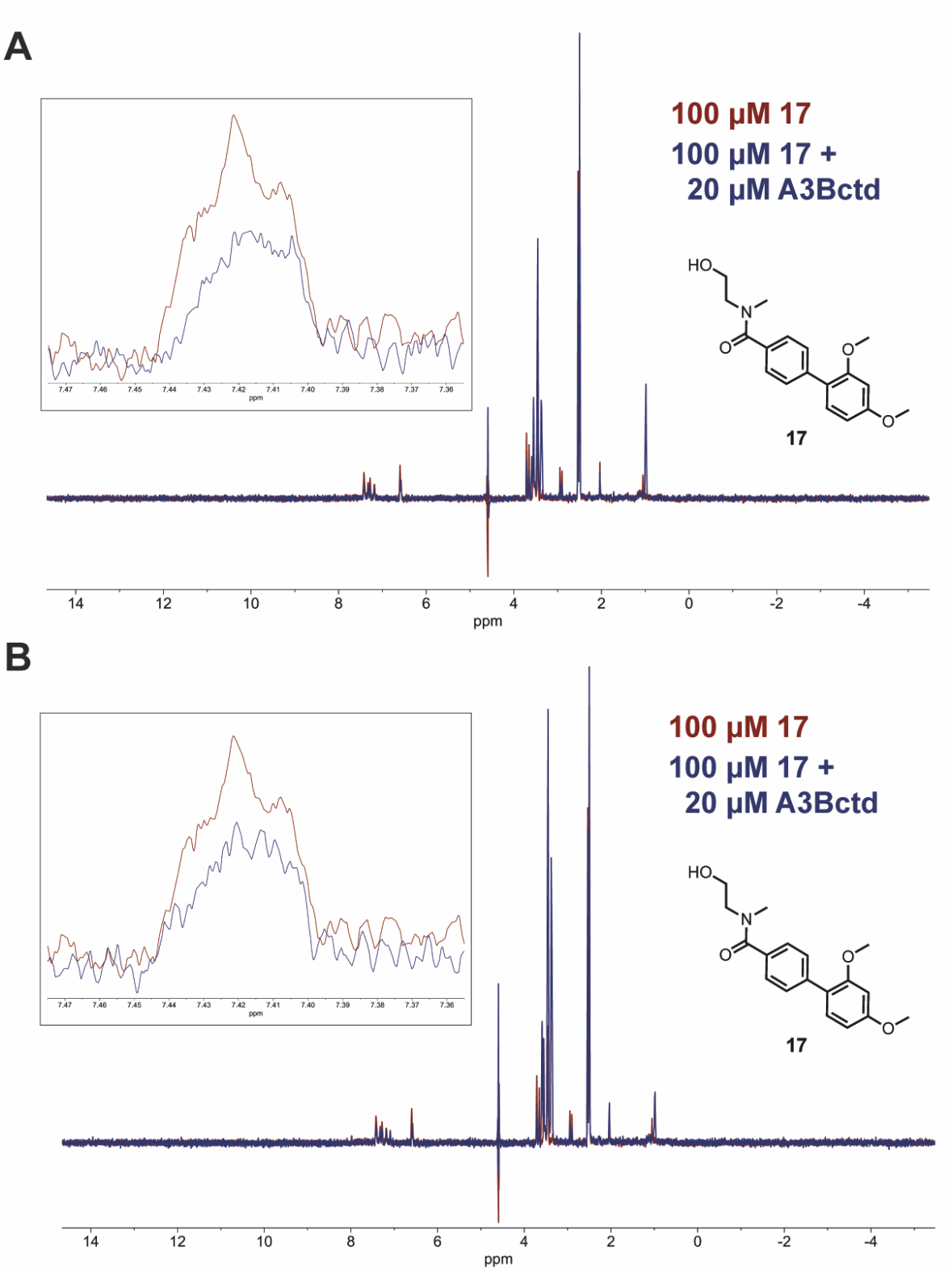

Figure S57. Biological replicate 1 (A) and 2 (B) of ligand-observed ^{1}H CPMG NMR, measuring the binding of **17** to A3Bctd. Red spectrum is compound alone, blue spectrum is compound incubated with protein. Peak used to measure signal attenuation is at 7.42 ppm. Spectra are normalized to DMSO peak at 2.5 ppm.

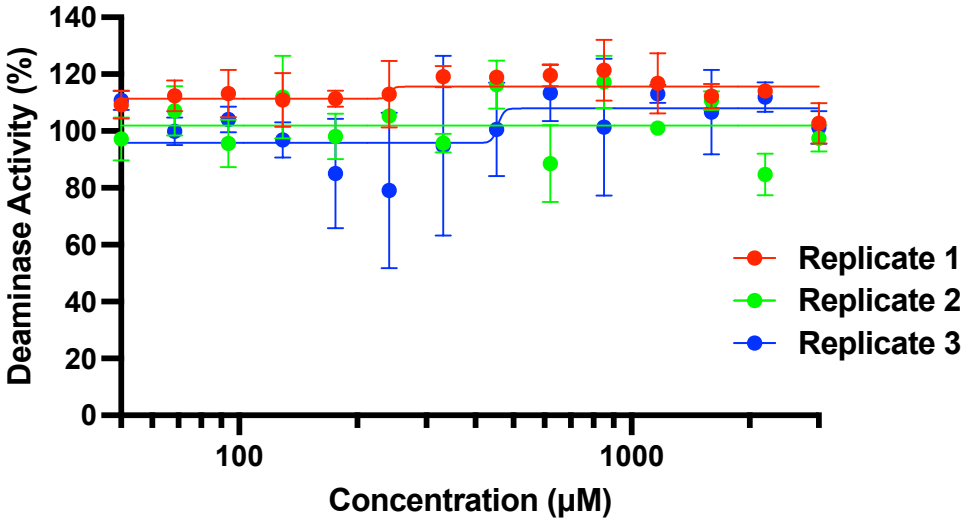

Figure S58. Three biological replicates of the deaminase activity assay with A3A against **1**. Each point is mean ± standard deviation of N = 3 technical replicates. IC_{50} values were unable to be determined.

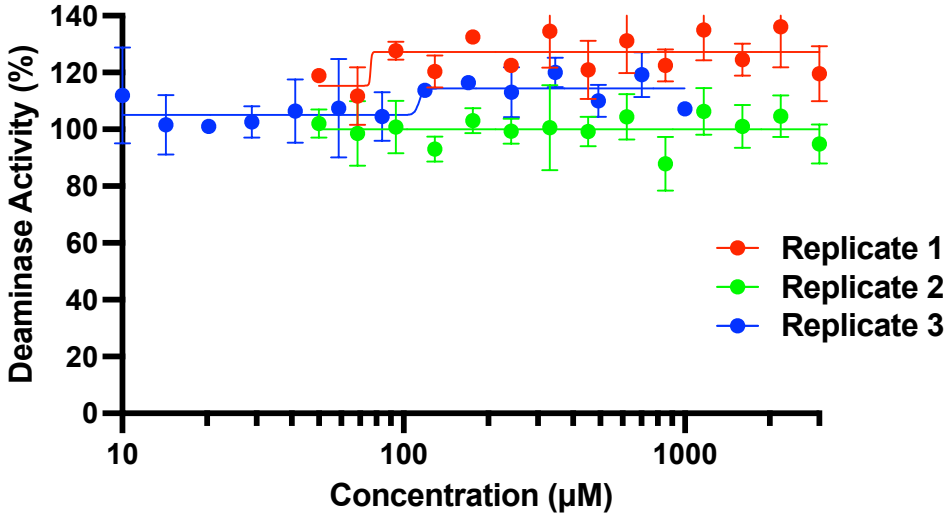

Figure S59. Three biological replicates of the deaminase activity assay with A3A against **2**. Each point is mean ± standard deviation of N = 3 technical replicates. IC_{50} values were unable to be determined.

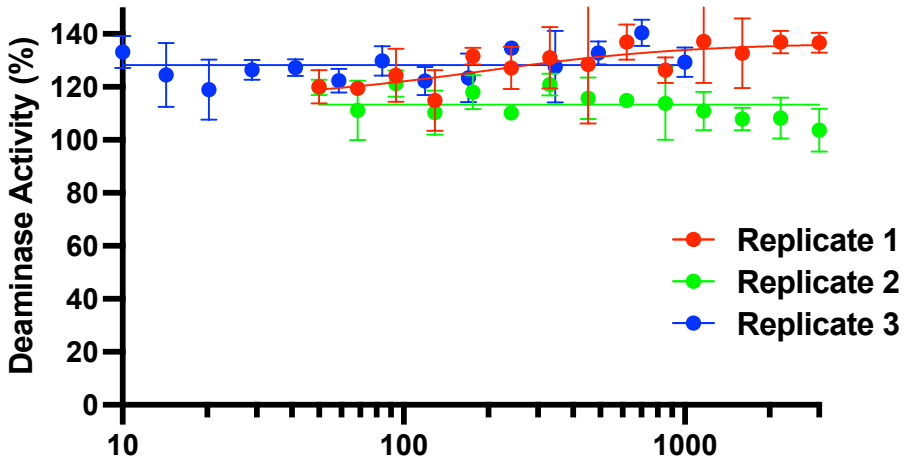

Figure S60. Three biological replicates of the deaminase activity assay with A3A against **3**. Each point is mean ± standard deviation of N = 3 technical replicates. IC_{50} values were unable to be determined.

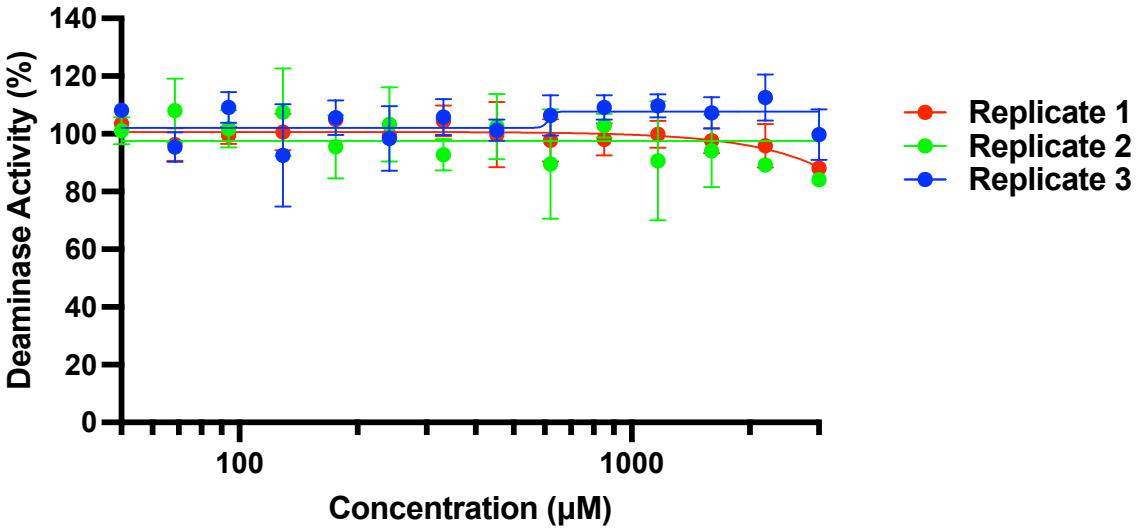

Figure S61. Three biological replicates of the deaminase activity assay with A3A against **4**. Each point is mean ± standard deviation of N = 3 technical replicates. IC_{50} values were unable to be determined.

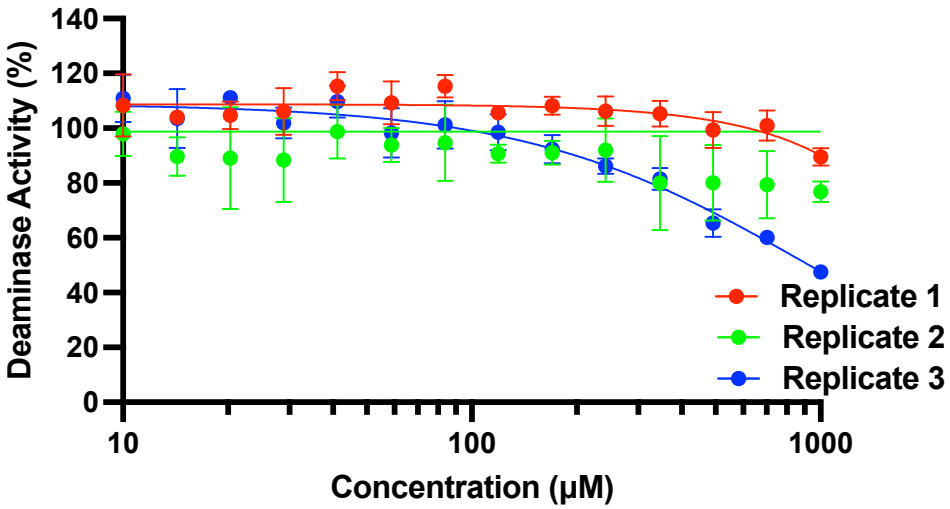

Figure S62. Three biological replicates of the deaminase activity assay with A3A against **6**. Each point is mean ± standard deviation of N = 3 technical replicates. IC_{50} values were unable to be determined.

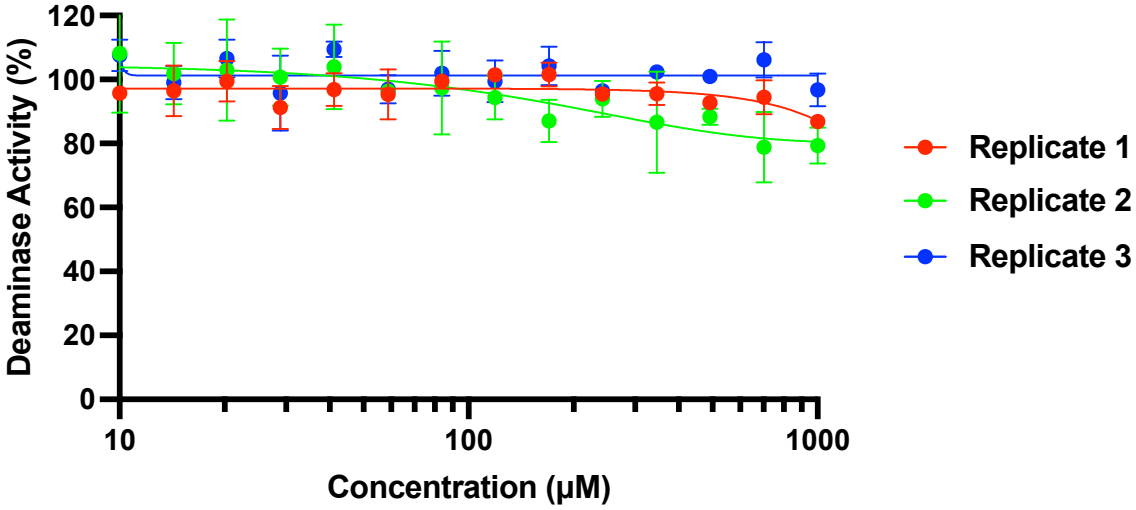

Figure S63. Three biological replicates of the deaminase activity assay with A3A against **7**. Each point is mean ± standard deviation of N = 3 technical replicates. IC_{50} values were unable to be determined.

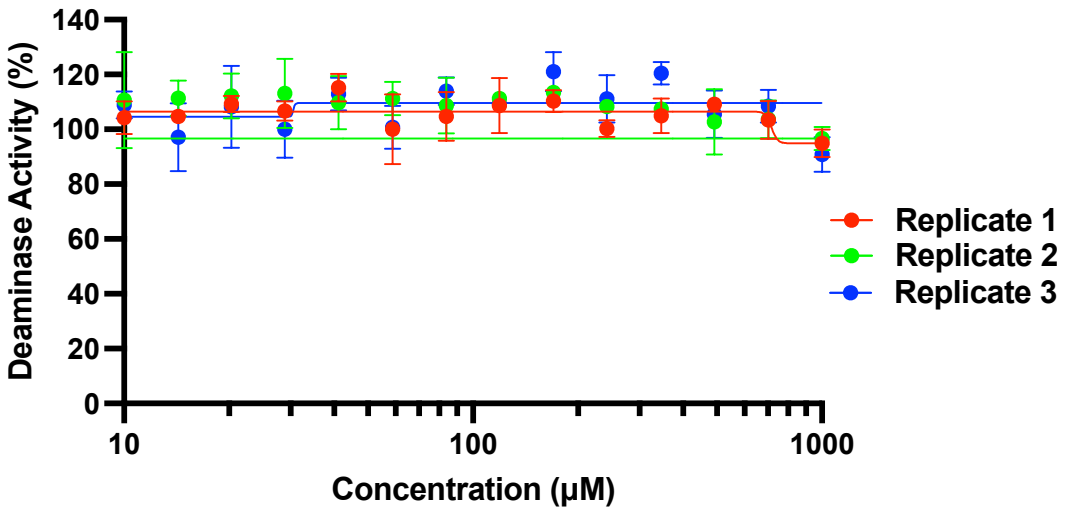

Figure S64. Three biological replicates of the deaminase activity assay with A3A against **8**. Each point is mean ± standard deviation of N = 3 technical replicates. IC_{50} values were unable to be determined.

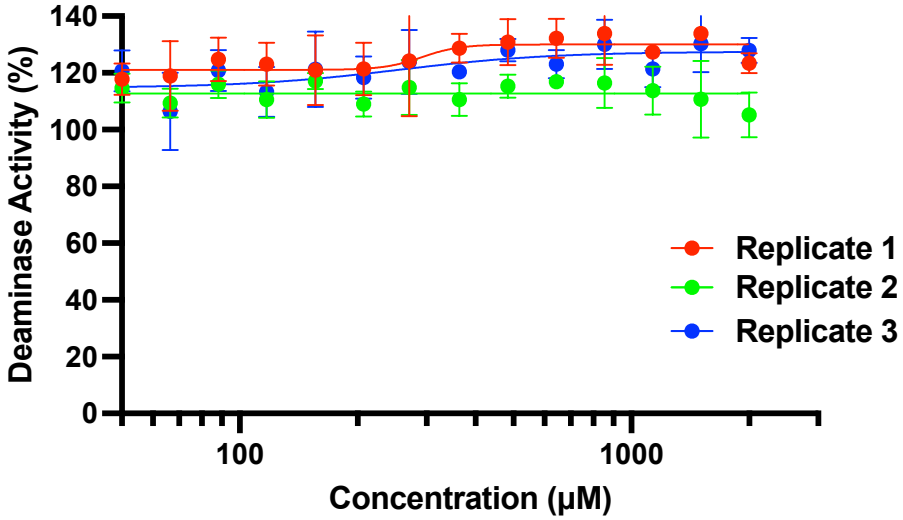

Figure S65. Three biological replicates of the deaminase activity assay with A3A against **9**. Each point is mean ± standard deviation of N = 3 technical replicates. IC_{50} values were unable to be determined.

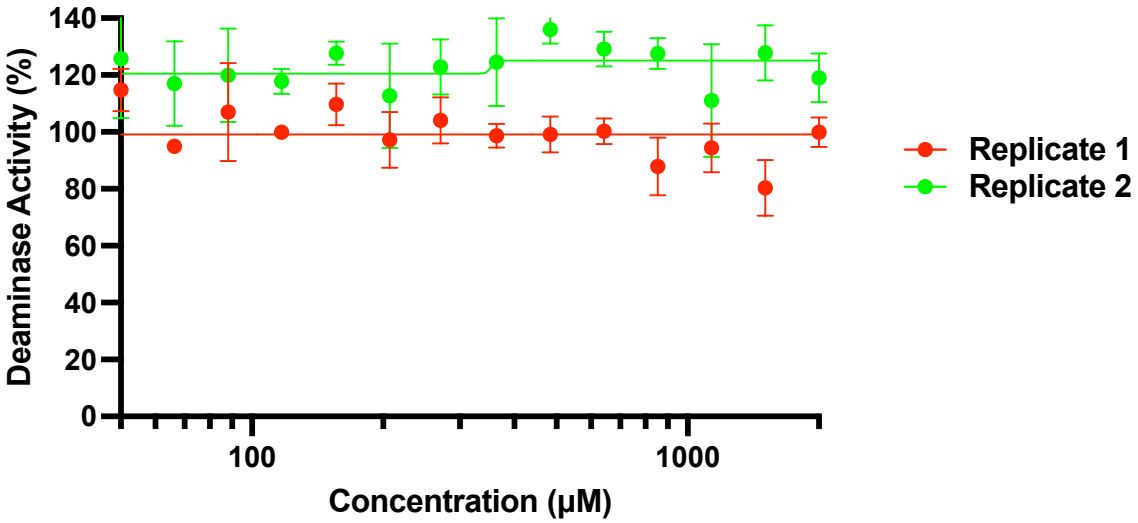

Figure S66. Two biological replicates of the deaminase activity assay with A3A against **10***. Each point is mean ± standard deviation of N = 3 technical replicates. IC_{50} values were unable to be determined.

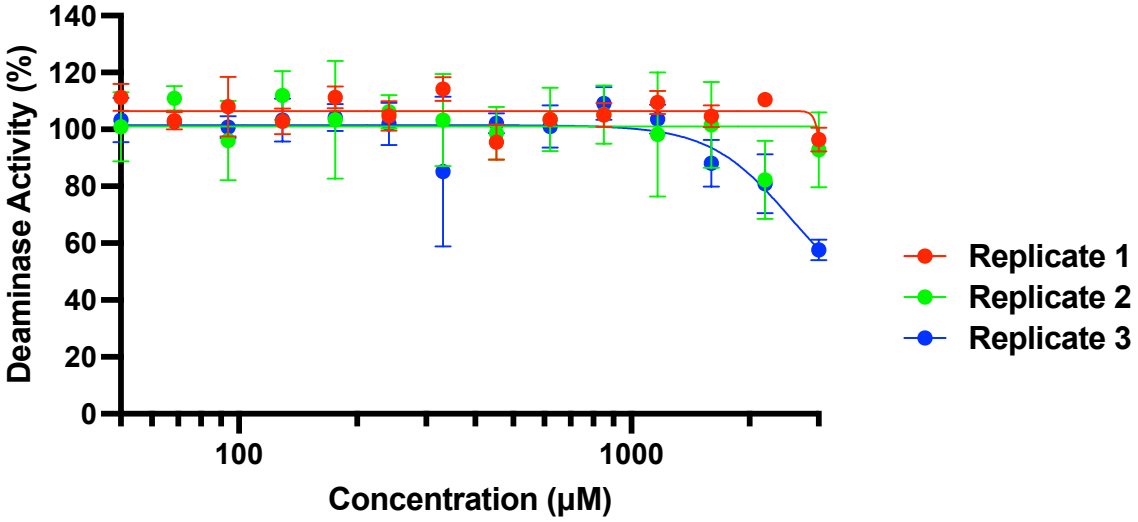

Figure S67. Three biological replicates of the deaminase activity assay with A3A against **11**. Each point is mean ± standard deviation of N = 3 technical replicates. IC_{50} values were unable to be determined.

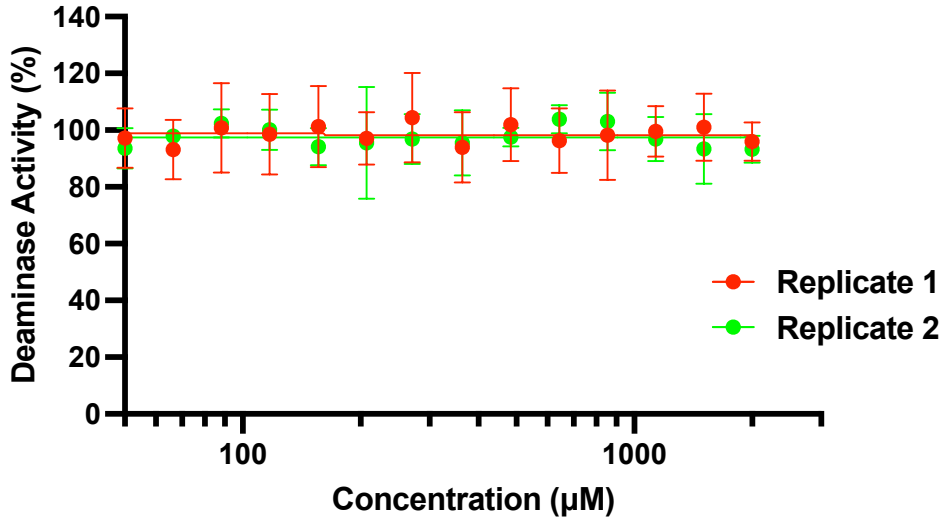

Figure S68. Two biological replicates of the deaminase activity assay with A3A against **12**. Each point is mean ± standard deviation of N = 3 technical replicates. IC_{50} values were unable to be determined.

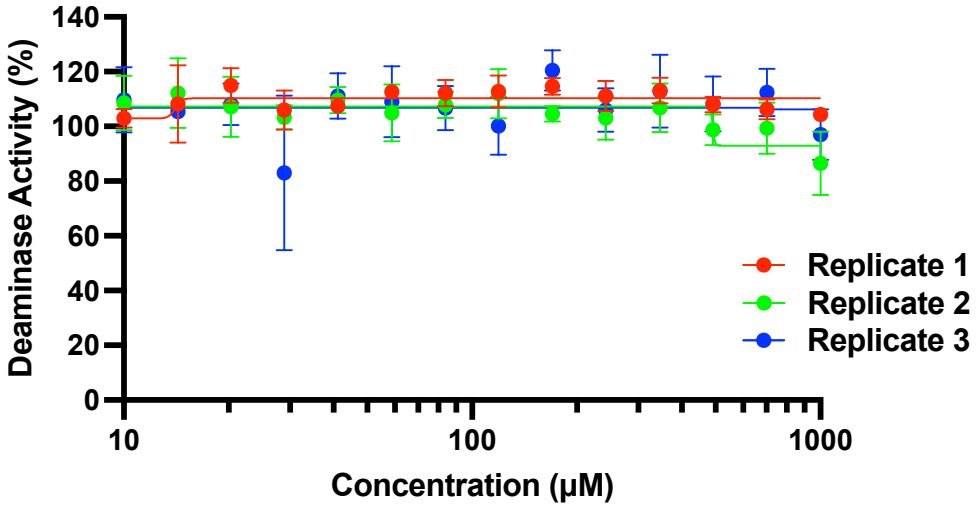

Figure S69. Three biological replicates of the deaminase activity assay with A3A against **13**. Each point is mean ± standard deviation of N = 3 technical replicates. IC_{50} values were unable to be determined.

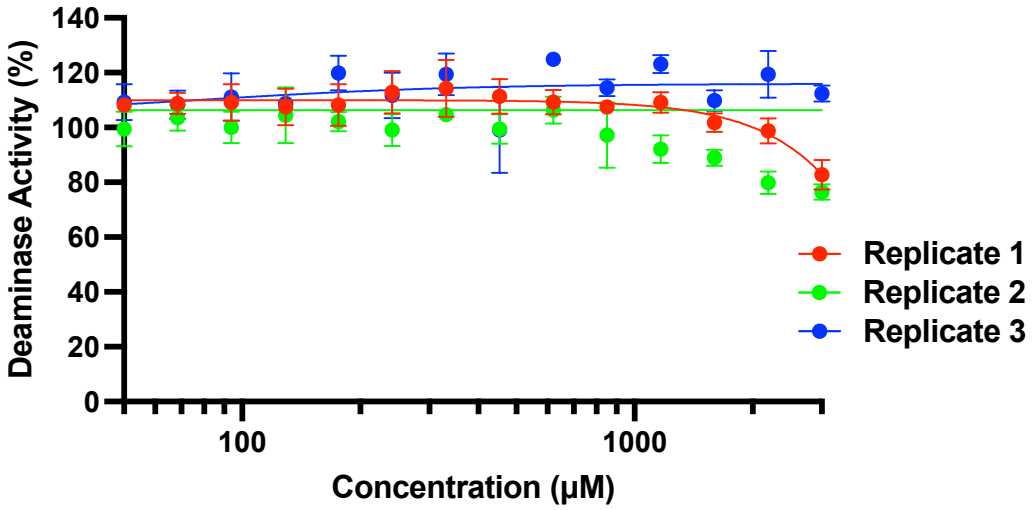

Figure S70. Three biological replicates of the deaminase activity assay with A3A against **14**. Each point is mean ± standard deviation of N = 3 technical replicates. IC_{50} values were unable to be determined.

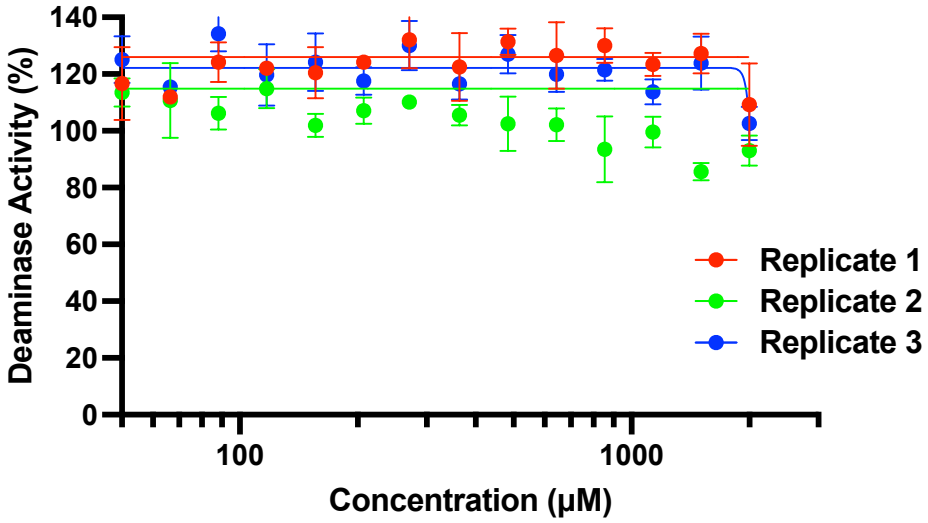

Figure S71. Three biological replicates of the deaminase activity assay with A3Bctd against **15**. Each point is mean ± standard deviation of N = 3 technical replicates. IC_{50} values were unable to be determined.

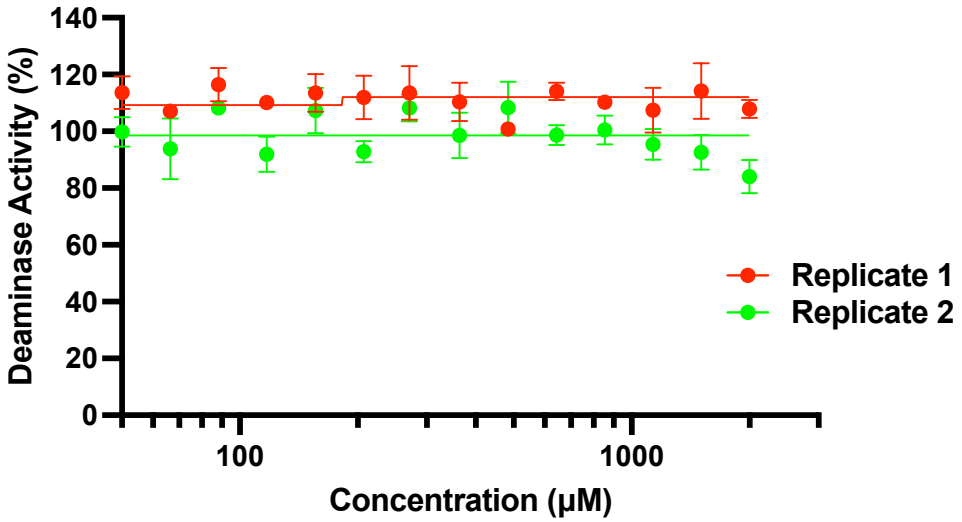

Figure S72. Two biological replicates of the deaminase activity assay with A3A against **16**. Each point is mean ± standard deviation of N = 3 technical replicates. IC_{50} values were unable to be determined.

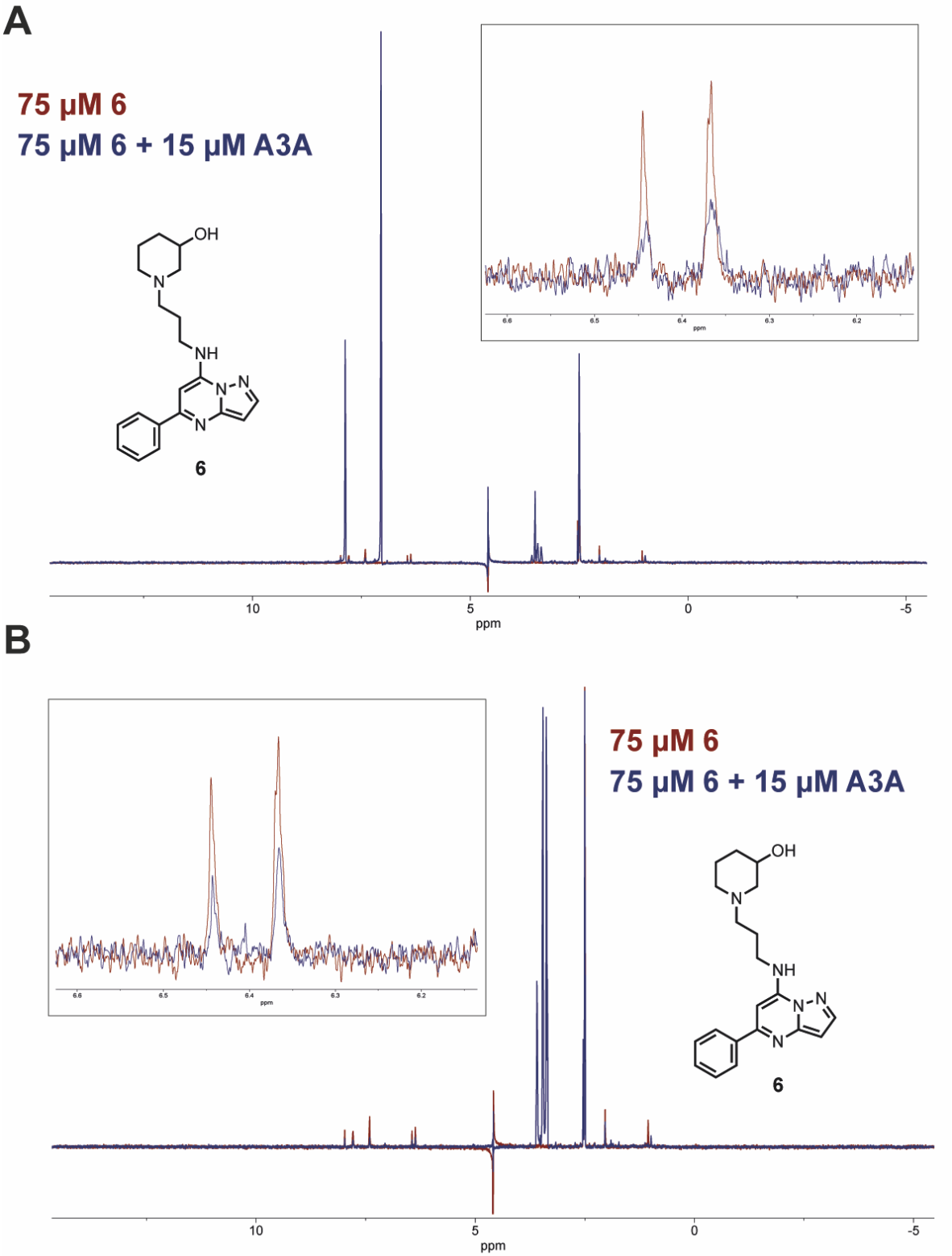

Figure S73. Biological replicate 1 (A) and 2 (B) of ligand-observed ^{1}H CPMG NMR, measuring the binding of **6** to A3A. Red spectrum is compound alone, blue spectrum is compound incubated with protein. Peak used to measure signal attenuation is at 6.37 ppm. Spectra are normalized to DMSO peak at 2.5 ppm.

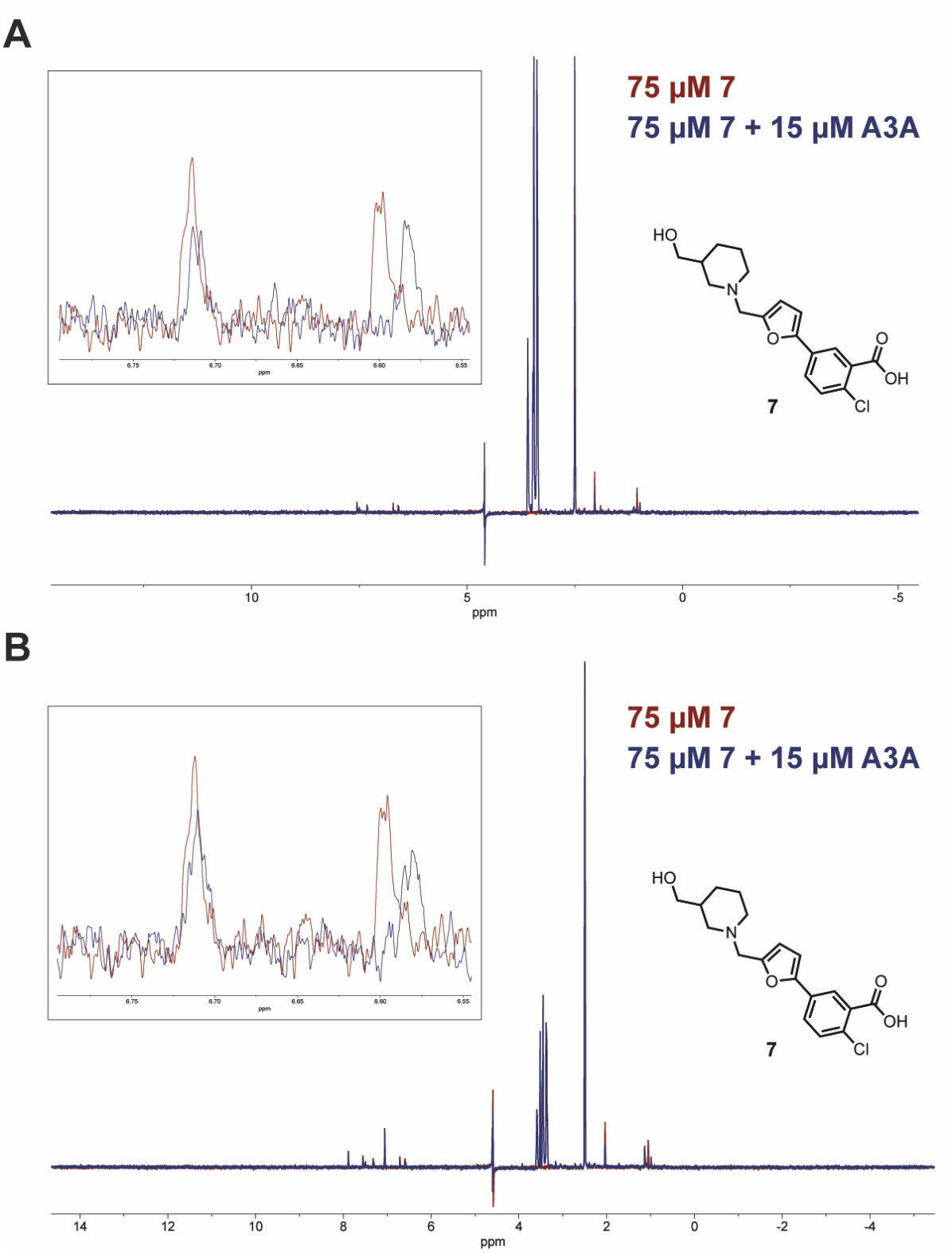

Figure S74. Biological replicate 1 (A) and 2 (B) of ligand-observed ^{1}H CPMG NMR, measuring the binding of **7** to A3A. Red spectrum is compound alone, blue spectrum is compound incubated with protein. Peak used to measure signal attenuation is at 6.72 ppm. Spectra are normalized to DMSO peak at 2.5 ppm.

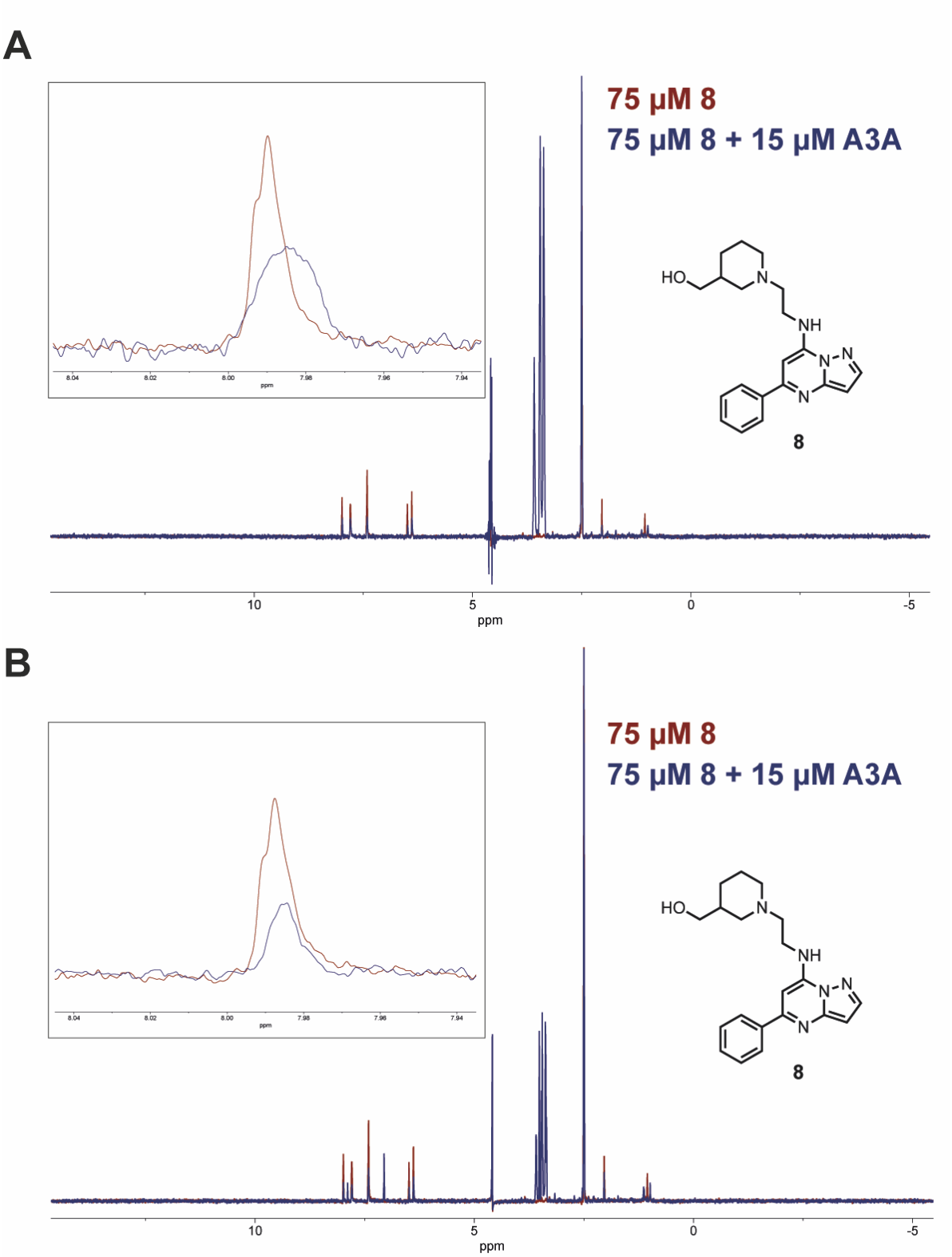

Figure S75. Biological replicate 1 (A) and 2 (B) of ligand-observed ^{1}H CPMG NMR, measuring the binding of **8** to A3A. Red spectrum is compound alone, blue spectrum is compound incubated with protein. Peak used to measure signal attenuation is at 7.99 ppm. Spectra are normalized to DMSO peak at 2.5 ppm.

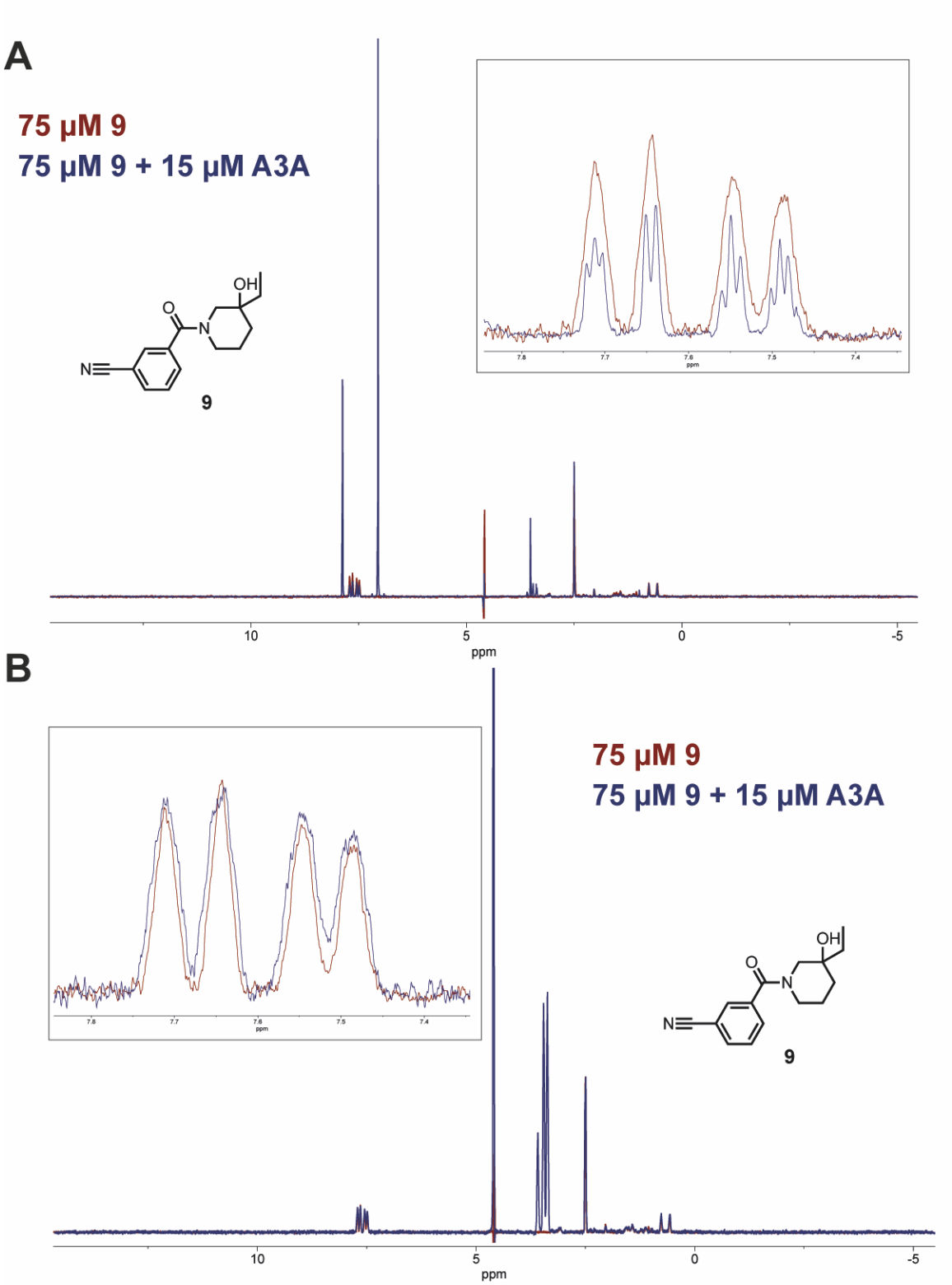

Figure S76. Biological replicate 1 (A) and 2 (B) of ligand-observed ^{1}H CPMG NMR, measuring the binding of **9** to A3A. Red spectrum is compound alone, blue spectrum is compound incubated with protein. Peak used to measure signal attenuation is at 7.55 ppm. Spectra are normalized to DMSO peak at 2.5 ppm.

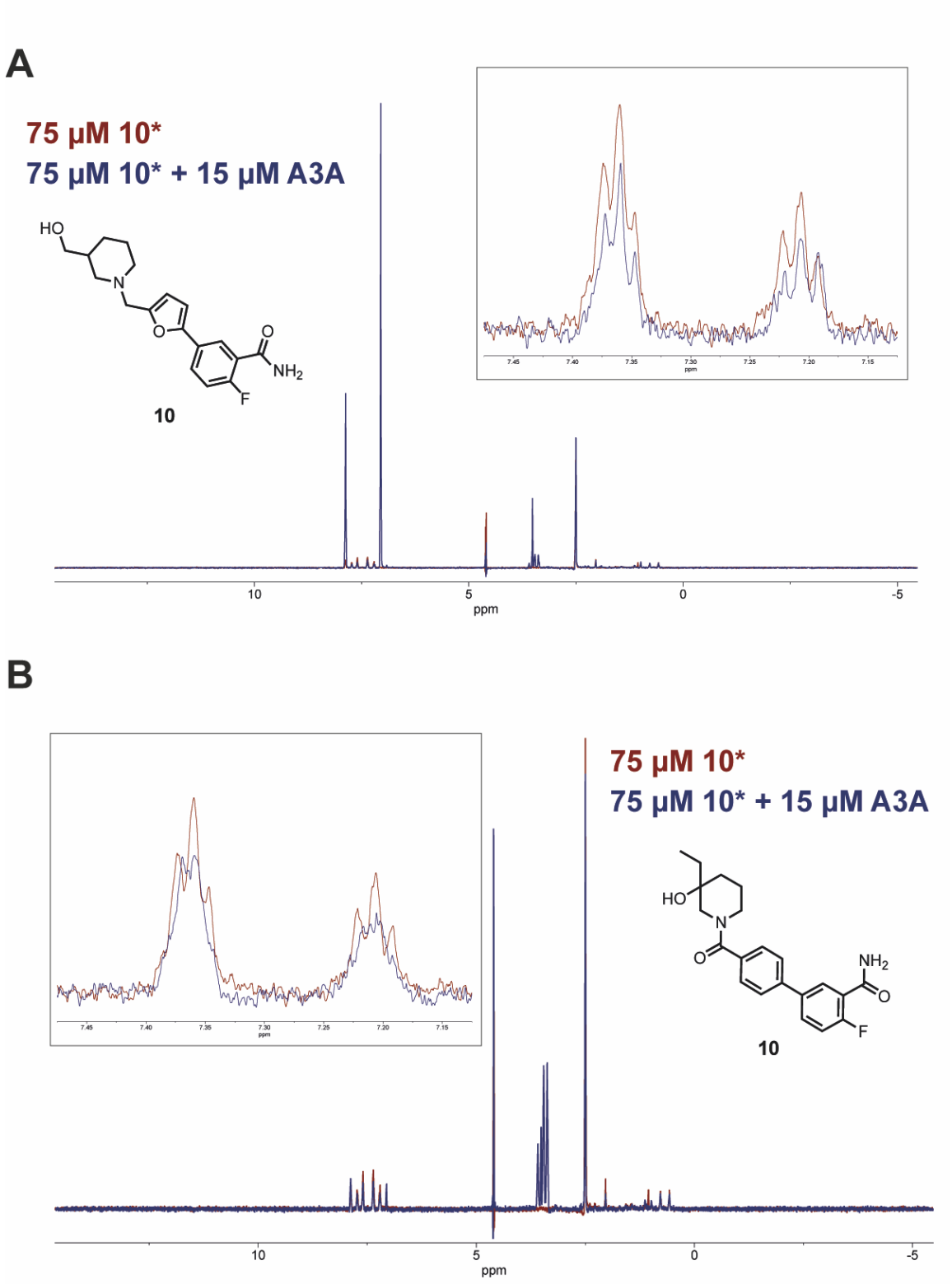

Figure S77. Biological replicate 1 (A) and 2 (B) of ligand-observed ^{1}H CPMG NMR, measuring the binding of **10*** to A3A. Red spectrum is compound alone, blue spectrum is compound incubated with protein. Peak used to measure signal attenuation is at 7.36 ppm. Spectra are normalized to DMSO peak at 2.5 ppm.

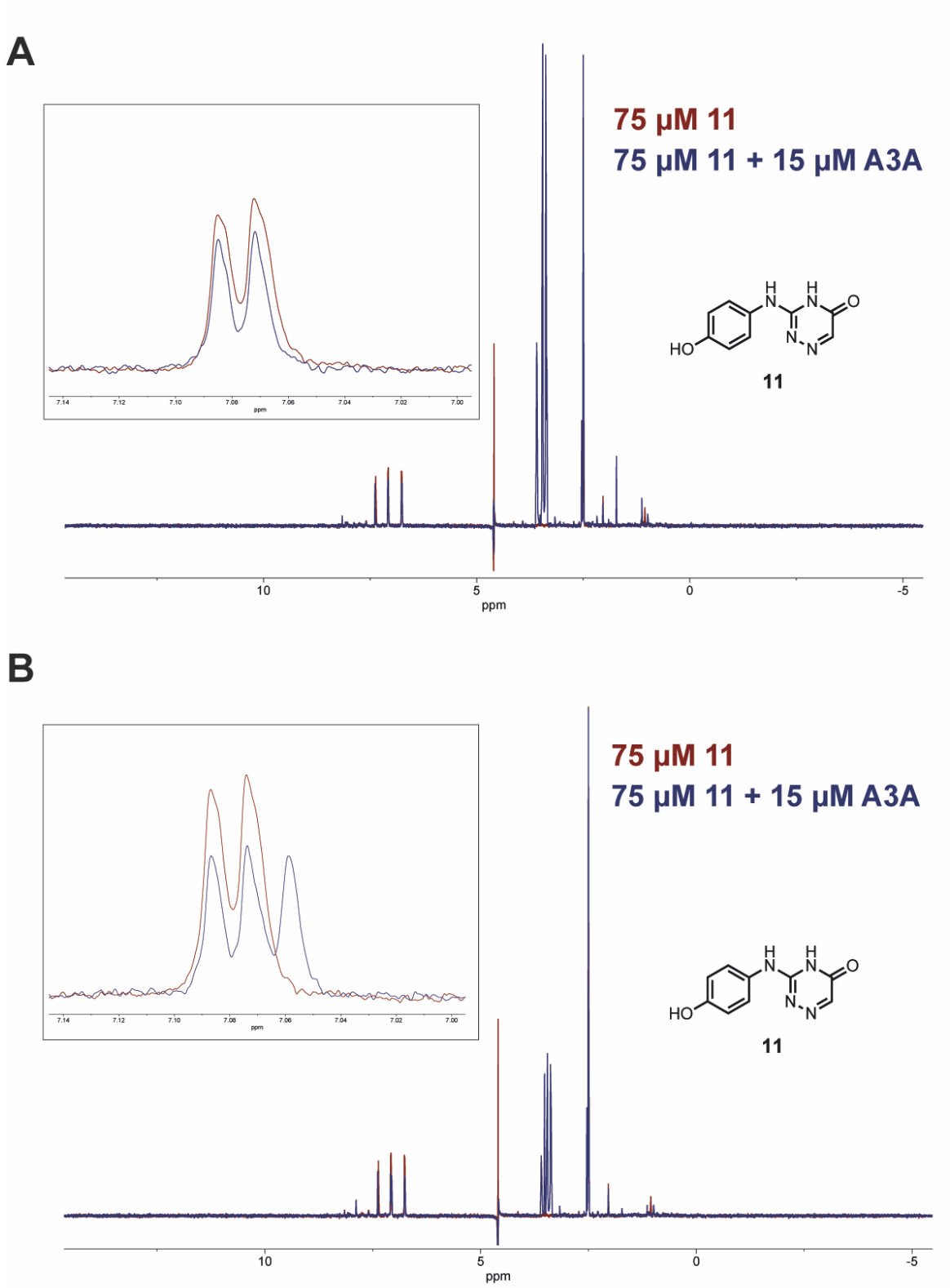

Figure S78. Biological replicate 1 (A) and 2 (B) of ligand-observed ^{1}H CPMG NMR, measuring the binding of **11** to A3A. Red spectrum is compound alone, blue spectrum is compound incubated with protein. Peak used to measure signal attenuation is at 7.08 ppm. Spectra are normalized to DMSO peak at 2.5 ppm.

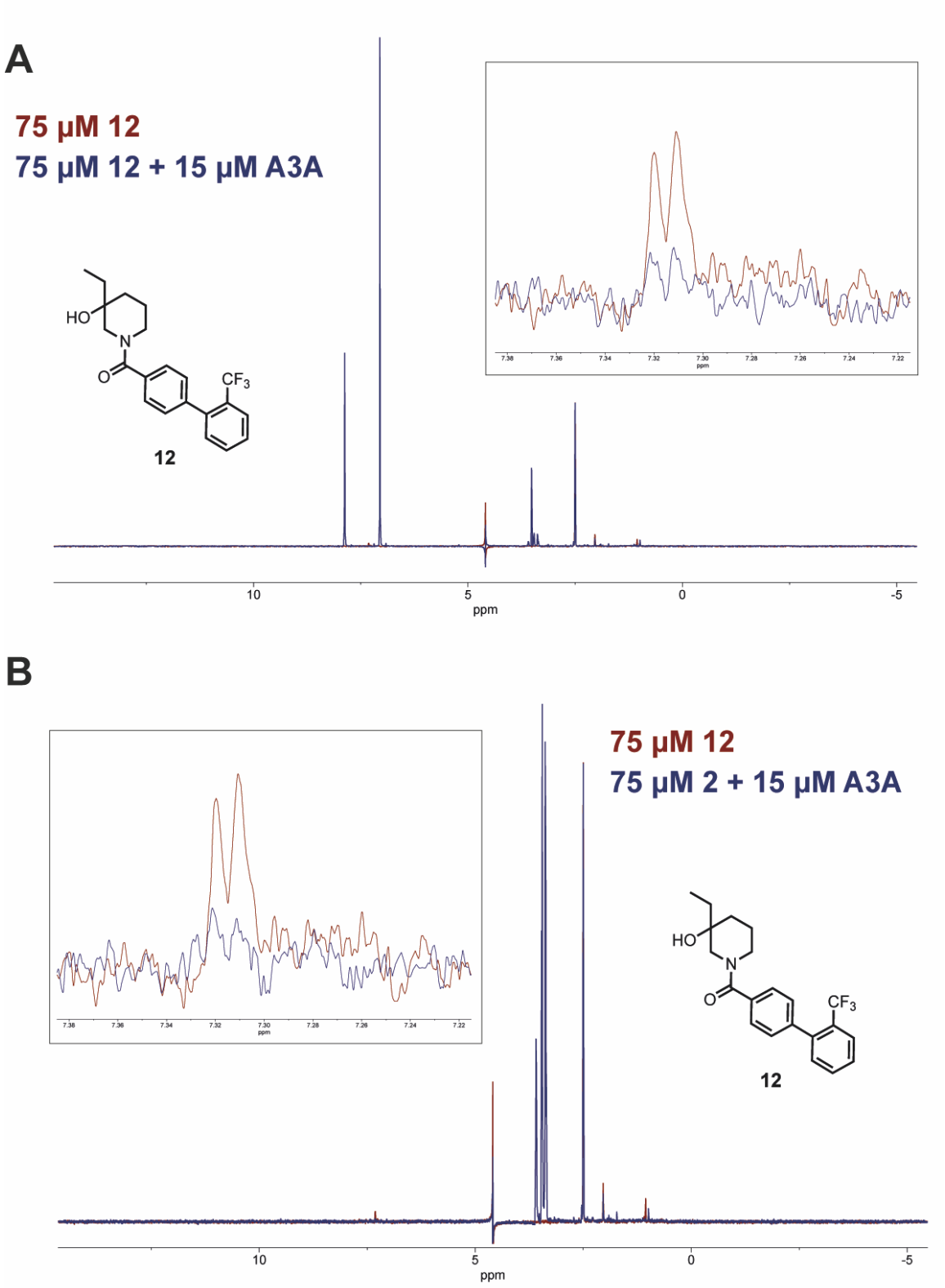

Figure S79. Biological replicate 1 (A) and 2 (B) of ligand-observed ^{1}H CPMG NMR, measuring the binding of **12** to A3A. Red spectrum is compound alone, blue spectrum is compound incubated with protein. Peak used to measure signal attenuation is at 7.32 ppm. Spectra are normalized to DMSO peak at 2.5 ppm.

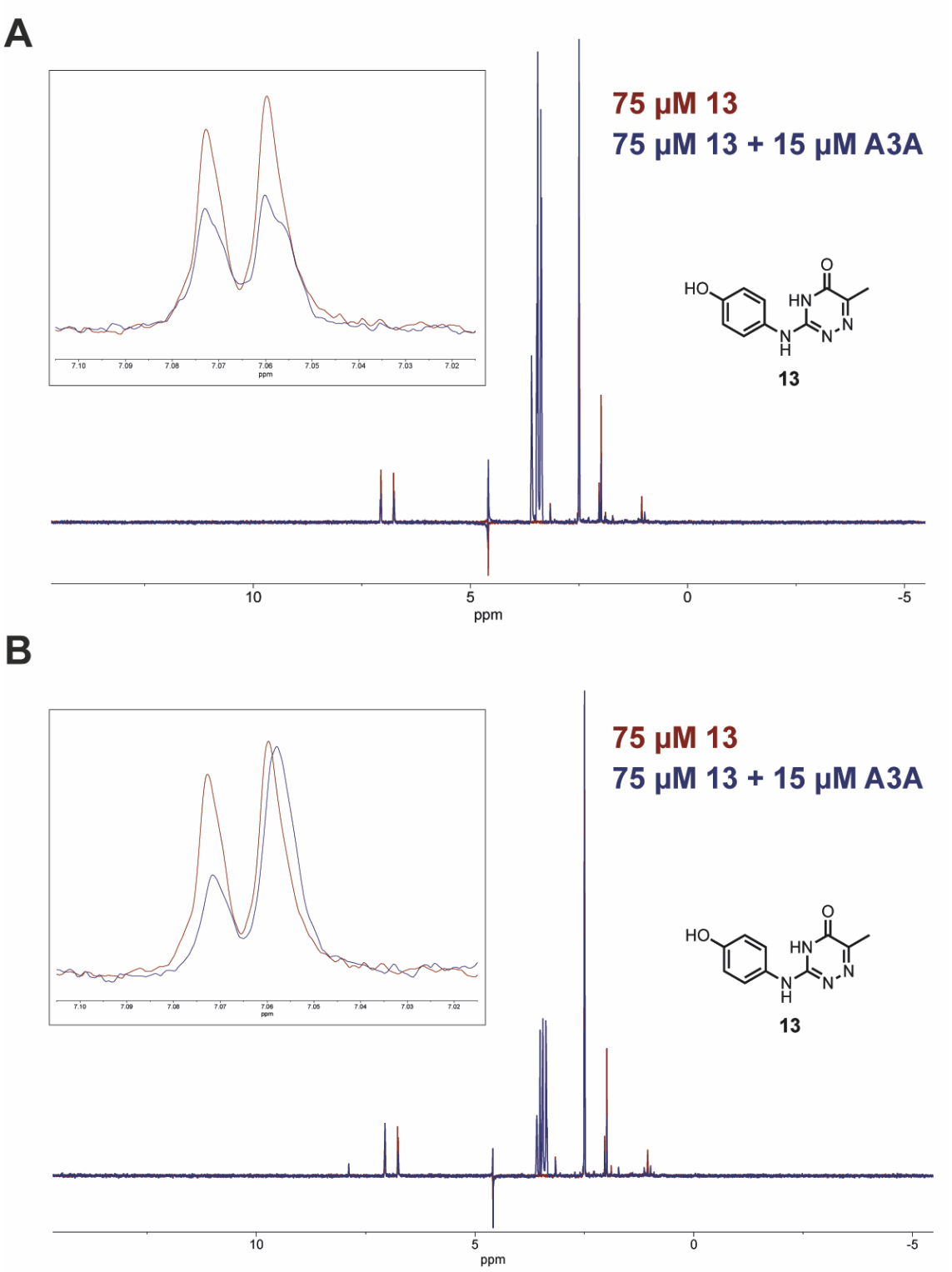

Figure S80. Biological replicate 1 (A) and 2 (B) of ligand-observed ^{1}H CPMG NMR, measuring the binding of **13** to A3A. Red spectrum is compound alone, blue spectrum is compound incubated with protein. Peak used to measure signal attenuation is at 7.07 ppm. Spectra are normalized to DMSO peak at 2.5 ppm.

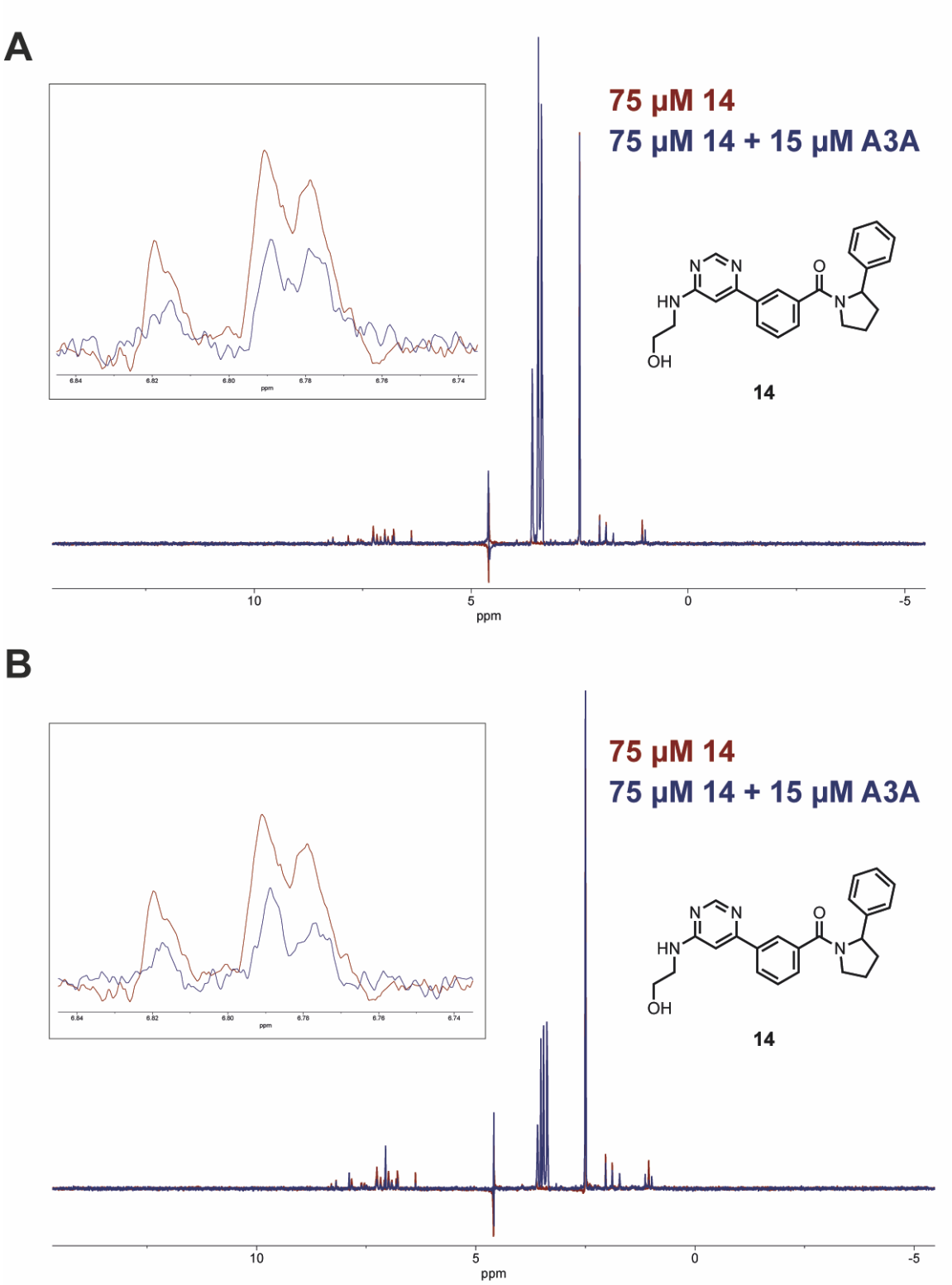

Figure S81. Biological replicate 1 (A) and 2 (B) of ligand-observed ^{1}H CPMG NMR, measuring the binding of **14** to A3A. Red spectrum is compound alone, blue spectrum is compound incubated with protein. Peak used to measure signal attenuation is at 6.79 ppm. Spectra are normalized to DMSO peak at 2.5 ppm.

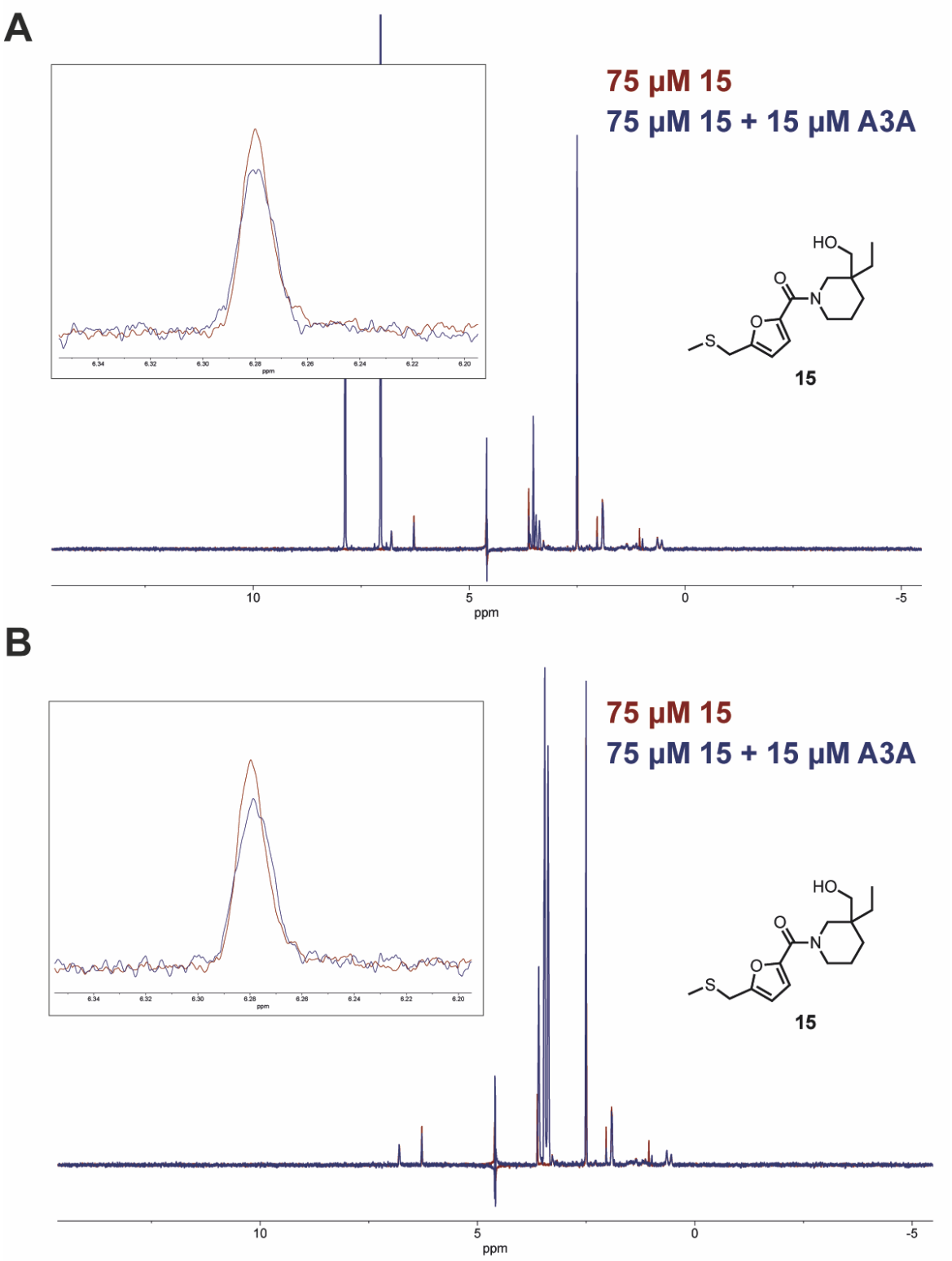

Figure S82. Biological replicate 1 (A) and 2 (B) of ligand-observed ^{1}H CPMG NMR, measuring the binding of **15** to A3A. Red spectrum is compound alone, blue spectrum is compound incubated with protein. Peak used to measure signal attenuation is at 6.28 ppm. Spectra are normalized to DMSO peak at 2.5 ppm.

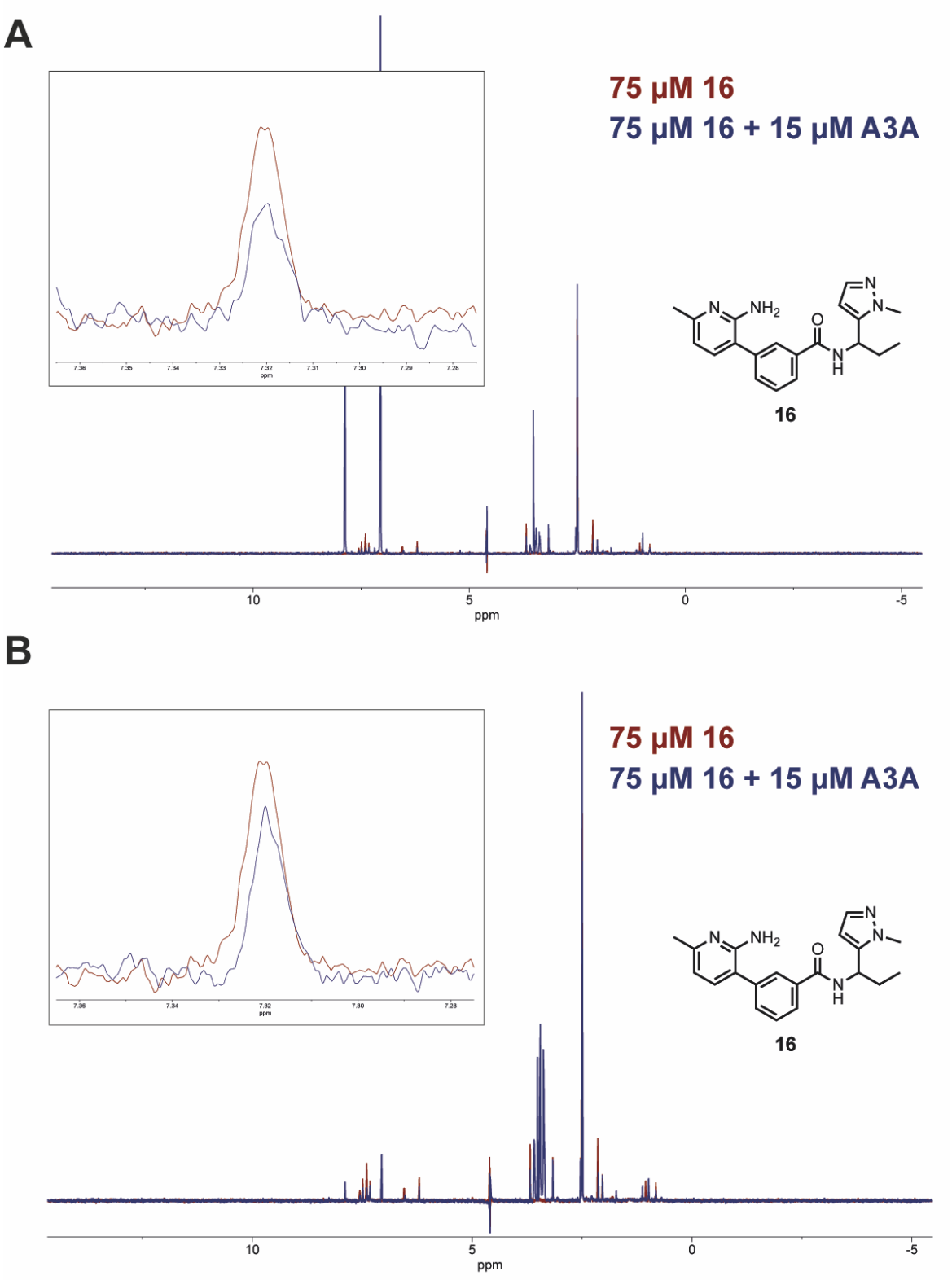

Figure S83. Biological replicate 1 (A) and 2 (B) of ligand-observed ^{1}H CPMG NMR, measuring the binding of **16** to A3A. Red spectrum is compound alone, blue spectrum is compound incubated with protein. Peak used to measure signal attenuation is at 7.32 ppm. Spectra are normalized to DMSO peak at 2.5 ppm.

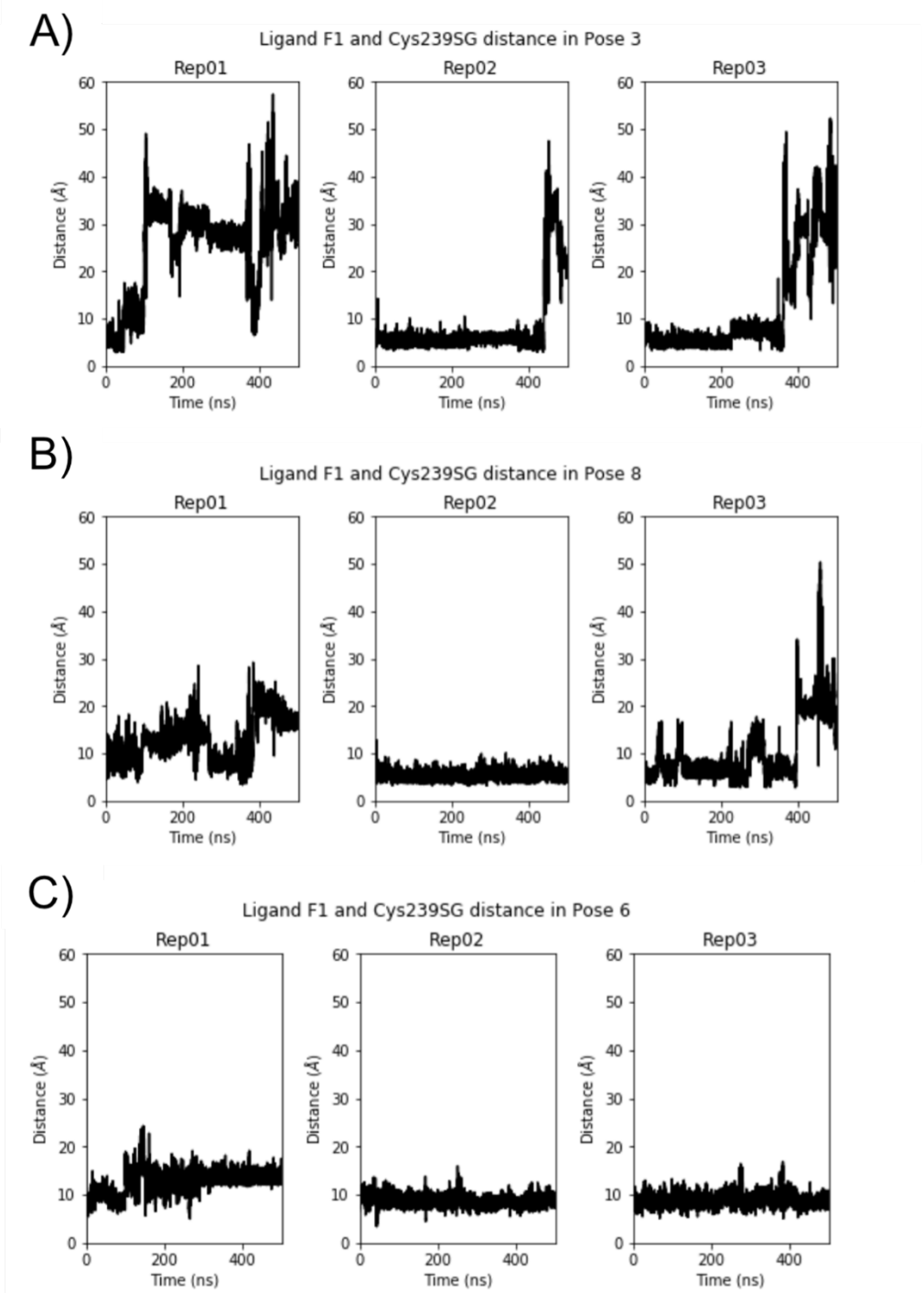

Figure S84. Initial binding pose stabilities between A3B-ctd and allosteric ligand **10**. Distance between ligand 4-fluoride atom and C239 SG atom of A3Bctd through 100ns of A) pose3, B) pose 8, and C) pose 6. These initial simulations and distance metrics were used evaluate the stability of the ligand in the allosteric pocket, which determined the final binding pose (pose6) to be used in further simulations.

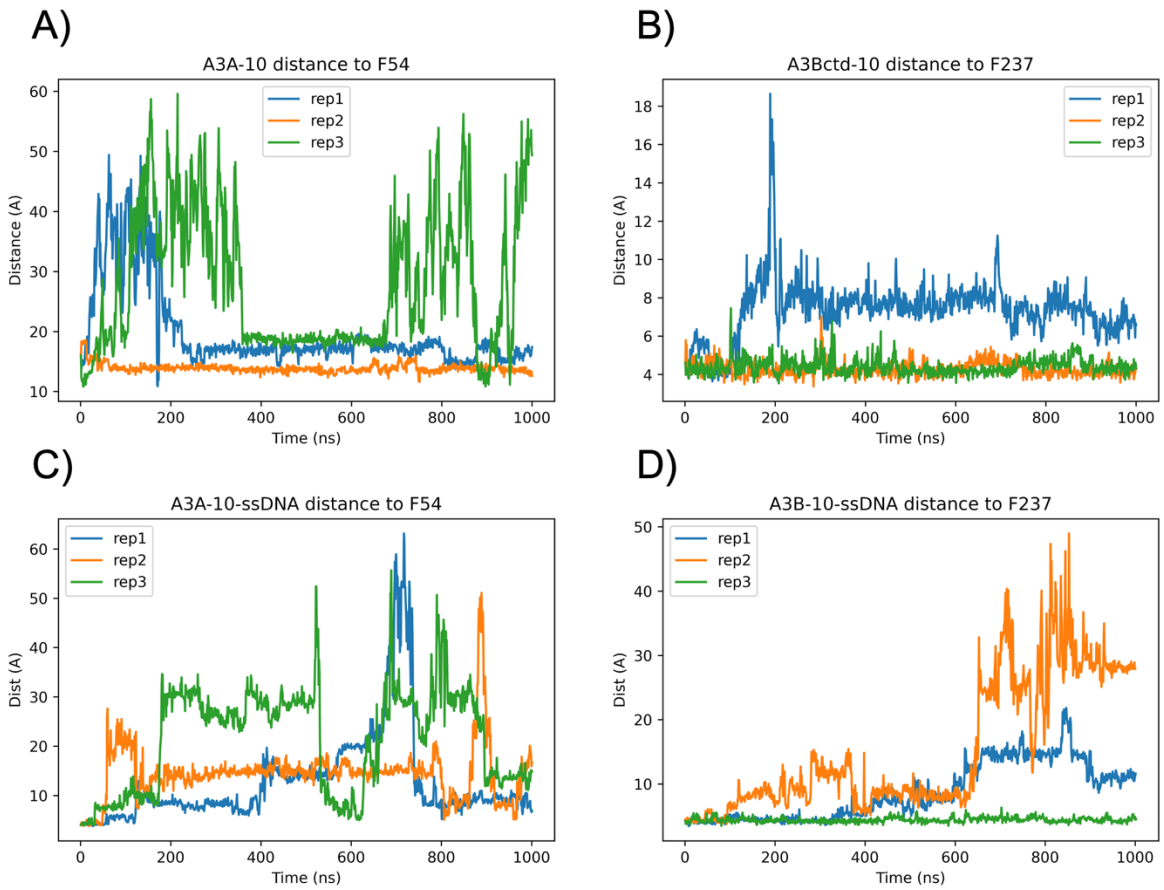

Figure S85. Distances between **10** and allosteric pocket COM (F237/F54 in A3Bctd and A3A respectively). Panels A & B show simulations of protein and **10** when ssDNA is not present. Panels C & D show simulations of protein, **10**, and ssDNA.

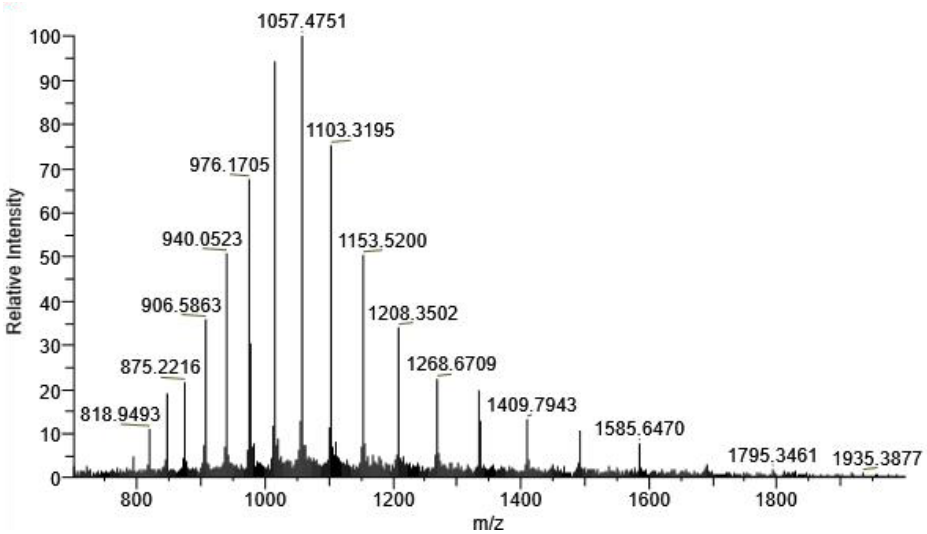

Figure S86. One biological replicate m/z spectrum of DMSO treated A3Bctd (25 μM).

Xtract Masses Table					
Monoisotopic Mass	Sum Intensity	Number of Charge States	Average Charge	Delta Mass	Relative Abundance
25339.2008	3684786.55	14	24.13	0.0000	100.0000

Table S5. Deconvolution intensities of **Figure S86**.

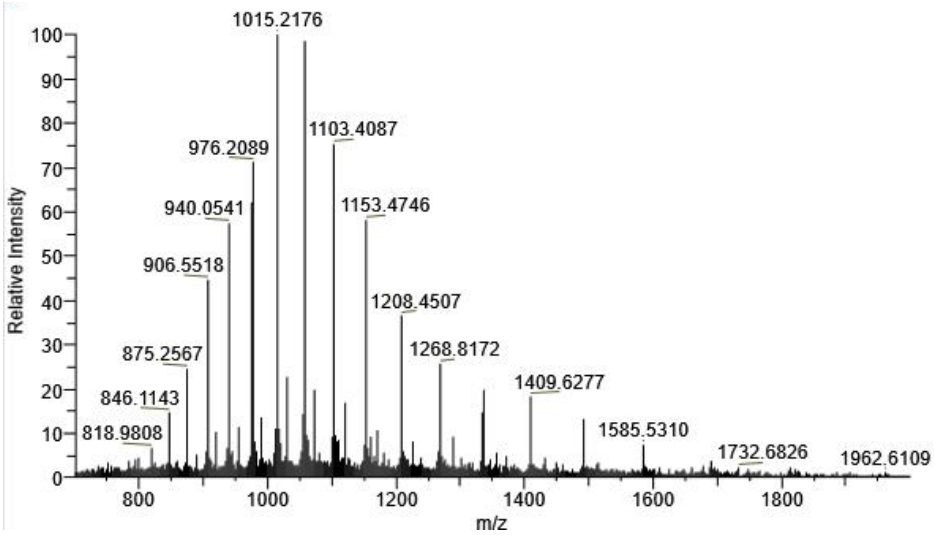

Figure S87. One biological replicate m/z spectrum of **24** (25 μM, 1X) treated A3Bctd (25 μM), incubated for one hour.

Xtract Masses Table					
Monoisotopic Mass	Sum Intensity	Number of Charge States	Average Charge	Delta Mass	Relative Abundance
25339.2062	2731371.78	15	23.94	0.0000	100.0000
25722.3857	385867.96	9	24.44	383.1795	14.1273

Table S6. Deconvolution intensities of **Figure S87.**

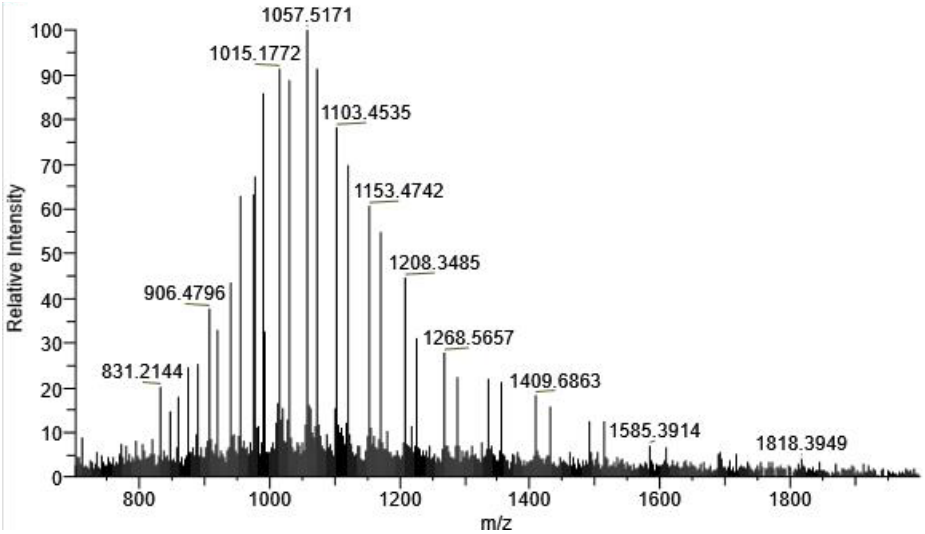

Figure S88. One biological replicate m/z spectrum of **24** (125 μM, 5X) treated A3Bctd (25 μM), incubated for one hour.

Xtract Masses Table					
Monoisotopic Mass	Sum Intensity	Number of Charge States	Average Charge	Delta Mass	Relative Abundance
25339.1716	3039076.14	12	24.16	0.0000	100.0000
25721.3676	2793136.65	11	24.47	382.1960	91.9074

Table S7. Deconvolution intensities of **Figure S88.**

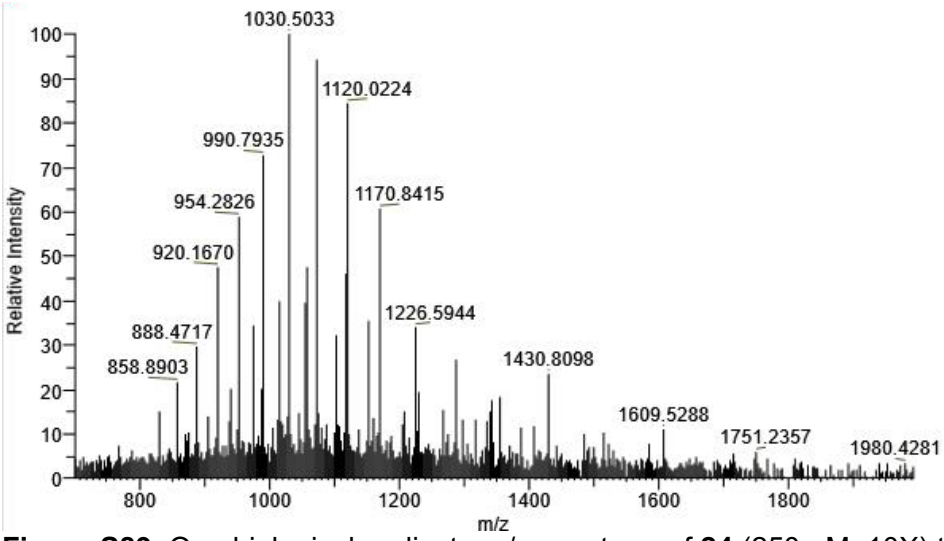

Figure S89. One biological replicate m/z spectrum of **24** (250 μM, 10X) treated A3Bctd (25 μM), incubated for one hour.

Xtract Masses Table					
Monoisotopic Mass	Sum Intensity	Number of Charge States	Average Charge	Delta Mass	Relative Abundance
25721.3589	2880461.97	10	24.53	0.0000	100.0000
25338.2303	740631.51	5	25.23	-383.1286	25.7122

Table S8. Deconvolution intensities of **Figure S89.**

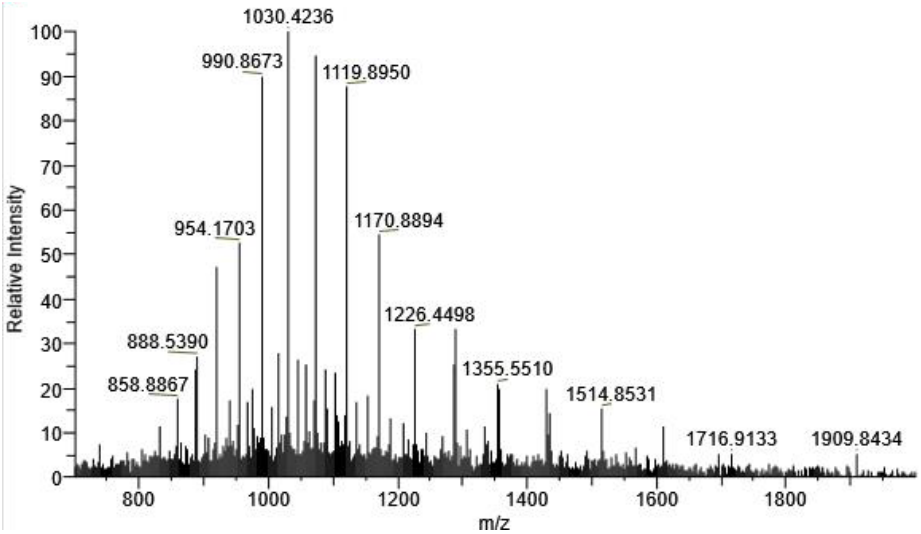

Figure S90. One biological replicate m/z spectrum of **24** (500 µM, 20X) treated A3Bctd (25 µM), incubated for one hour.

Xtract Masses Table					
Monoisotopic Mass	Sum Intensity	Number of Charge States	Average Charge	Delta Mass	Relative Abundance
25722.3730	3486301.84	12	24.19	0.0000	100.0000
25338.2100	422157.39	5	23.96	-384.1630	12.1090
26104.5488	209553.57	3	24.95	382.1758	6.0108

Table S9. Deconvolution intensities of **Figure S90.**

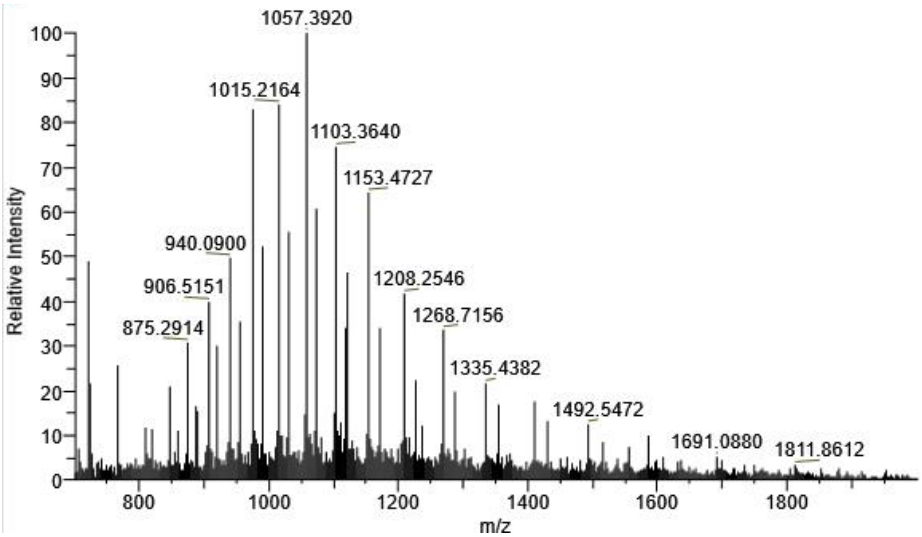

Figure S91. One biological replicate m/z spectrum of **24** (25 µM, 1X) treated A3Bctd (25 µM), incubated for three hours.

Xtract Masses Table					
Monoisotopic Mass	Sum Intensity	Number of Charge States	Average Charge	Delta Mass	Relative Abundance
25339.1902	859949.10	13	24.13	0.0000	100.0000
25721.4055	506509.67	11	24.39	382.2153	58.9000

Table S10. Deconvolution intensities of **Figure S91.**

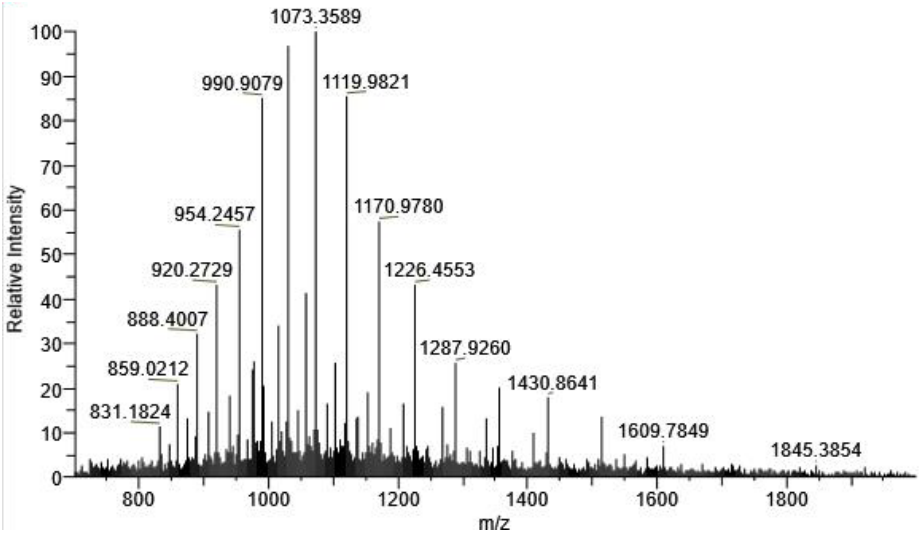

Figure S92. One biological replicate m/z spectrum of **24** (125 μM, 5X) treated A3Bctd (25 μM), incubated for three hours.

Xtract Masses Table					
Monoisotopic Mass	Sum Intensity	Number of Charge States	Average Charge	Delta Mass	Relative Abundance
25721.3915	2824750.54	13	24.34	0.0000	100.0000
25338.1922	684892.33	7	24.55	-383.1993	24.2461
26104.5388	203944.39	5	24.72	383.1473	7.2199

Table S11. Deconvolution intensities of **Figure S92.**

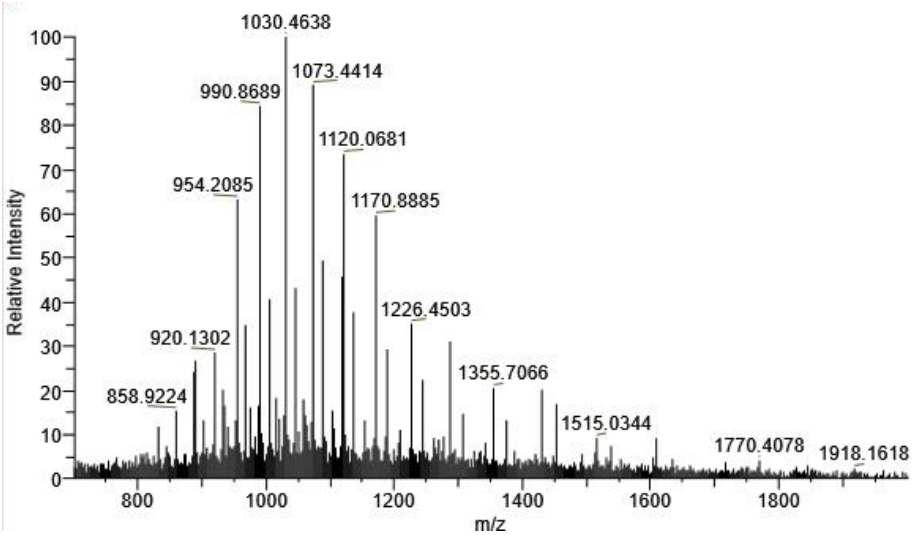

Figure S93. One biological replicate m/z spectrum of **24** (250 μM, 10X) treated A3Bctd (25 μM), incubated for three hours.

Xtract Masses Table					
Monoisotopic Mass	Sum Intensity	Number of Charge States	Average Charge	Delta Mass	Relative Abundance
25721.3369	3450587.76	12	24.46	0.0000	100.0000
26103.5700	477383.72	5	24.65	382.2331	13.8349
25338.2010	384890.32	5	23.87	-383.1359	11.1543

Table S12. Deconvolution intensities of **Figure S93.**

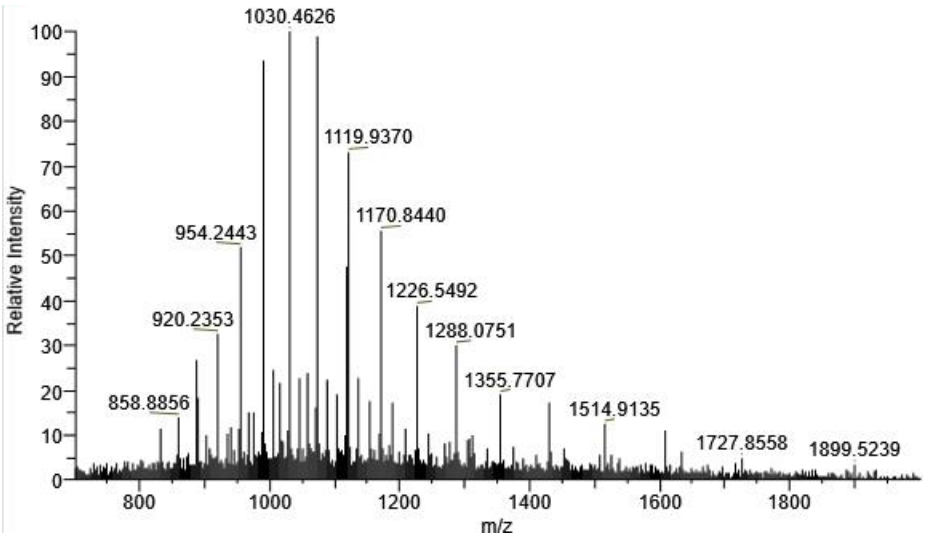

Figure S94. One biological replicate m/z spectrum of **24** (500 μM, 20X) treated A3Bctd (25 μM), incubated for three hours.

Xtract Masses Table					
Monoisotopic Mass	Sum Intensity	Number of Charge States	Average Charge	Delta Mass	Relative Abundance
25721.3789	1261041.70	12	24.67	0.0000	100.0000
26104.5200	612945.30	9	25.08	383.1411	48.6063
26487.6827	75978.06	3	24.92	766.3038	6.0250

Table S13. Deconvolution intensities of **Figure S94.**

Table S14. Average percent adduction of A3Bctd treated with **24** at variable concentration and time, from intact protein mass spectrometry deconvolution.

MW of species (Da)		Incubation = 1 hr			
		25 µM (1X)	125 µM (5X)	250 µM (10X)	500 µM (20X)
25338 no adduct	Replicate 1	88%	52%	20%	7%
	Replicate 2	89%	64%	35%	22%
	Average	88.5%	58%	27.5%	14.5%
25721 (+383)	Replicate 1	12%	48%	80%	88%
	Replicate 2	11%	36%	65%	72%
	Average	11.5%	42%	72.5%	80%
26104 (+766)	Replicate 1	0	0	0	5%
	Replicate 2	0	0	0	6%
	Average	0	0	0	5.5%

MW of species (Da)		Incubation = 3 hr			
		25 µM (1X)	125 µM (5X)	250 µM (10X)	500 µM (20X)
25338 no adduct	Replicate 1	37%	19%	9%	0
	Replicate 2	60%	28%	22%	0
	Average	48.5%	23.5%	15.5%	0
25721 (+383)	Replicate 1	63%	76%	80%	67%
	Replicate 2	40%	68%	73%	63%
	Average	51.5%	72%	76.5%	65%
26104 (+766)	Replicate 1	0	5%	11%	25%
	Replicate 2	0	4%	5%	25%
	Average	0	4.5%	8%	25%
26487 (+1149)	Replicate 1	0	0	0	8%
	Replicate 2	0	0	0	12%
	Average	0	0	0	10%

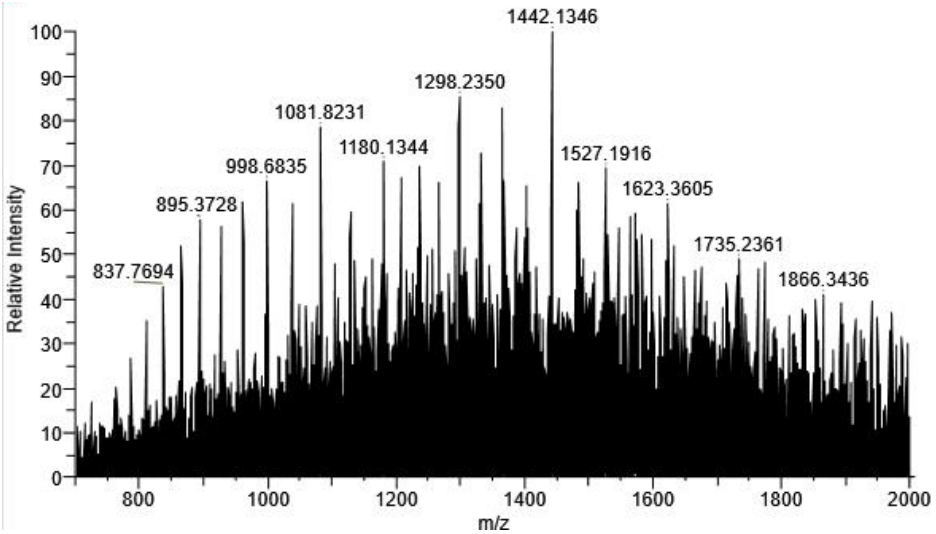

Figure S95. One biological replicate m/z spectrum of DMSO treated A3A.

Xtract Masses Table					
Monoisotopic Mass	Sum Intensity	Number of Charge States	Average Charge	Delta Mass	Relative Abundance
25925.5609	350925.03	7	26.69	0.0000	100.0000

Table S15. Deconvolution intensities of **Figure S95.**

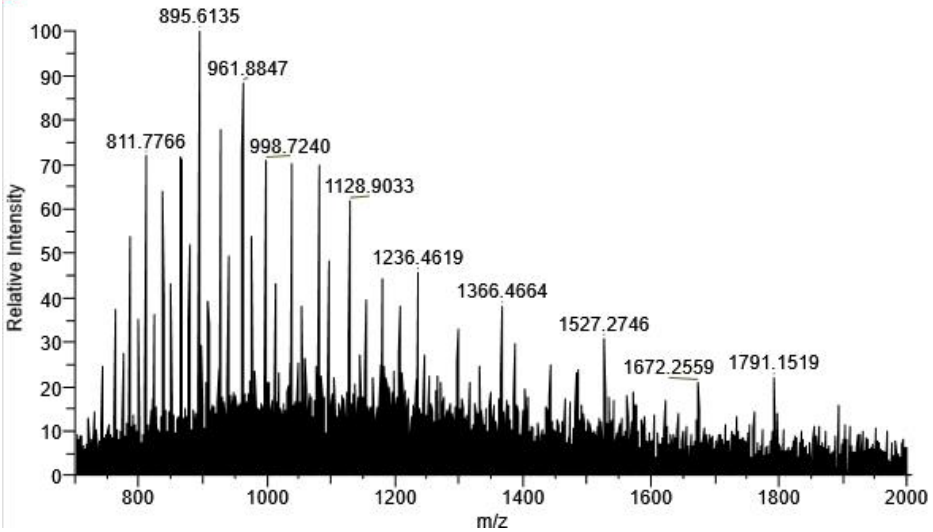

Figure S96. One biological replicate m/z spectrum of **24** (25 μM, 1X) treated A3A (25 μM), incubated for one hour.

Xtract Masses Table					
Monoisotopic Mass	Sum Intensity	Number of Charge States	Average Charge	Delta Mass	Relative Abundance
25927.5710	1619336.29	8	27.82	0.0000	100.0000
26309.7697	932737.05	8	29.07	382.1987	57.6000

Table S16. Deconvolution intensities of **Figure S96.**

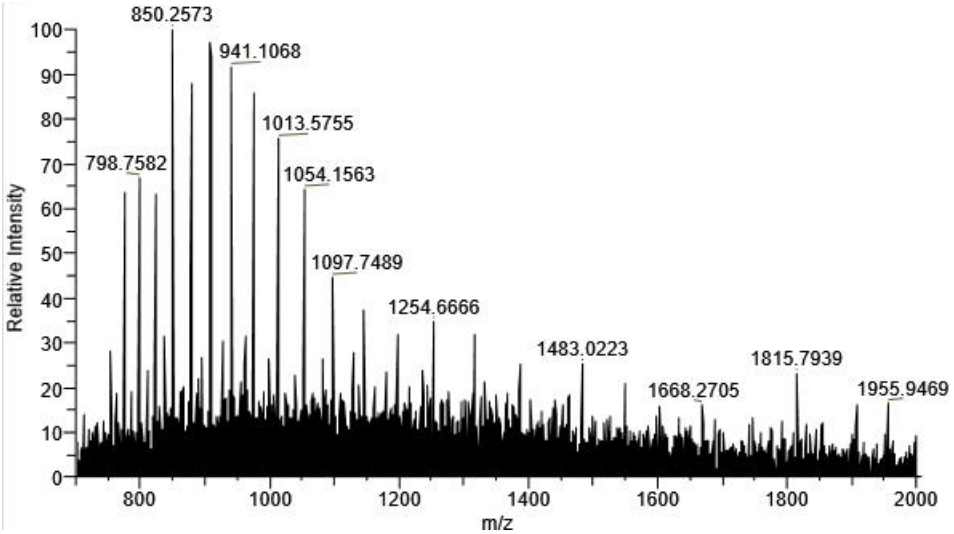

Figure S97. One biological replicate m/z spectrum of **24** (125 μM, 5X) treated A3A (25 μM), incubated for one hour.

Xtract Masses Table					
Monoisotopic Mass	Sum Intensity	Number of Charge States	Average Charge	Delta Mass	Relative Abundance
26309.7615	3020966.02	12	28.78	0.0000	100.0000
25929.6134	163198.95	4	32.29	-380.1481	5.4022

Table S17. Deconvolution intensities of **Figure S97.**

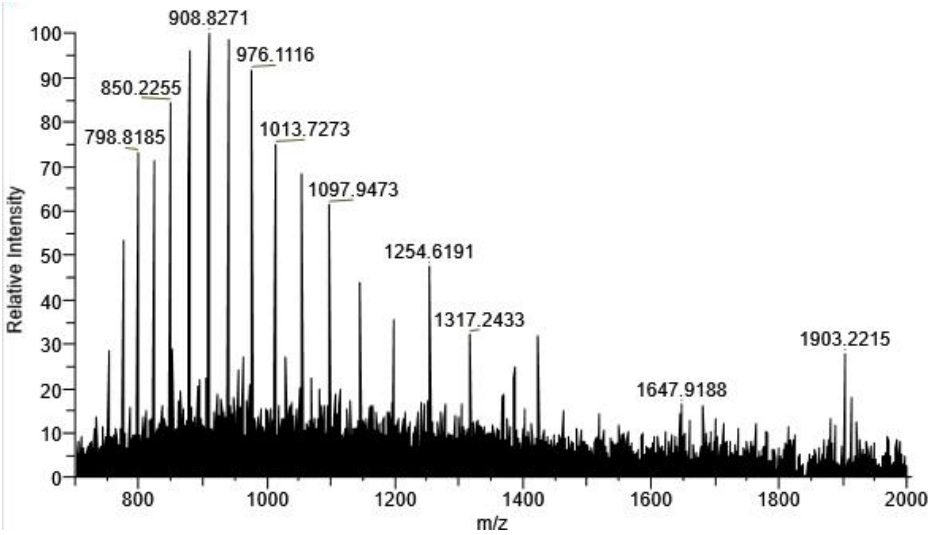

Figure S98. One biological replicate m/z spectrum of **24** (250 μM, 10X) treated A3A (25 μM), incubated for one hour.

Xtract Masses Table					
Monoisotopic Mass	Sum Intensity	Number of Charge States	Average Charge	Delta Mass	Relative Abundance
26310.7608	3151546.28	11	28.99	0.0000	100.0000

Table S18. Deconvolution intensities of **Figure S98.**

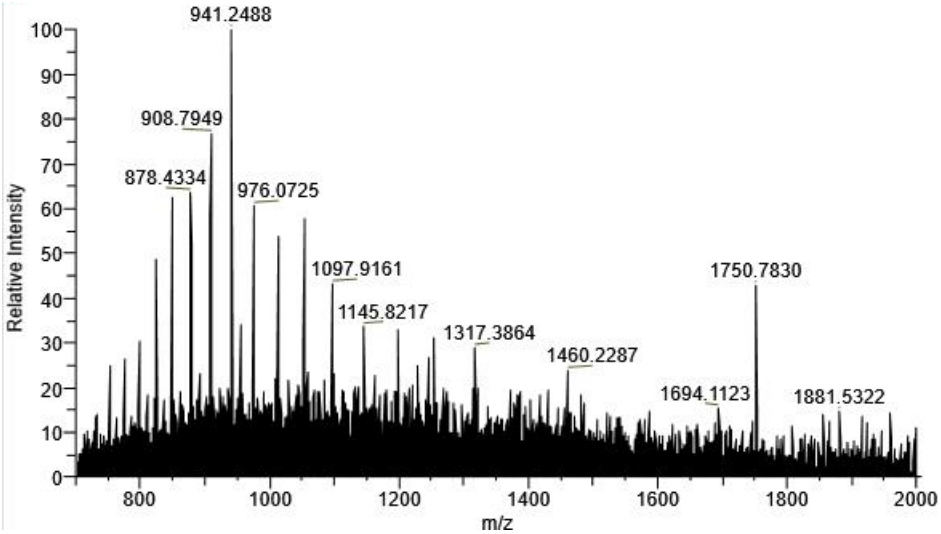

Figure S99. One biological replicate m/z spectrum of **24** (500 μM, 20X) treated A3A (25 μM), incubated for one hour.

Xtract Masses Table					
Monoisotopic Mass	Sum Intensity	Number of Charge States	Average Charge	Delta Mass	Relative Abundance
26309.7631	1444750.65	9	29.22	0.0000	100.0000

Table S19. Deconvolution intensities of **Figure S99.**

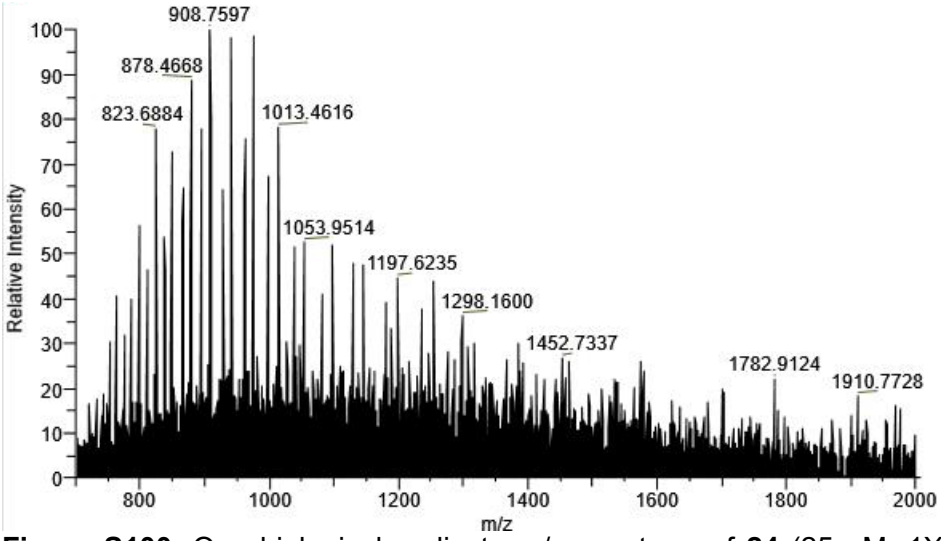

Figure S100. One biological replicate m/z spectrum of **24** (25 μM, 1X) treated A3A (25 μM), incubated for three hours.

Xtract Masses Table					
Monoisotopic Mass	Sum Intensity	Number of Charge States	Average Charge	Delta Mass	Relative Abundance
26309.7180	1577133.95	10	28.83	0.0000	100.0000
25928.5998	921842.29	8	29.03	-381.1182	58.4505

Table S20. Deconvolution intensities of **Figure S100.**

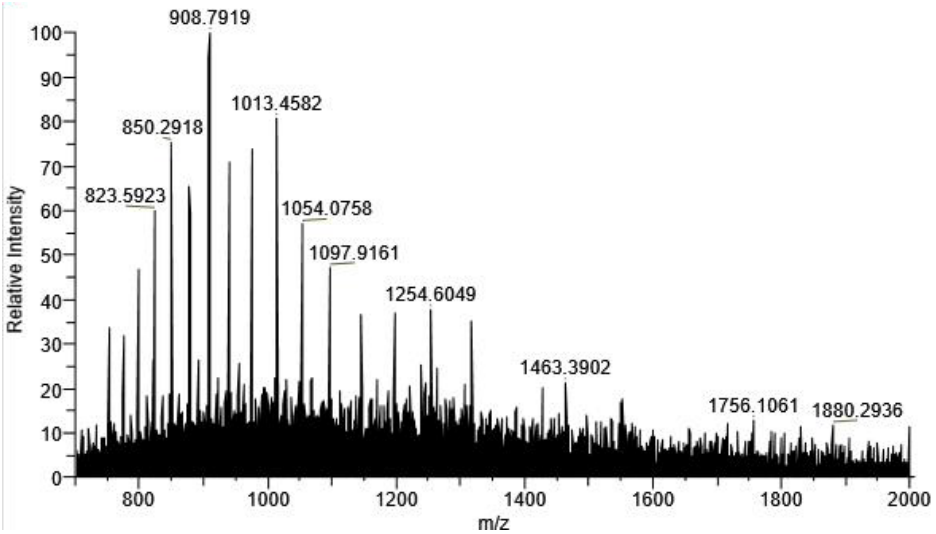

Figure S101. One biological replicate m/z spectrum of **24** (125 μM, 5X) treated A3A (25 μM), incubated for three hours.

Xtract Masses Table					
Monoisotopic Mass	Sum Intensity	Number of Charge States	Average Charge	Delta Mass	Relative Abundance
26309.7524	2322192.67	11	28.67	0.0000	100.0000

Table S21. Deconvolution intensities of **Figure S101.**

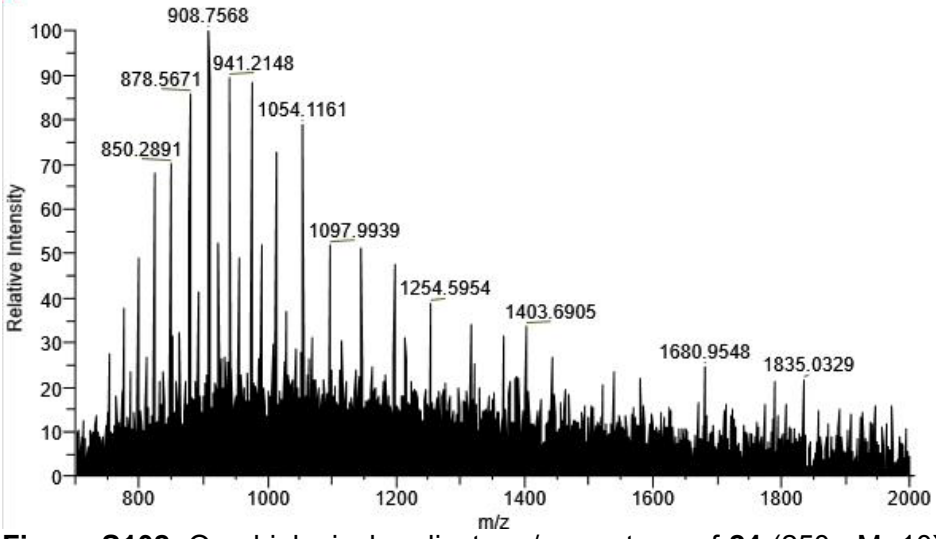

Figure S102. One biological replicate m/z spectrum of **24** (250 μM, 10X) treated A3A (25 μM), incubated for three hours.

Xtract Masses Table					
Monoisotopic Mass	Sum Intensity	Number of Charge States	Average Charge	Delta Mass	Relative Abundance
26310.7725	1791651.39	12	28.63	0.0000	100.0000
26692.8934	402307.42	6	28.96	382.1209	22.4546

Table S22. Deconvolution intensities of **Figure S102.**

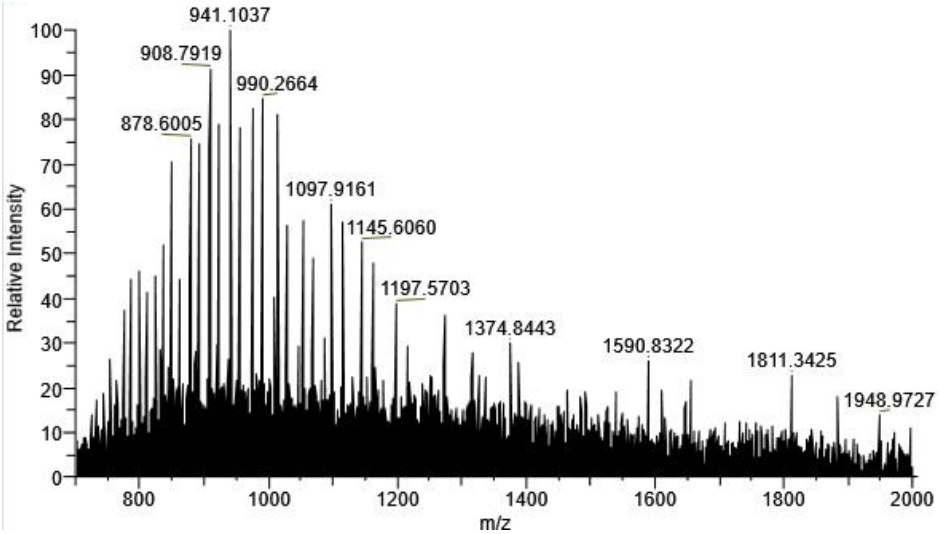

Figure S103. One biological replicate m/z spectrum of **24** (500 μM, 20X) treated A3A (25 μM), incubated for three hours.

Xtract Masses Table					
Monoisotopic Mass	Sum Intensity	Number of Charge States	Average Charge	Delta Mass	Relative Abundance
26691.9561	1025069.21	8	28.94	0.0000	100.0000
26310.7441	849168.08	8	29.05	-381.2120	82.8401

Table S23. Deconvolution intensities of **Figure S103.**

Table S24. Average percent adduction of A3A treated with **24** at variable concentration and time, from intact protein mass spectrometry deconvolution.

MW of species (Da)		Incubation = 1 hr			
		25 µM (1X)	125 µM (5X)	250 µM (10X)	500 µM (20X)
25927 no adduct	Replicate 1	76%	0	0	0
	Replicate 2	64%	5%	0	0
	Average	70%	2.5%	0	0
26309 (+382)	Replicate 1	24%	100%	100%	85%
	Replicate 2	36%	95%	100%	100%
	Average	30%	97.5%	100%	92%
26691 (+764)	Replicate 1	0	0	0	15%
	Replicate 2	0	0	0	0
	Average	0	0	0	7.5%

MW of species (Da)		Incubation = 3 hr			
		25 µM (1X)	125 µM (5X)	250 µM (10X)	500 µM (20X)
25927 no adduct	Replicate 1	30%	0	0	0
	Replicate 2	37%	0	0	0
	Average	33.5%	0	0	0
26309 (+382)	Replicate 1	70%	100%	80%	49%
	Replicate 2	63%	100%	82%	45%
	Average	66.5%	100%	81%	47%
26691 (+764)	Replicate 1	0	0	20%	51%
	Replicate 2	0	0	18%	55%
	Average	0	0	19%	53%

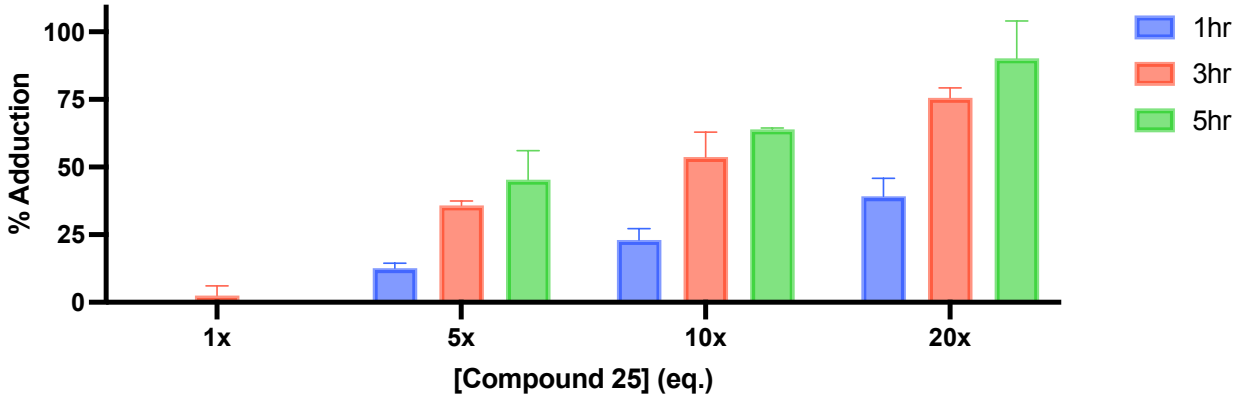

Figure S104. Bar graph of percent adduction of the acrylamide, **25**, to A3Bctd (25 μM) at 1x (25 μM), 5x (125 μM), 10x (250 μM), and 20x (500 μM). Percent adduction determined by intensity of mass species from deconvoluted spectra. N = 2 biological replicates, error bars represent standard deviation.

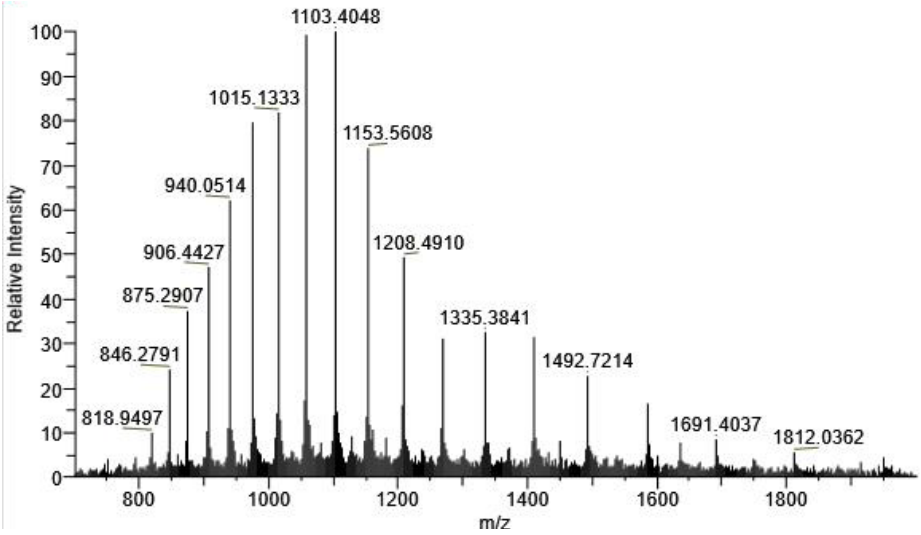

Figure S105. One biological replicate m/z spectrum of DMSO treated A3Bctd (25 μM).

Xtract Masses Table					
Monoisotopic Mass	Sum Intensity	Number of Charge States	Average Charge	Delta Mass	Relative Abundance
25339.1471	20328438.68	14	23.82	0.0000	100.0000

Table S25. Deconvolution intensities of **Figure S105.**

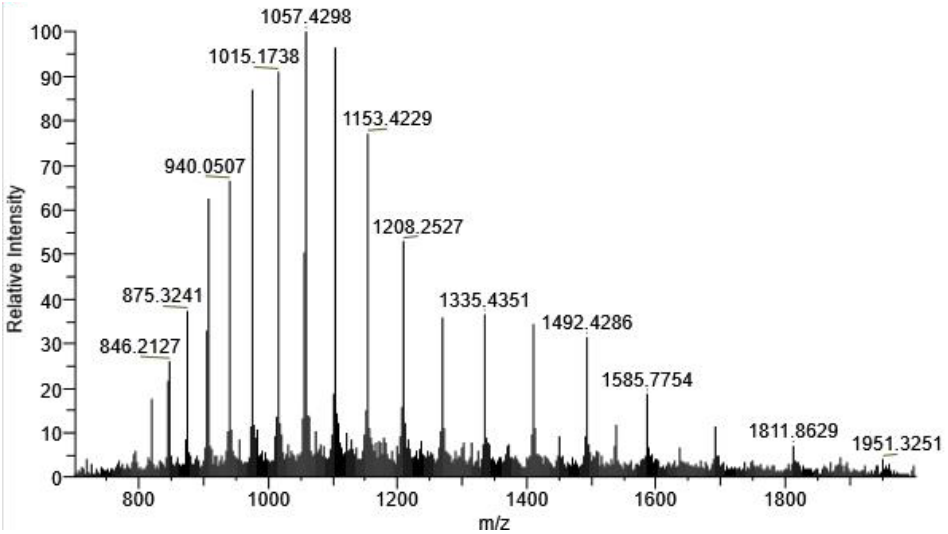

Figure S106. One biological replicate m/z spectrum of **25** (25 μM, 1X) treated A3Bctd (25 μM) incubated for one hour.

Xtract Masses Table					
Monoisotopic Mass	Sum Intensity	Number of Charge States	Average Charge	Delta Mass	Relative Abundance
25339.1325	20046771.18	16	23.45	0.0000	100.0000

Table S26. Deconvolution intensities of **Figure S106.**

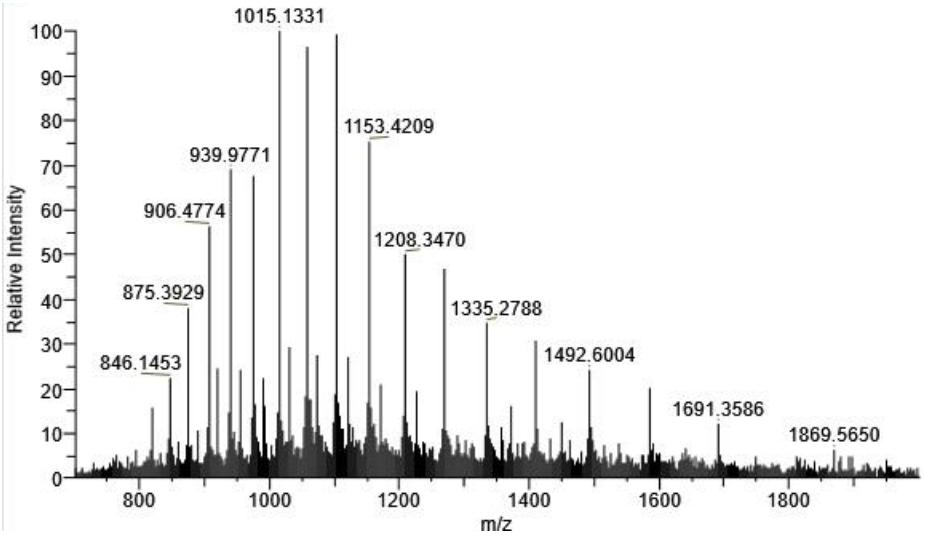

Figure S107. One biological replicate m/z spectrum of **25** (125 μM, 5X) treated A3Bctd (25 μM) incubated for one hour.

Xtract Masses Table					
Monoisotopic Mass	Sum Intensity	Number of Charge States	Average Charge	Delta Mass	Relative Abundance
25339.1316	10542034.72	15	23.45	0.0000	100.0000
25735.2943	1410875.18	6	24.22	396.1627	13.3833

Table S27. Deconvolution intensities of **Figure S107.**

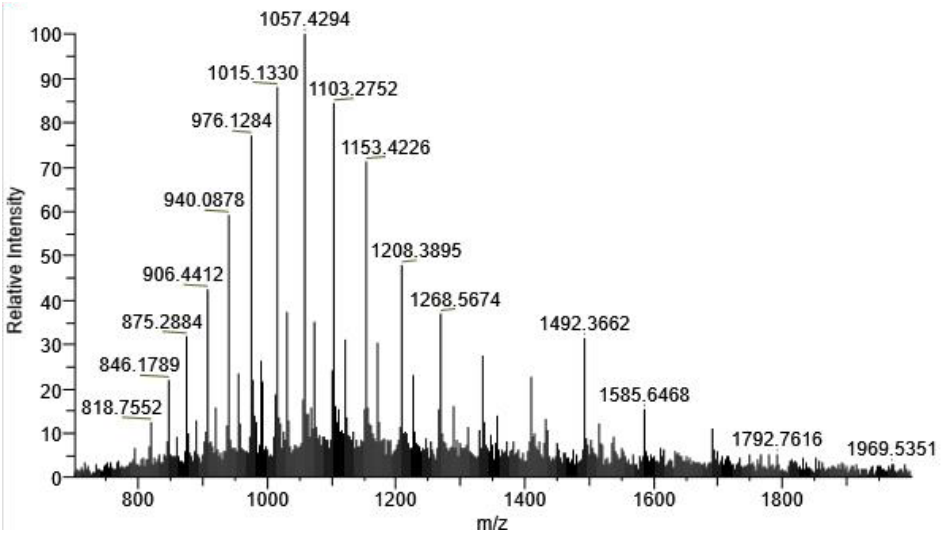

Figure S108. One biological replicate m/z spectrum of **25** (250 μM, 10X) treated A3Bctd (25 μM) incubated for one hour.

Xtract Masses Table					
Monoisotopic Mass	Sum Intensity	Number of Charge States	Average Charge	Delta Mass	Relative Abundance
25339.1338	6911094.52	13	23.58	0.0000	100.0000
25736.2909	1745386.65	7	24.47	397.1571	25.2549

Table S28. Deconvolution intensities of **Figure S108.**

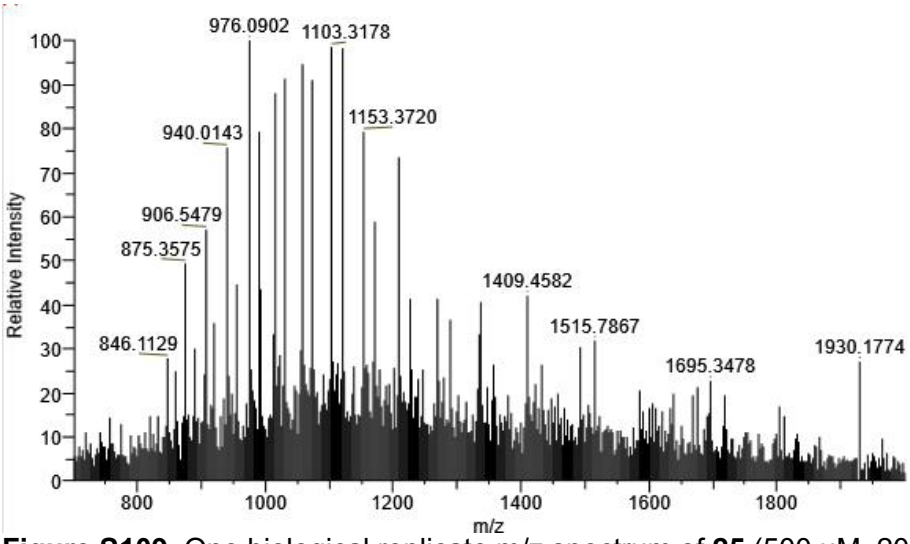

Figure S109. One biological replicate m/z spectrum of **25** (500 μM, 20X) treated A3Bctd (25 μM) incubated for one hour.

Xtract Masses Table					
Monoisotopic Mass	Sum Intensity	Number of Charge States	Average Charge	Delta Mass	Relative Abundance
25338.0772	3948645.71	9	24.43	0.0000	100.0000
25735.2897	3087905.61	9	24.29	397.2125	78.2016

Table S29. Deconvolution intensities of **Figure S109.**

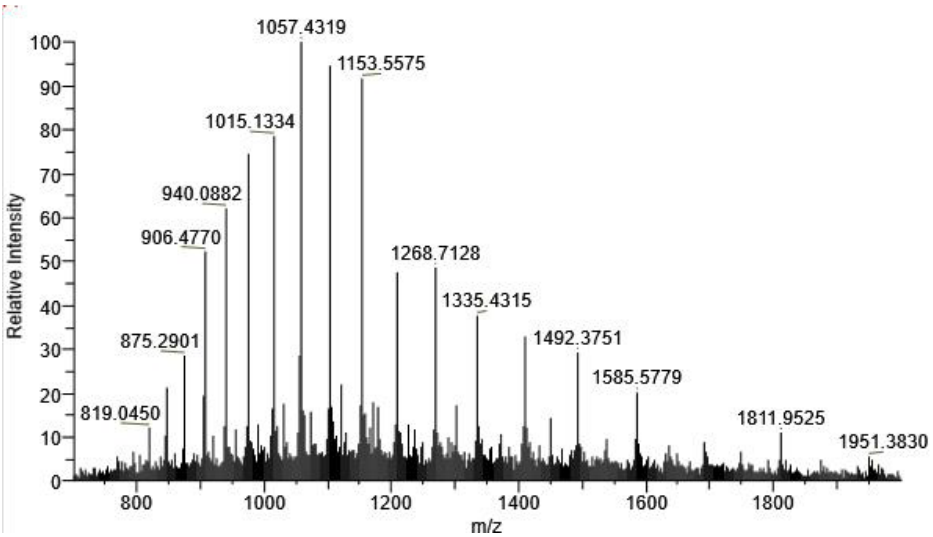

Figure S110. One biological replicate m/z spectrum of **25** (25 μM, 1X) treated A3Bctd (25 μM) incubated for three hours.

Xtract Masses Table					
Monoisotopic Mass	Sum Intensity	Number of Charge States	Average Charge	Delta Mass	Relative Abundance
25339.1202	12389084.49	14	23.24	0.0000	100.0000

Table S30. Deconvolution intensities of **Figure S110.**

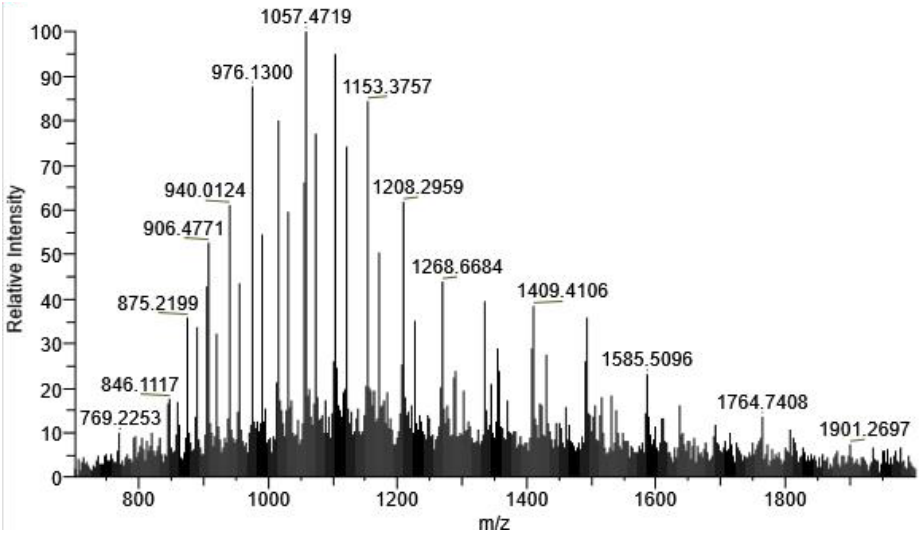

Figure S111. One biological replicate m/z spectrum of **25** (125 μM, 5X) treated A3Bctd (25 μM) incubated for three hours.

Xtract Masses Table					
Monoisotopic Mass	Sum Intensity	Number of Charge States	Average Charge	Delta Mass	Relative Abundance
25338.0977	6694300.41	10	24.32	0.0000	100.0000
25735.2513	3925709.40	9	24.20	397.1536	58.6426

Table S31. Deconvolution intensities of **Figure S111.**

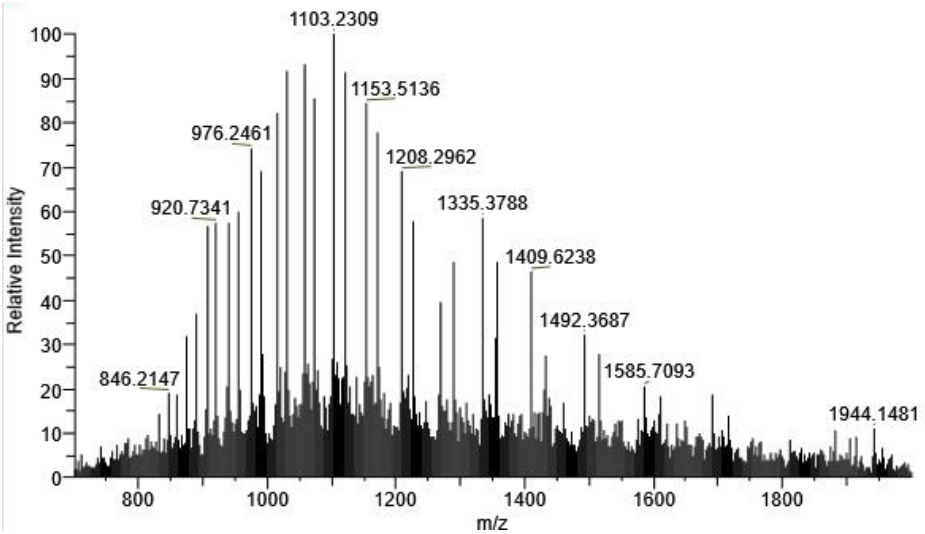

Figure S112. One biological replicate m/z spectrum of **25** (250 μM, 10X) treated A3Bctd (25 μM) incubated for three hours.

Xtract Masses Table					
Monoisotopic Mass	Sum Intensity	Number of Charge States	Average Charge	Delta Mass	Relative Abundance
25338.0915	4423994.09	10	23.81	0.0000	100.0000
25735.3090	3953827.79	9	24.39	397.2175	89.3724

Table S32. Deconvolution intensities of **Figure S112.**

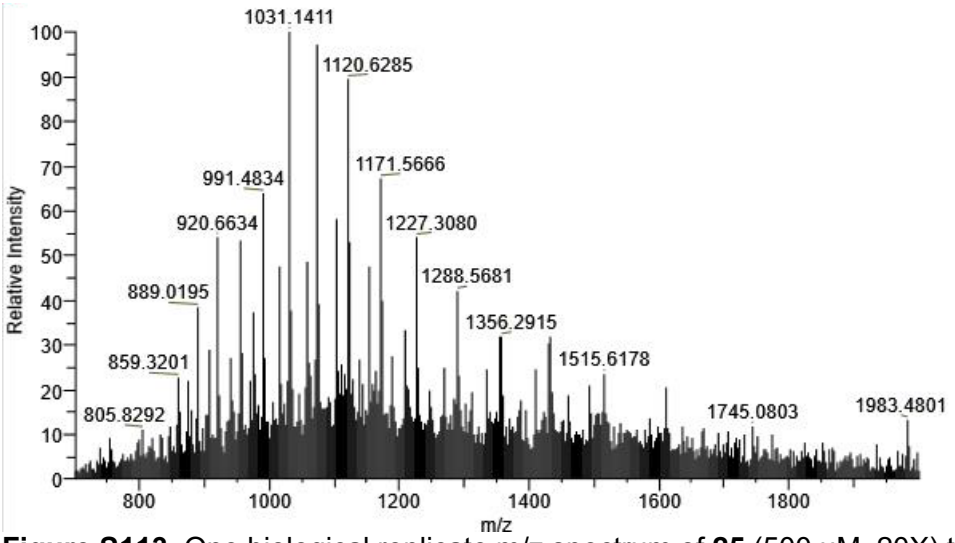

Figure S113. One biological replicate m/z spectrum of **25** (500 μM, 20X) treated A3Bctd (25 μM) incubated for three hours.

Xtract Masses Table					
Monoisotopic Mass	Sum Intensity	Number of Charge States	Average Charge	Delta Mass	Relative Abundance
25735.2817	4569511.77	10	24.12	0.0000	100.0000
25338.1102	1690661.51	7	24.38	-397.1715	36.9987

Table S33. Deconvolution intensities of **Figure S113.**

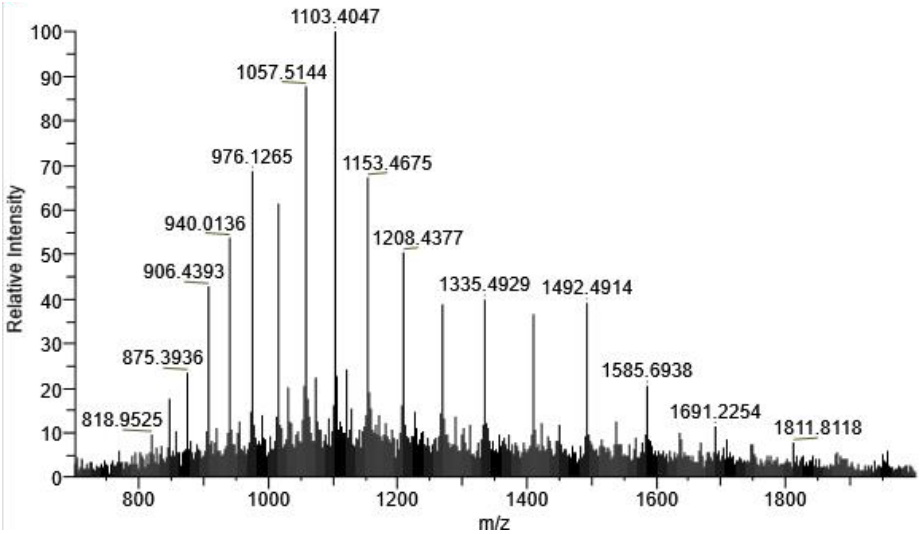

Figure S114. One biological replicate m/z spectrum of **25** (25 μM, 1X) treated A3Bctd (25 μM) incubated for five hours.

Xtract Masses Table					
Monoisotopic Mass	Sum Intensity	Number of Charge States	Average Charge	Delta Mass	Relative Abundance
25338.0929	3033212.40	12	23.18	0.0000	100.0000

Table S34. Deconvolution intensities of **Figure S114.**

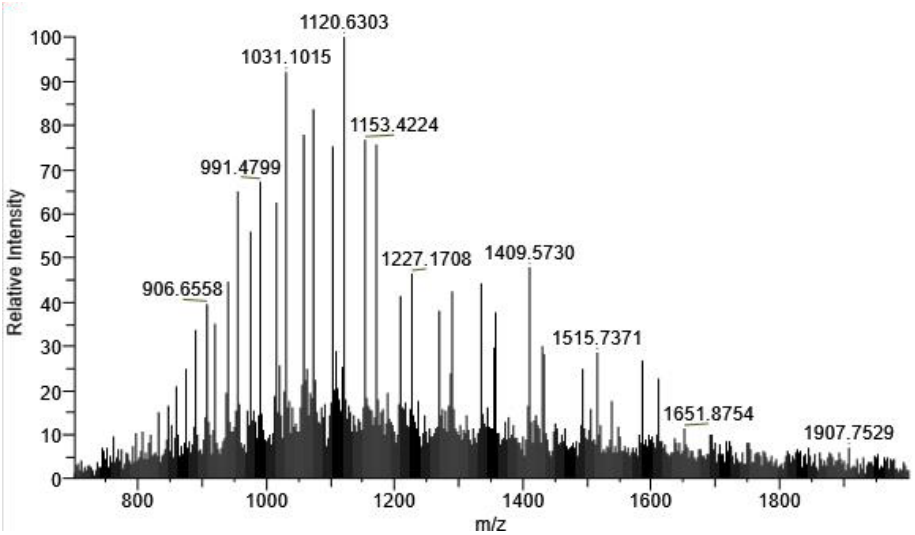

Figure S115. One biological replicate m/z spectrum of **25** (125 μM, 5X) treated A3Bctd (25 μM) incubated for five hours.

Xtract Masses Table					
Monoisotopic Mass	Sum Intensity	Number of Charge States	Average Charge	Delta Mass	Relative Abundance
25735.2758	4000941.60	10	24.01	0.0000	100.0000
25338.1062	2420819.20	8	24.29	-397.1696	60.5062

Table S35. Deconvolution intensities of **Figure S115.**

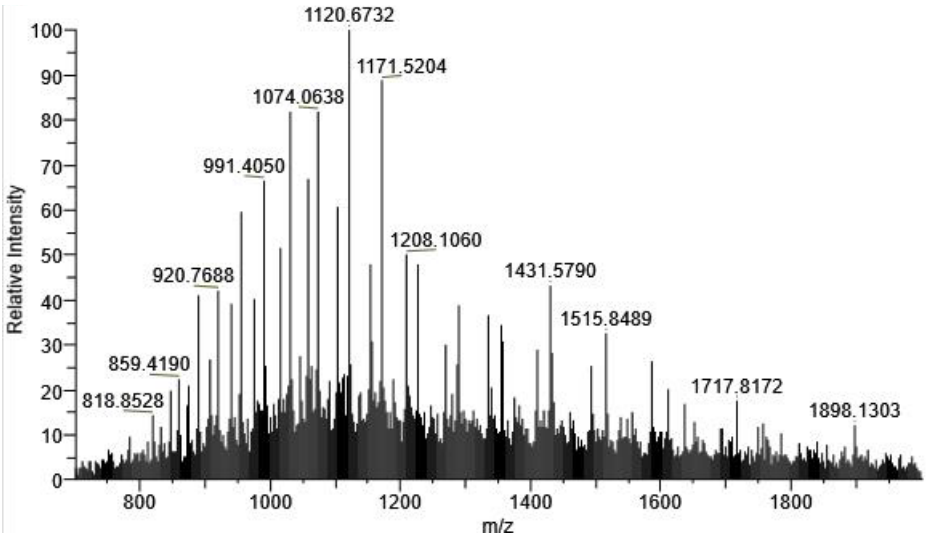

Figure S116. One biological replicate m/z spectrum of **25** (250 μM, 10X) treated A3Bctd (25 μM) incubated for five hours.

Xtract Masses Table					
Monoisotopic Mass	Sum Intensity	Number of Charge States	Average Charge	Delta Mass	Relative Abundance
25735.2778	3755471.18	10	23.94	0.0000	100.0000
25338.1038	2159754.28	8	23.94	-397.1740	57.5095

Table S36. Deconvolution intensities of **Figure S116.**

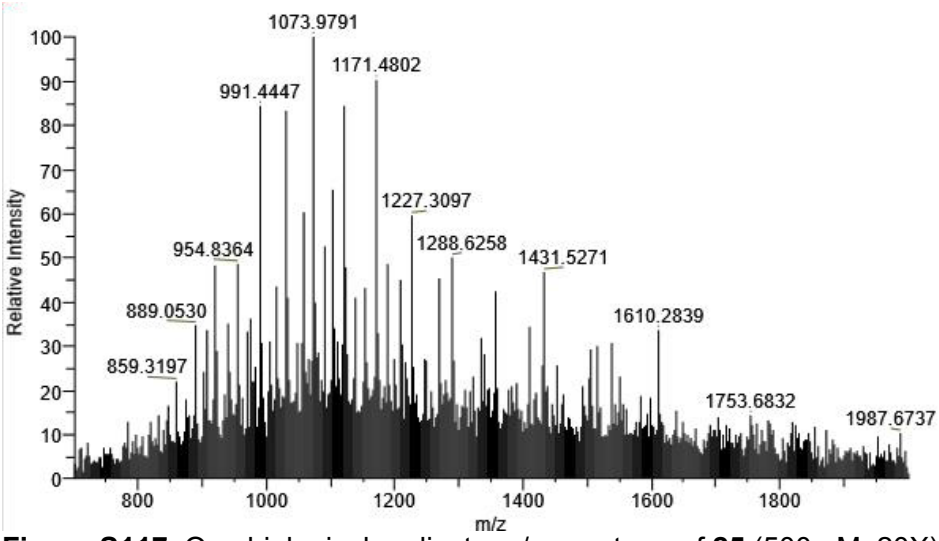

Figure S117. One biological replicate m/z spectrum of **25** (500 μM, 20X) treated A3Bctd (25 μM) incubated for five hours.

Xtract Masses Table					
Monoisotopic Mass	Sum Intensity	Number of Charge States	Average Charge	Delta Mass	Relative Abundance
25735.2969	3014874.38	9	24.17	0.0000	100.0000
25338.0842	736700.82	5	23.96	-397.2127	24.4355

Table S37. Deconvolution intensities of **Figure S117.**

Table S38. Average percent adduction of A3Bctd treated with **25** at variable concentration and time, from intact protein mass spectrometry deconvolution.

MW of species (Da)		Incubation = 1 hr			
		25 µM (1X)	**125 µM (5X)**	**250 µM (10X)**	**500 µM (20X)**
25338 no adduct	Replicate 1	100%	89%	80%	65%
	Replicate 2	100%	86%	74%	56%
	Average	100%	87.5%	77%	60.5%
25735 (+397)	Replicate 1	0	11%	20%	35%
	Replicate 2	0	14%	26%	44%
	Average	0	12.5%	23%	39.5%

MW of species (Da)		Incubation = 3 hr			
		25 µM (1X)	**125 µM (5X)**	**250 µM (10X)**	**500 µM (20X)**
5338 no adduct	Replicate 1	100%	63%	53%	27%
	Replicate 2	95%	65%	40%	22%
	Average	97.5%	64%	46.5%	24.5%
25735 (+397)	Replicate 1	0	37%	47%	73%
	Replicate 2	5%	35%	60%	78%
	Average	2.5%	36%	53.5%	75.5%

MW of species (Da)		Incubation = 5 hr			
		25 µM (1X)	**125 µM (5X)**	**250 µM (10X)**	**500 µM (20X)**
25339 no adduct	Replicate 1	100%	47%	36%	0
	Replicate 2	100%	62%	36%	20%
	Average	100%	54.5%	36%	10%
25735 (+397)	Replicate 1	0	53%	64%	100%
	Replicate 2	0	38%	64%	80%
	Average	0	45.5%	64%	90%

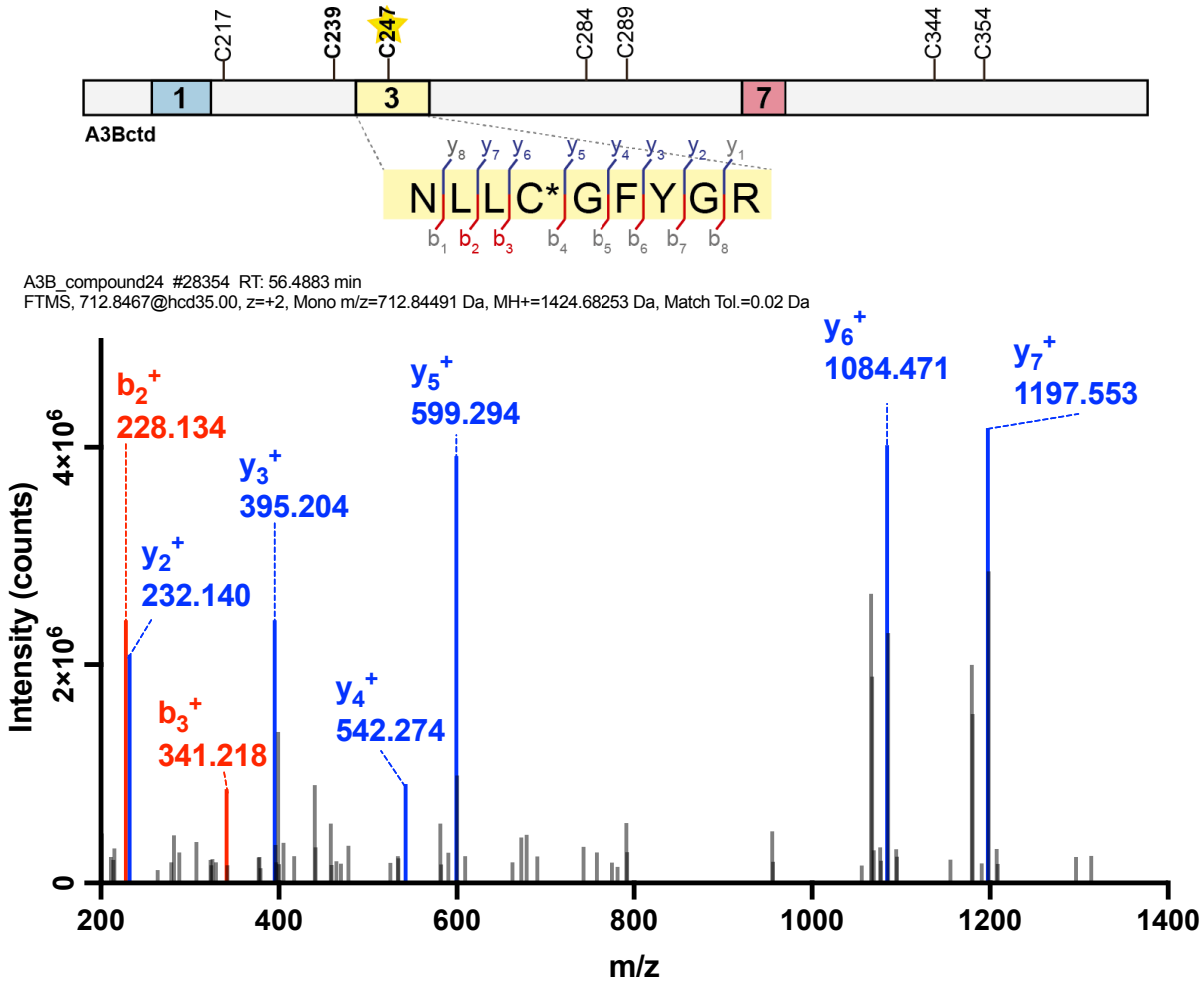

Figure S118. Collision-induced fragmentation pattern of major adducted peptide from A3Bctd (25 μM) treated with 500 μM (20x) **24**, incubated for one hour. 12 peptide-spectrum matches (PSM) identified.

Table S39. Table of calculated and identified ions from **Figure S118.**

b^+	calculated	detected	sequence	y^+	calculated	observed
1	115.05020	nd	**N**	**9**	-	-
2	228.13427	228.13443	**L**	**8**	1310.64133	nd
3	341.21833	341.21680	**L**	**7**	1197.55727	1197.55847
4	826.398	nd	**C+adduct**	**6**	1084.47321	1084.47046
5	883.419	nd	**G**	**5**	599.29362	599.29279
6	1030.488	nd	**F**	**4**	542.27216	542.27228
7	1193.551	nd	**Y**	**3**	395.20374	395.20349
8	1250.573	nd	**G**	**2**	232.14042	232.14072
9	-	-	**R**	**1**	175.11895	nd

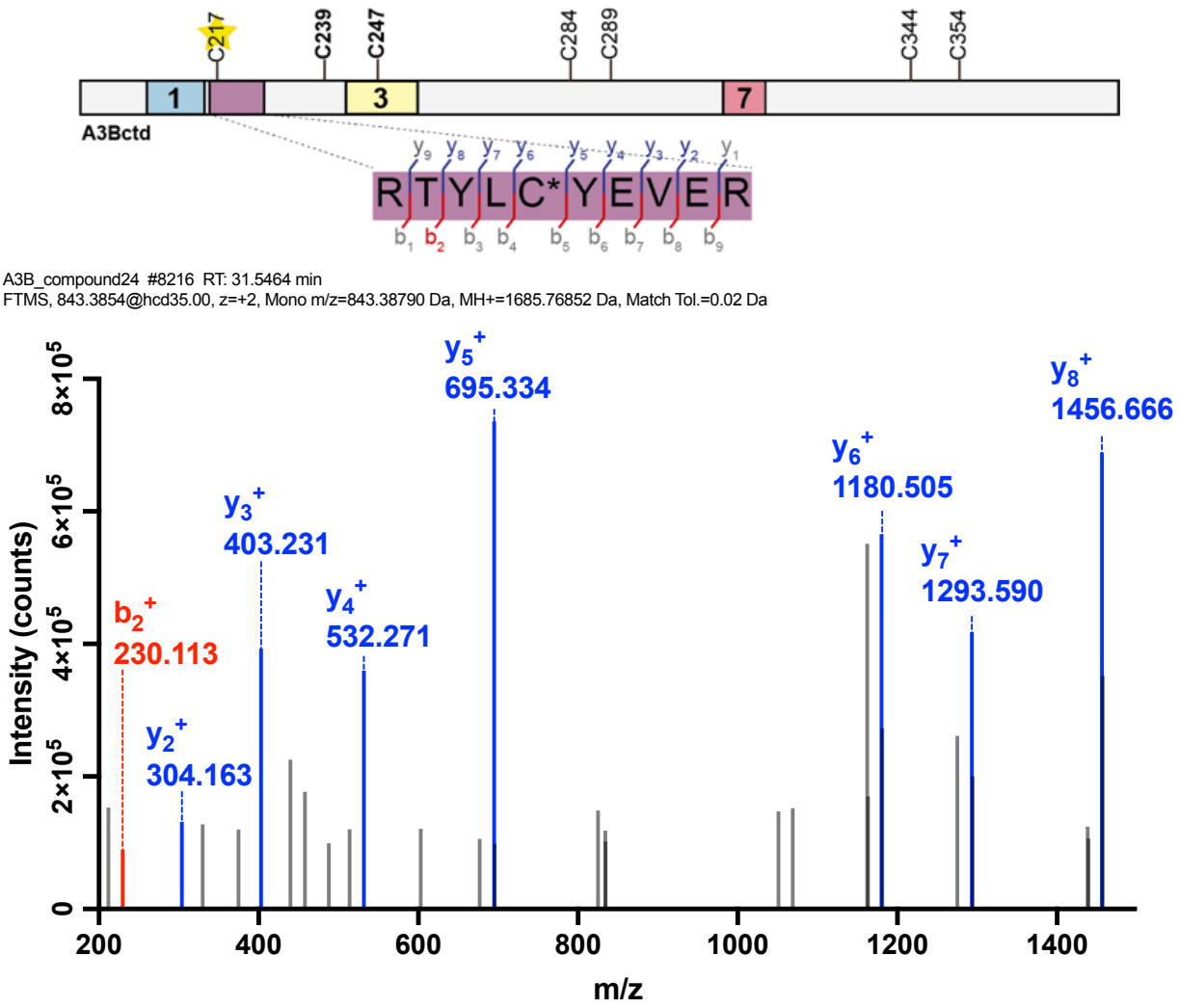

Figure S119. Collision-induced fragmentation pattern of minor adducted peptide from A3Bctd (25 μM) treated with 500 μM (20x) **24**, incubated for one hour. 6 peptide-spectrum matches (PSM) identified.

Table S40. Table of calculated and identified ions from **Figure S119.**

b^+	calculated	detected	sequence	y^+	calculated	observed
1	129.06585	nd	**Q**	**10**	-	-
2	230.11353	230.11304	**T**	**9**	1557.71054	nd
3	393.17686	nd	**Y**	**8**	1456.66286	1456.66565
4	506.26092	nd	**L**	**7**	1293.59953	1293.59033
5	991.44051	nd	**C+adduct**	**6**	1180.51547	1180.50537
6	1154.50384	nd	**Y**	**5**	695.33588	695.33826
7	1283.54643	nd	**E**	**4**	532.27255	532.27112
8	1382.61484	nd	**V**	**3**	403.22996	403.23105
9	1511.65744	nd	**E**	**2**	304.16155	304.16333
10	-	-	**R**	**1**	175.11895	nd

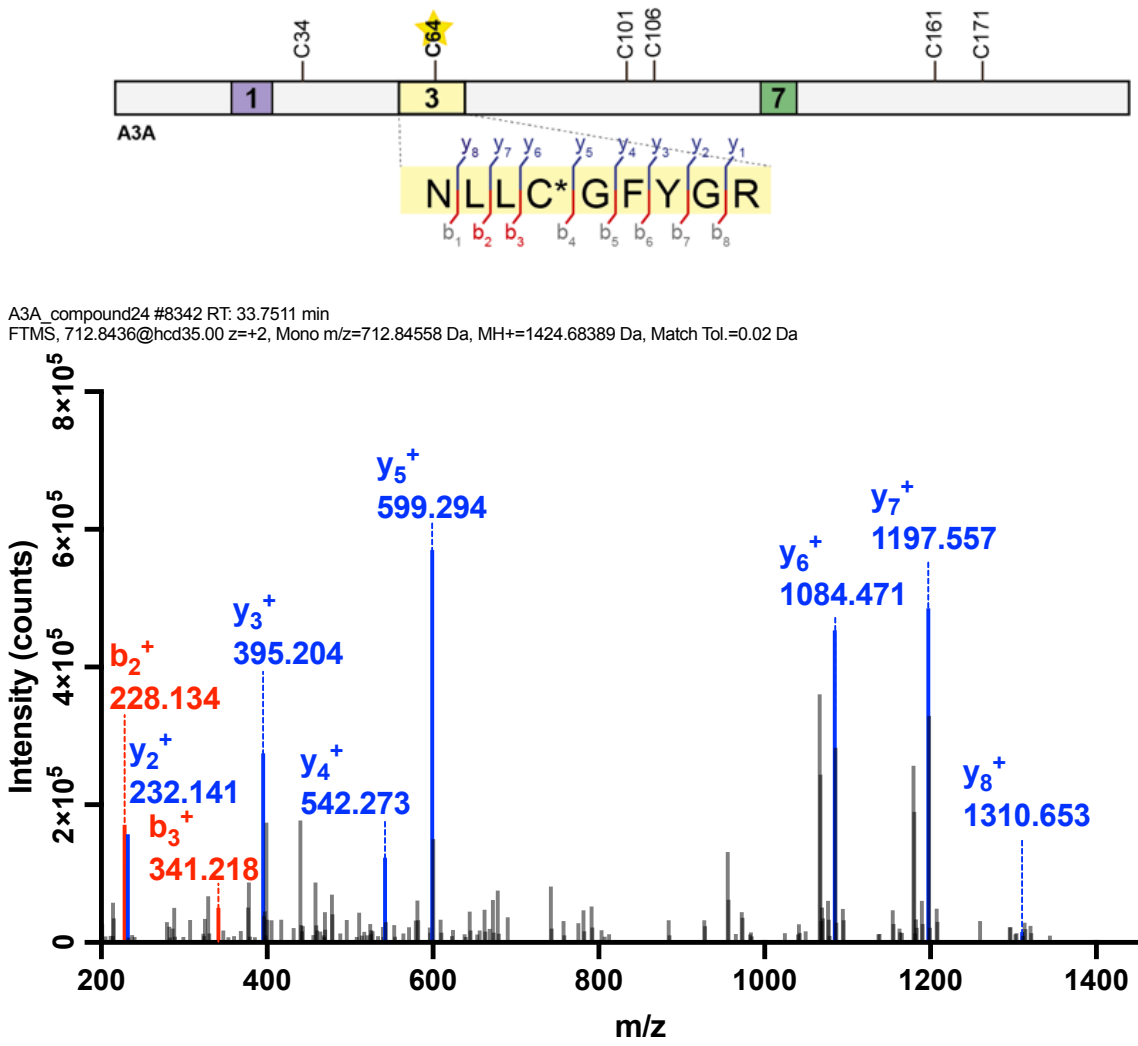

Figure S120. Collision-induced fragmentation pattern of major adducted peptide from A3A (25 μM) treated with 250 μM (10x) **24**, incubated for one hour. 32 peptide-spectrum matches (PSM) identified.

Table S41. Table of calculated and identified ions from **Figure S120.**

b^+	calculated	detected	sequence	y^+	calculated	observed
1	115.05020	nd	**N**	**9**	-	-
2	228.13427	228.13437	**L**	**8**	1310.64133	1310.63367
3	341.21833	341.21887	**L**	**7**	1197.55727	1197.55481
4	826.39792	nd	**C+adduct**	**6**	1084.47321	1084.47058
5	883.41938	nd	**G**	**5**	599.29362	599.29413
6	1030.48779	nd	**F**	**4**	542.27216	542.27344
7	1193.55112	nd	**Y**	**3**	395.20374	395.20432
8	1250.57259	nd	**G**	**2**	232.14042	232.14059
9	-	-	**R**	**1**	175.11895	nd

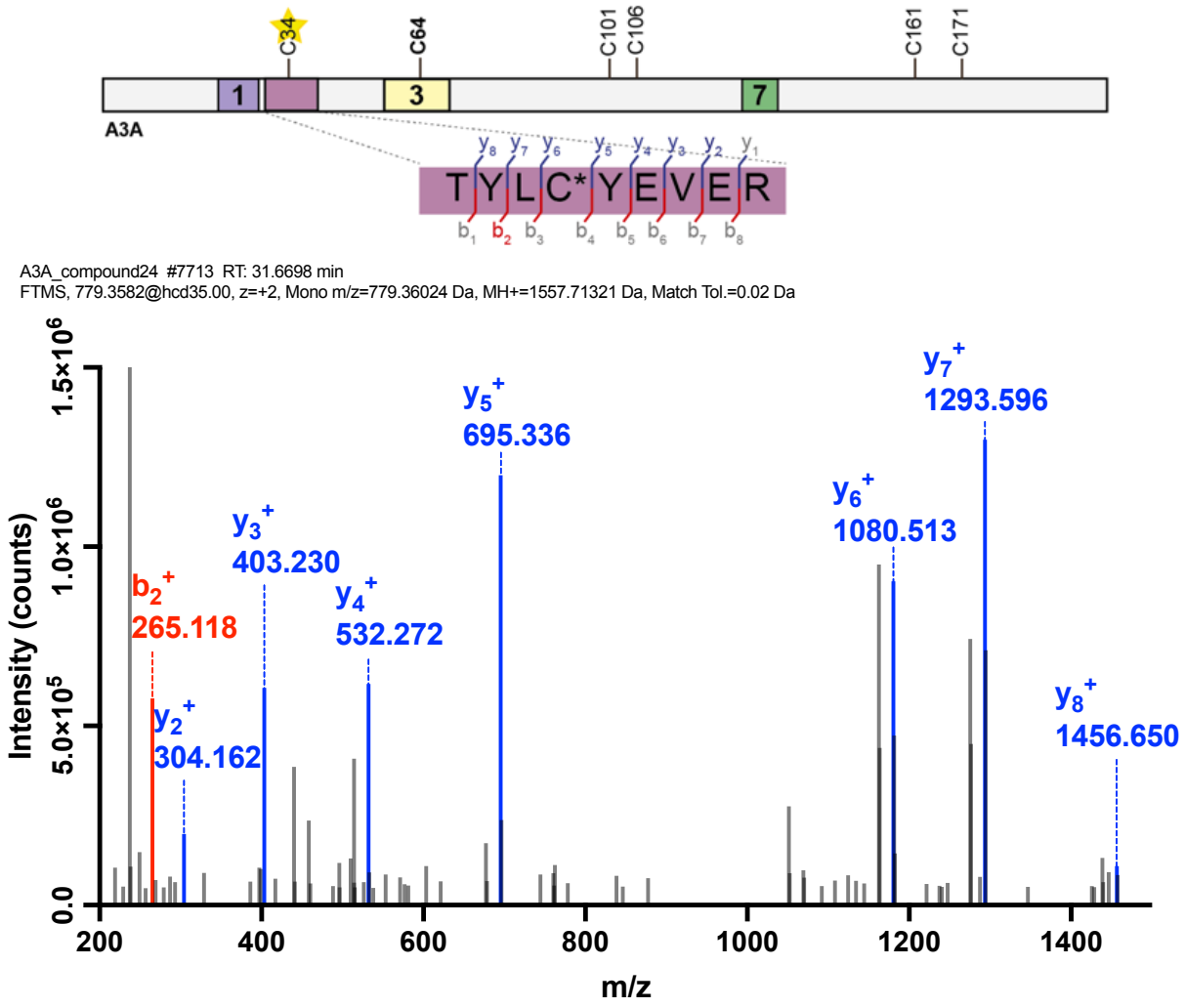

Figure S121. Collision-induced fragmentation pattern of minor adducted peptide from A3A (25 μM) treated with 250 μM (10x) **24**, incubated for one hour. 7 peptide-spectrum matches (PSM) identified.

Table S42. Table of calculated and identified ions from **Figure S121.**

b^+	calculated	detected	sequence	y^+	calculated	observed
1	102.05496	nd	**T**	**9**	-	-
2	265.11828	265.11844	**Y**	**8**	1456.66286	1456.65881
3	378.20235	nd	**L**	**7**	1293.59953	1293.59631
4	863.38193	nd	**C+adduct**	**6**	1180.51547	1180.51355
5	1026.44526	nd	**Y**	**5**	695.33588	695.33630
6	1155.48785	nd	**E**	**4**	532.27255	532.27203
7	1254.55627	nd	**V**	**3**	403.22996	403.23026
8	1383.59886	nd	**E**	**2**	304.16155	304.16165
9	-	-	**R**	**1**	175.11895	nd

19 ^{1}H NMR ($CDCl_3$, 0.05% TMS)

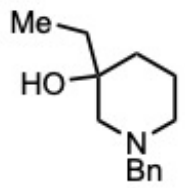

19

20 ^{1}H NMR (MeOD, 0.05% TMS)

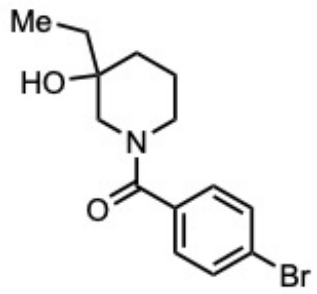

20

20 ^{13}C NMR (MeOD)

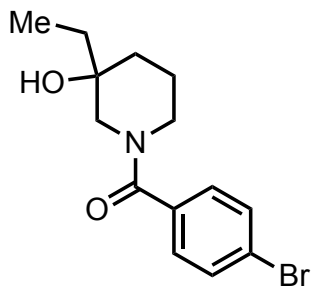

20

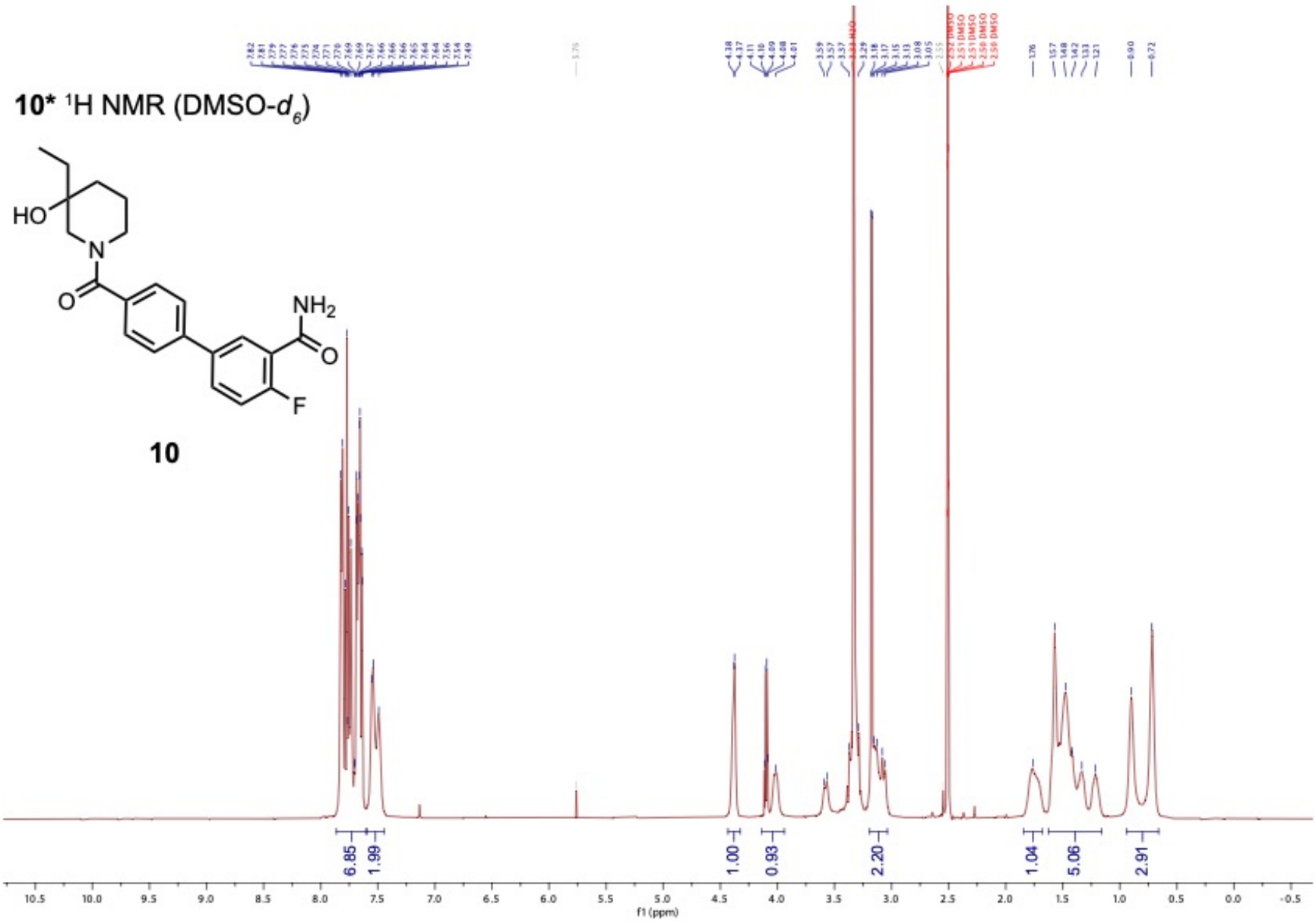
10* 1H NMR (DMSO-d6)
HO
N
O
NH2
O
F
10
6.85
1.99
1.00
0.93
2.20
1.04
5.06
2.91
f1 (ppm)

10* ^{13}C NMR (DMSO-d_6)

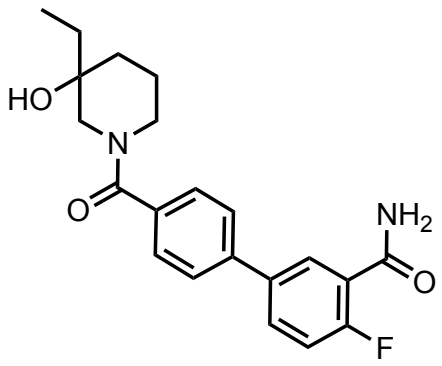

10

10* ^{19}F NMR (DMSO-d_6)

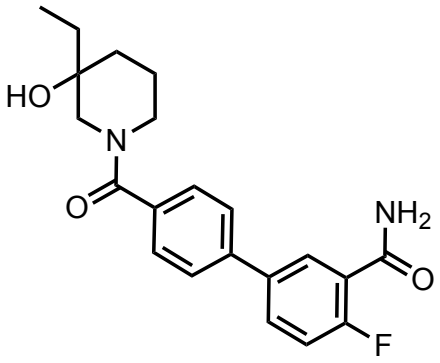

10

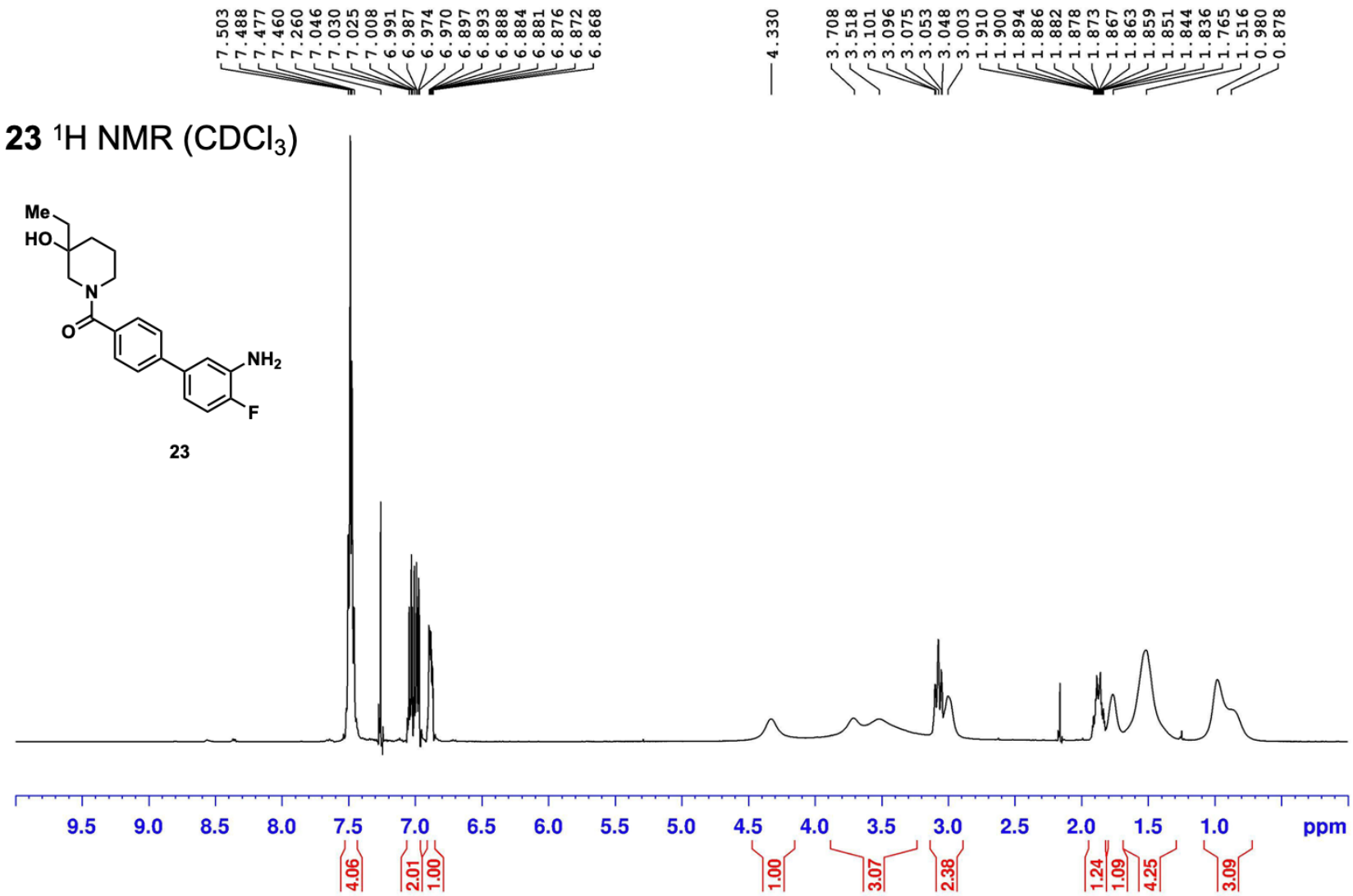
7.503
7.488
7.477
7.460
7.260
7.046
7.030
7.025
7.008
6.991
6.987
6.974
6.970
6.897
6.893
6.888
6.884
6.881
6.876
6.872
6.868
4.330
3.708
3.518
3.101
3.096
3.075
3.053
3.048
3.003
1.910
1.900
1.894
1.886
1.882
1.878
1.873
1.867
1.863
1.859
1.851
1.844
1.836
1.765
1.516
0.980
0.878
23 ^{1}H NMR ($CDCl_3$)
Me
HO
N
O
NH$_2$
F
23
9.5
9.0
8.5
8.0
7.5
7.0
6.5
6.0
5.5
5.0
4.5
4.0
3.5
3.0
2.5
2.0
1.5
1.0
ppm
4.06
2.01
1.00
1.00
3.07
2.38
1.24
1.09
4.25
3.09

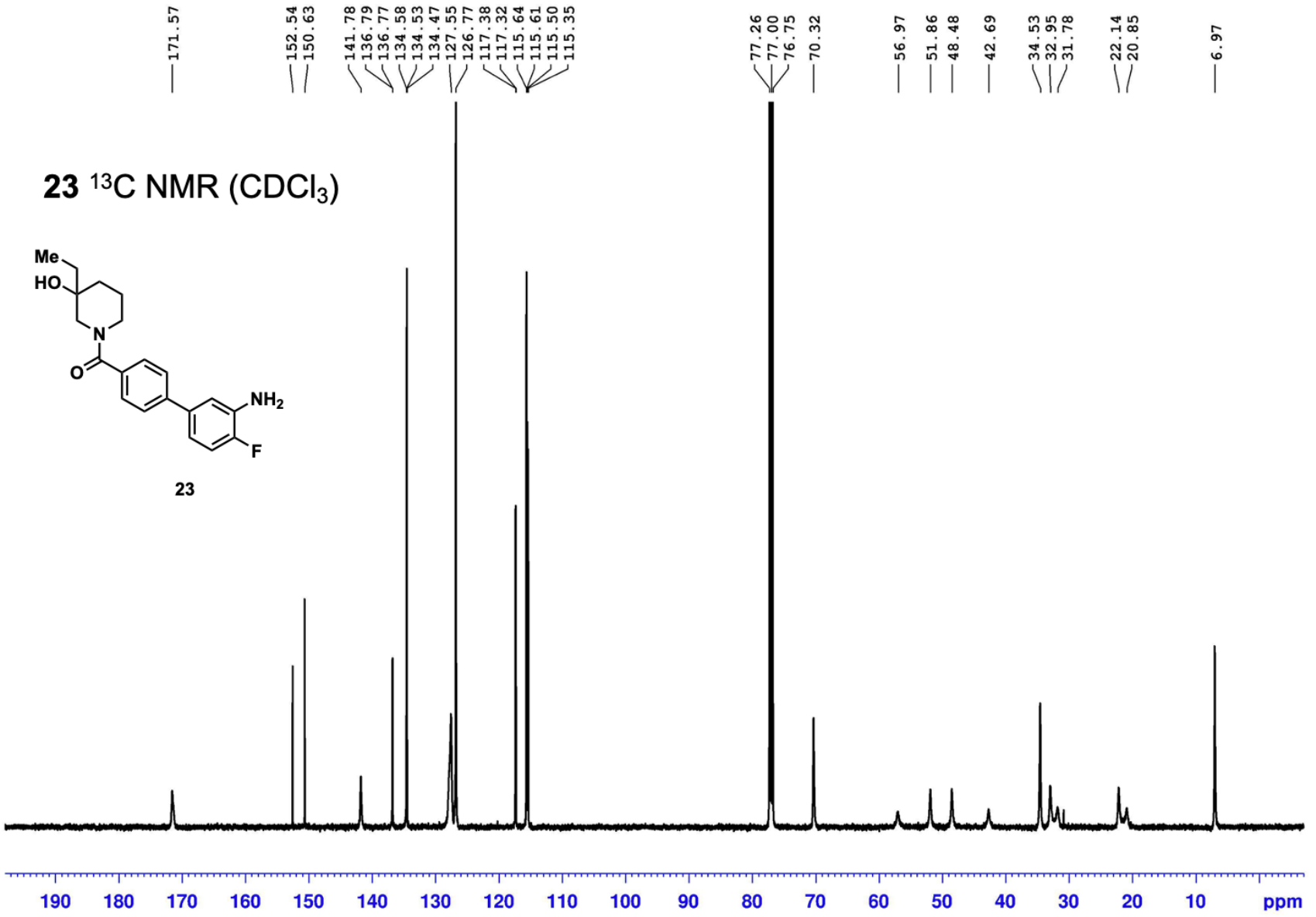
171.57
152.54
150.63
141.78
136.79
136.77
134.58
134.53
134.47
127.55
126.77
117.38
117.32
115.64
115.61
115.50
115.35
77.26
77.00
76.75
70.32
56.97
51.86
48.48
42.69
34.53
32.95
31.78
22.14
20.85
6.97
23 13C NMR (CDCl3)
Me
HO
N
O
NH2
F
23
190
180
170
160
150
140
130
120
110
100
90
80
70
60
50
40
30
20
10
ppm

23 ^{19}F NMR ($CDCl_3$)

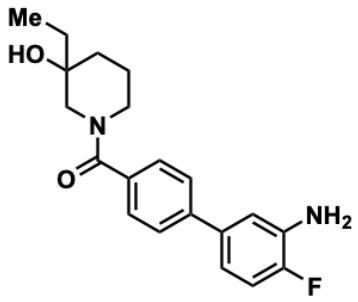

23

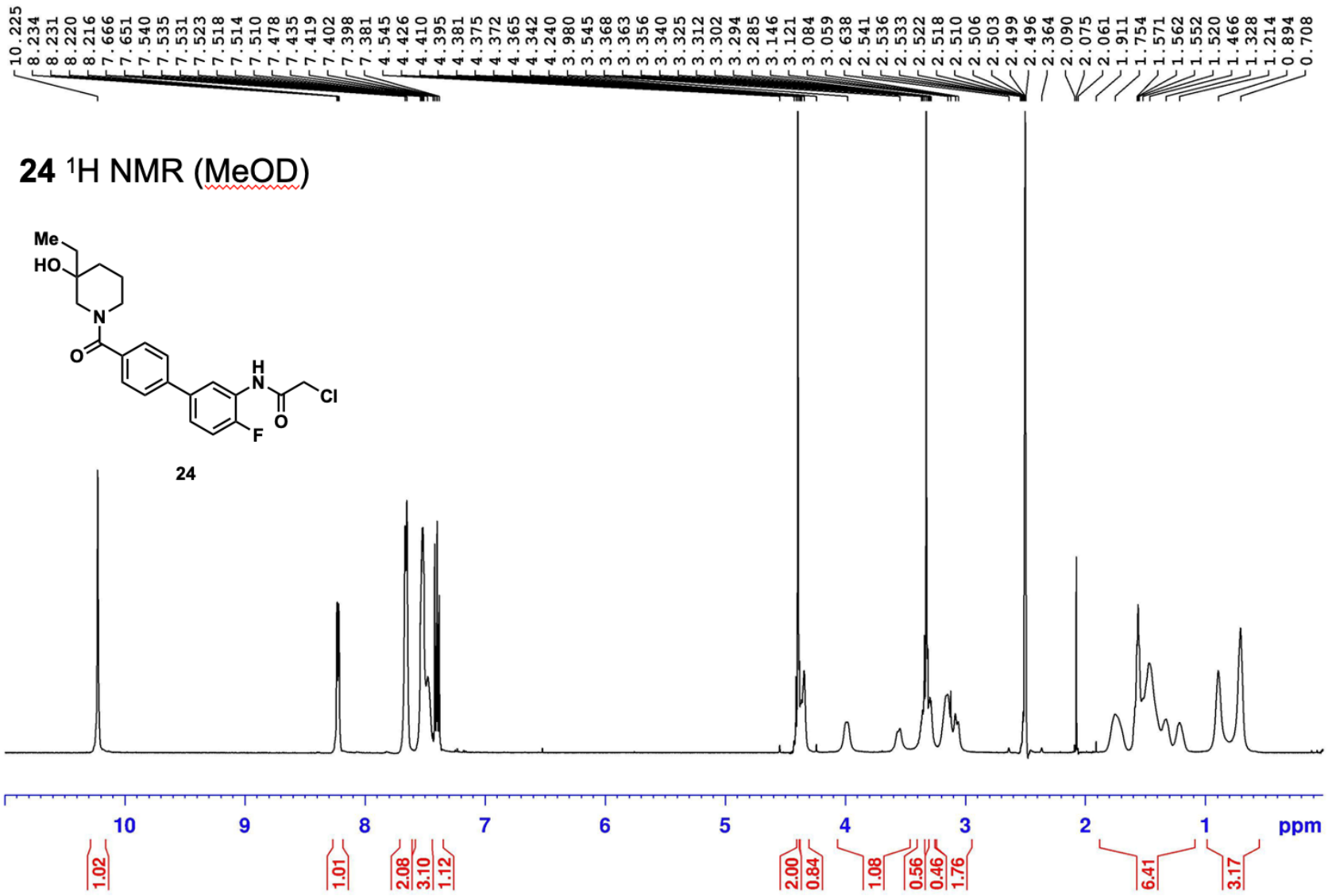
10.225
8.234
8.231
8.220
8.216
7.666
7.651
7.540
7.535
7.531
7.523
7.518
7.514
7.510
7.478
7.435
7.419
7.402
7.398
7.381
4.545
4.426
4.410
4.395
4.381
4.375
4.372
4.365
4.342
4.240
3.980
3.545
3.368
3.363
3.356
3.340
3.325
3.312
3.302
3.294
3.285
3.146
3.121
3.084
3.059
2.638
2.541
2.536
2.533
2.522
2.518
2.510
2.506
2.503
2.499
2.496
2.364
2.090
2.075
2.061
1.911
1.754
1.571
1.562
1.552
1.520
1.466
1.328
1.214
0.894
0.708
24 1H NMR (MeOD)
Me
HO
N
O
H
N
O
Cl
F
24
10
9
8
7
6
5
4
3
2
1
ppm
1.02
1.01
2.08
3.10
1.12
2.00
0.84
1.08
0.56
0.46
1.76
6.41
3.17

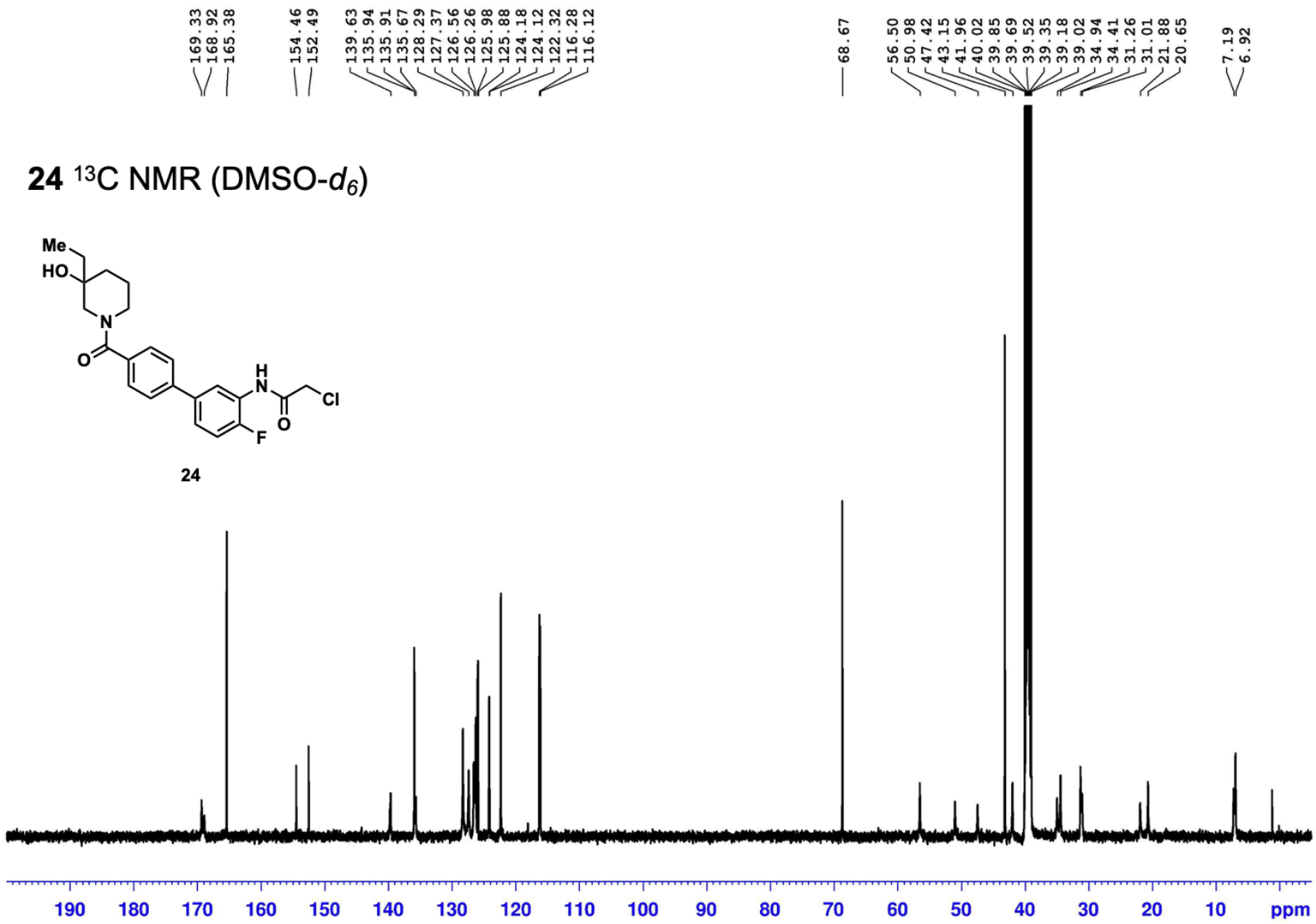
169.33
168.92
165.38
154.46
152.49
139.63
135.94
135.91
135.67
128.29
127.37
126.56
126.26
125.98
125.88
124.18
124.12
122.32
116.28
116.12
68.67
56.50
50.98
47.42
43.15
41.96
40.02
39.85
39.69
39.52
39.35
39.18
39.02
34.94
34.41
31.26
31.01
21.88
20.65
7.19
6.92
24 13C NMR (DMSO-d6)
Me
HO
N
O
H
N
O
Cl
F
24
190
180
170
160
150
140
130
120
110
100
90
80
70
60
50
40
30
20
10
ppm

24 ^{19}F NMR ($CDCl_3$)

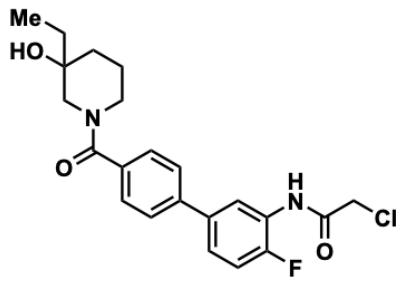

24

25 ^{1}H NMR ($CDCl_3$)

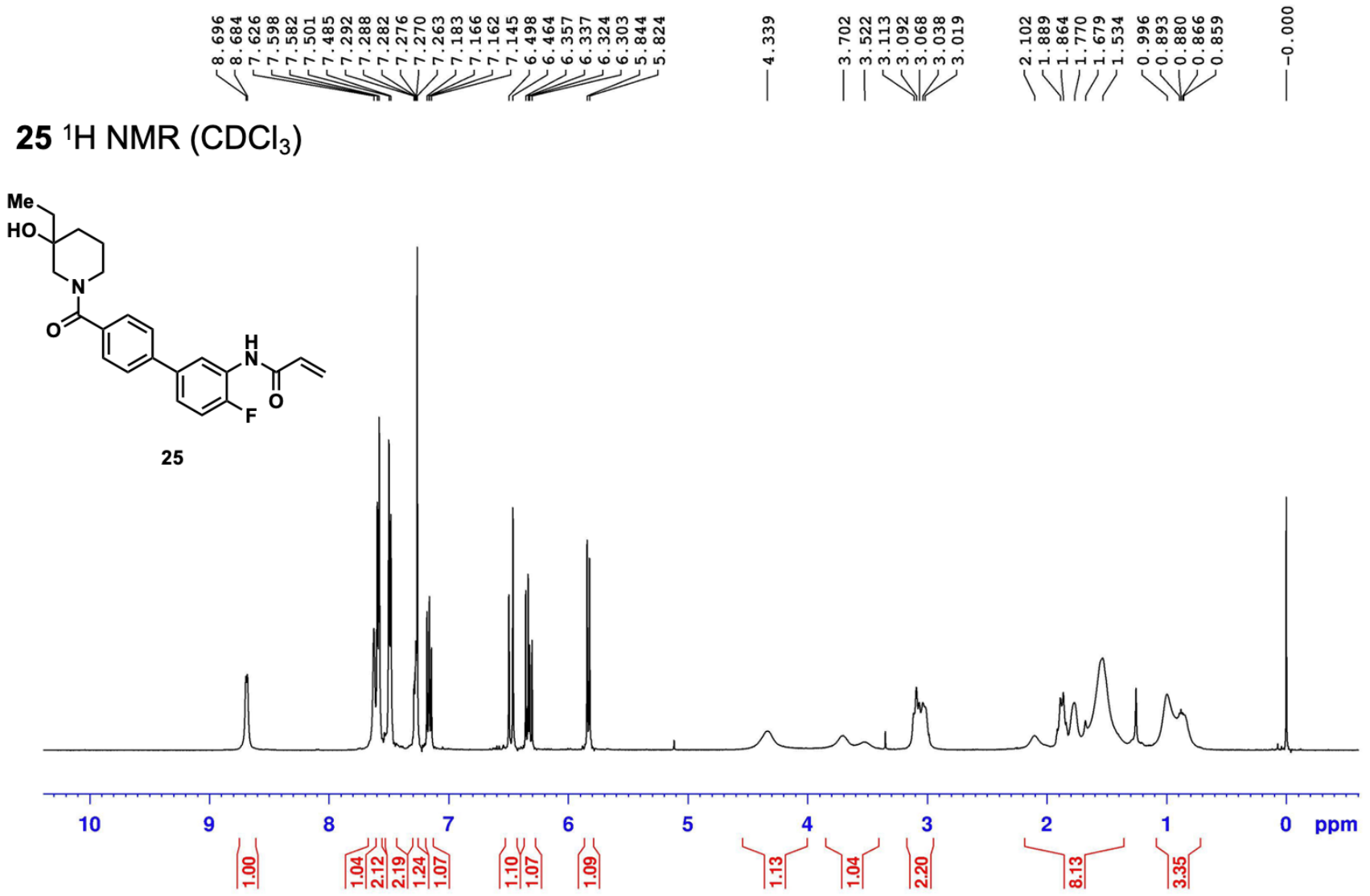

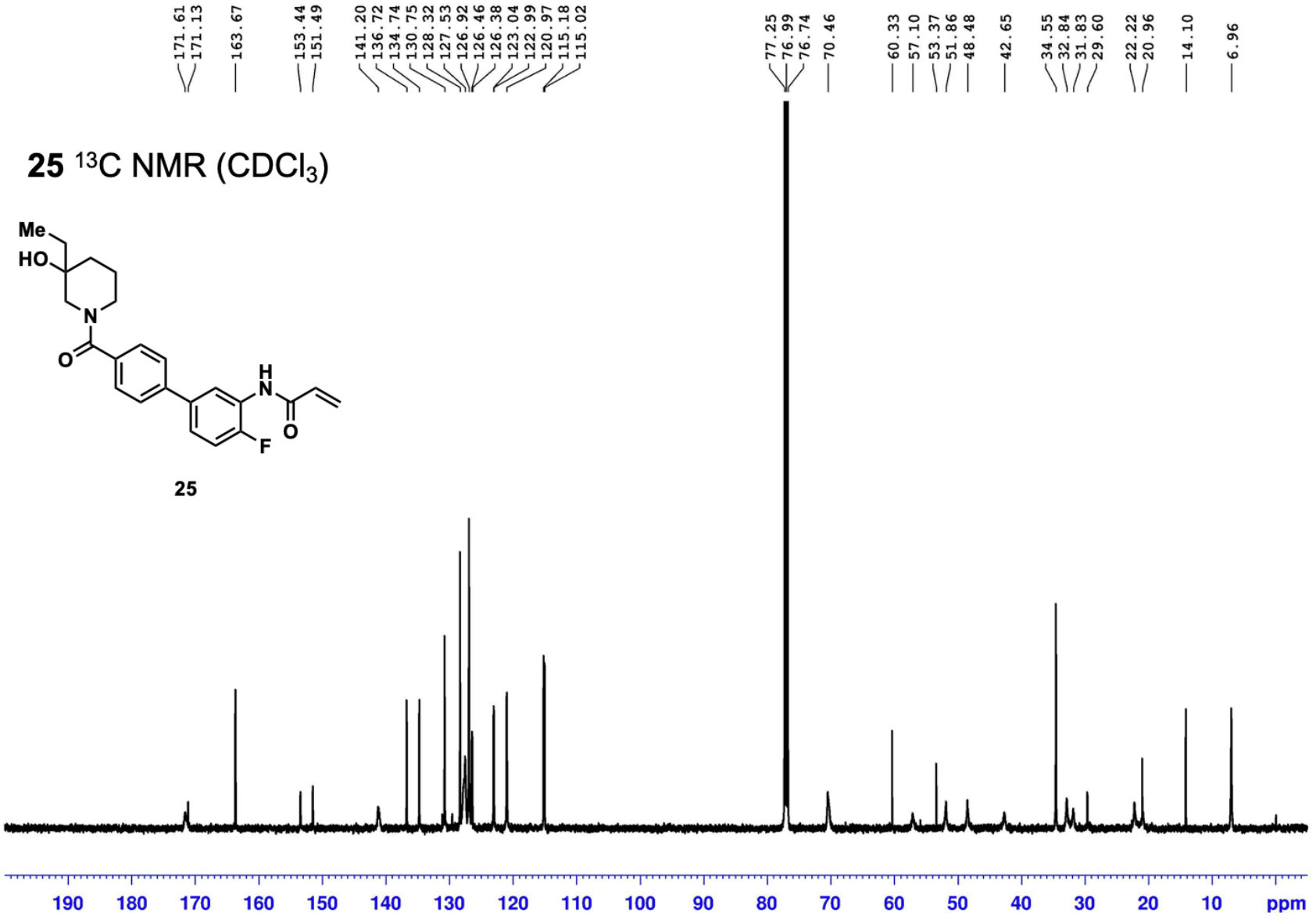
171.61
171.13
163.67
153.44
151.49
141.20
136.72
134.74
130.75
128.32
127.53
126.92
126.46
126.38
123.04
122.99
120.97
115.18
115.02
77.25
76.99
76.74
70.46
60.33
57.10
53.37
51.86
48.48
42.65
34.55
32.84
31.83
29.60
22.22
20.96
14.10
6.96
25 13C NMR (CDCl3)
Me
HO
N
O
H
N
O
F
25
190
180
170
160
150
140
130
120
110
100
90
80
70
60
50
40
30
20
10
ppm

25 ^{19}F NMR ($CDCl_3$)

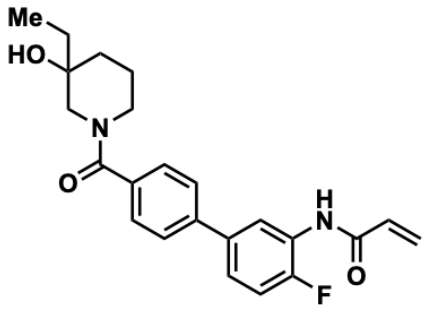

25

References

1. Cossy, J, Dumas, C, Michel, P, Pardo, DG. *Tetrahedron Lett.* **1995**, *36*, 549. DOI: 10.1016/0040-4039(94)02338-C.

2. Wagner, JR, Sørensen, J, Hensley, N, Wong, C, Zhu, C, Perison, T, Amaro, RE. *J. Chem. Theory Comput.* **2017,** *13*, 4584. DOI: 10.1021/acs.jctc.7b00500.

3. Wagner, JR, Demir, O, Carpenter, MA, Aihara, H, Harki, DA, Harris, RS, Amaro, RE. *J. Chem. Inf. Model* **2019,** *59*, 2264. DOI: 10.1021/acs.jcim.8b00427

4. Kozakov, D, Grove, LE, Hall, DR, Bohnuud, T, Mottarella, SE, Luo, L, Xia, B, Beglov, D, Vajda, S. *Nat. Protoc.* **2015,** *10*, 733. DOI: 10.1038/nprot.2015.043

5. Votapka, L, Amaro, RE. *Bioinformatics* **2012,** *29*, 393. DOI: 10.1093/bioinformatics/bts689

6. Friesner, RA, Banks, JL, Murphy, RB, Halgren, TA, Klicic, JJ, Mainz, DT, Repasky, MP, Knoll, EH, Shelley, M, Perry, JK, Shaw, DE, Francis, P, Shenkin, PS. *J. Med. Chem.* **2004,** *47*, 1739. DOI: 10.1021/jm0306430

7. Friesner, RA, Murphy, RB, Repasky, MP, Frye, LL, Greenwood, JR, Halgren, TA, Sanschagrin, PC, Mainz, DT. *J. Med. Chem.* **2006,** *49*, 6177. DOI: 10.1021/jm051256o

8. Case, DA, Ben-Shalom, IY, Brozell, SR, Cerutti, DS, Cheatham III, TE, Cruzeiro, VWD, Darden, TA, Duke, RE, Ghoreishi, D, Gilson, MK, Gohlke, H, Goetz, AW, Greene, D, Harris, R, Homeyer, N, Huang, Y, Izadi, S, Kovalenko, A, Kurtzman, T, Lee, TS, LeGrand, S, Li, P, Lin, C, Liu, J, Luchko, T, Luo, R, Mermelstein, DJ, Merz, KM, Miao, Y, Monard, G, Nguyen, C, Nguyen, H, Omelyan, I, Onufriev, A, Pan, F, Qi, R, Roe, DR, Roitberg, A, Sagui, C, Schott-Verdugo, S, Shen, J, Simmerling, CL, Smith, J, Salomon-Ferrer, R, Swails, J, Walker, RC, Wang, J, Wei, H, Wolf, RM, Wu, X, Xiao, L, York, DM, Kollman, PA. AMBER 2018, 2018. *University of California, San Francisco* **2018**.

9. Wang, J, Wang, W, Kollman, PA, Case, DA. *J. Mol. Graph. Model.* **2006,** *25*, 247. DOI: 10.1016/j.jmgm.2005.12.005

10. Wang, J, Wolf, RM, Caldwell, JW, Kollman, PA, Case, DA. *J. Comput. Chem.* **2004,** *25*, 1157. DOI: 10.1002/jcc.20035

11. Frisch, ME, Trucks, G, Schlegel, H, Scuseria, G, Robb, M, Cheeseman, J, Scalmani, G, Barone, V, Petersson, G, Nakatsuji, H. Gaussian 16, revision C. 01. In Gaussian, Inc., Wallingford CT: 2016.

12. Shi, K, Carpenter, MA, Kurahashi, K, Harris, RS, Aihara, H.. *Biol. Chem.* **2015**, *290*, 28120. DOI: 10.1074/jbc.M115.679951

13. Shi, K, Carpenter, MA, Banerjee, S, Shaban, NM, Kurahashi, K, Salamango, DJ, McCann, JL, Starrett, GJ, Duffy, JV, Demir, O, Amaro, RE, Harki, DA, Harris, RS, Aihara, H. *Nat. Struct. Mol. Biol.* **2017,** *24*, 131. DOI: 10.1038/nsmb.3344

14. Søndergaard, CR, Olsson, MHM, Rostkowski, M, Jensen, JH. *J. Chem. Theory Comput.* **2011,** *7*, 2284. DOI: 10.1021/ct200133y

15. Olsson, MHM, Søndergaard, CR, Rostkowski, M, Jensen, JH. *J. Chem. Theory Comput.* **2011,** *7*, 525. DOI: 10.1021/ct100578z

16. Roe, DR, Cheatham III, TE. *J. Chem. Theory Comput.* **2013,** *9*, 3084. DOI: 10.1021/ct400341p

17. Scheurer, M, Rodenkirch, P, Siggel, M, Bernardi, RC, Schulten, K, Tajkhorshid, E, Rudack, T. *Biophys. J.* **2018,** *114*, 577. DOI: 10.1016/j.bpj.2017.12.003

18. Li, M, Shandilya, SM, Carpenter, MA, Rathore, A, Brown, WL, Perkins, AL, Harki, DA, Solberg, J, Hook, DJ, Pandey, KK. *ACS Chem. Biol.* **2012,** *7*, 506. DOI: 10.1021/cb200440y

19. Kvach, MV, Barzak, FM, Harjes, S, Schares, HAM, Kurup, HM, Jones, KFM, Sutton, L, Donahue, J, D'Aquila, RT, Jameson, GB, Harki, DA, Krause, KL, Harjes, E, Filichev, VV. *ChemBioChem* **2020,** *21*, 1028. DOI: 10.1002/cbic.201900505

20. Kvach, MV, Barzak, FM, Harjes, S, Schares, HAM, Jameson, GB, Ayoub, AM, Moorthy, R, Aihara, H, Harris, RS, Filichev, VV, Harki, DA, Harjes, E. *Biochemistry* **2019,** *58*, 391. DOI: 10.1021/acs.biochem.8b00858

21. Anderson, JJ, Grillo, MJ, Harki, DA. *ACS Med. Chem. Lett.* **2023,** *14*, 1815. DOI: 10.1021/acsmedchemlett.3c00429